AN INVESTIGATION OF THE NARROW-BAND AND WIDEBAND AMBIGUITY FUNCTIONS FOR COMPLEMENTARY CODES

by

Richard Mitsuo Akita

UNITED STATES NAVAL POSTGRADUATE SCHOOL

THESIS

AN INVESTIGATION OF THE

NARROW-BAND AND WIDEBAND

AMBIGUITY FUNCTIONS FOR COMPLEMENTARY CODES

by

Richard Mitsuo Akita

June 1968

[redacted]

AN INVESTIGATION OF THE NARROW-BAND AND WIDEBAND AMBIGUITY FUNCTIONS FOR COMPLEMENTARY CODES

by

Richard Mitsuo Akita
Lieutenant, United States Navy
B.S., Oregon State University, 1961

[redacted]

Submitted in partial fulfillment of the
requirements for the degree of

MASTER OF SCIENCE IN ELECTRICAL ENGINEERING

from the

NAVAL POSTGRADUATE SCHOOL
June 1968

ABSTRACT

A complementary code pair has the property that its autocorrelation function contains no range sidelobes. This property makes complementary codes attractive for use in signal waveform design for detection and tracking systems. An extensive list of the properties of these codes has been formulated by M J. Golay and additions were made by S. Jauregui. However, the ambiguity functions of complementary codes have not been previously formulated.

This thesis considers the ambiguity functions of complementary codes for two cases:

1. Narrow-band analysis
2. Wideband analysis.

In the narrow-band analysis it is assumed that the doppler effect does not significantly alter the envelope of the transmitted signal. Siebert's definition of the ambiguity function is utilized in the formulation of the narrow-band complementary code ambiguity function.

In the wideband analysis it is shown that the doppler effect significantly alters the envelope of the transmitted signal. This alteration of the envelope of the transmitted signal becomes significant when the product of the two factors, the relative velocity between the transmitter and the target, and the time-bandwidth product, approaches one-half the velocity of propagation in the medium. Siebert's ambiguity function is extended to include the wideband case.

TABLE OF CONTENTS

LIST OF TABLES

LIST OF ILLUSTRATIONS

FIGURE PAGE

FIGURE PAGE

ACKNOWLEDGMENTS

I wish to express my gratitude for the assistance and patient effort given me by Professor C. F. Klamm, Jr. in the investigation and writing of this thesis. It was Professor Klamm who brought to my attention, the area of my thesis.

Special thanks are given to various members of the faculty of the Department of Physics at the Naval Postgraduate School; in particular, Professor K. E. Woehler, whose many stimulating discussions enabled me to achieve a greater depth of understanding of the special theory of relativity.

CHAPTER I

INTRODUCTION

The detection problem in modern search radar systems is generally concerned with the optimization of four major factors. These four factors are:

1) Maximization of the effective range of the system.
2) Minimization of the number of false alarms due to impulse noise.
3) Maximization of range and velocity resolution.
4) Accurate measurement of the target's position and velocity without ambiguity.

The solution of this optimization proglem is predicated primarily on a suitable choice of a transmitted signal waveform. To emphasize this point let us analyze the four factors that are involved in the optimization problem.

The first factor can be analyzed from the standpoint of the radar range equation. The prominent result of this analysis is that the system designer may increase the range of the system by increasing the duration of the transmitted pulse.

The second factor can be disposed of by setting a high enough threshold such that very few noise impulses exceed the threshold, but not so high as to degrade the probability of detection below a tolerable level.

The last two factors depend almost entirely on a judicious choice of a signal waveform. Hence it is topical to consider a measure or cost function by which various waveforms may be compared. Siebert's[1] modification of Woodward's [2] ambiguity function provides such a comparison.

It is for this reason that the ambiguity function forms the basis of the modern radar detection philosophy.

This thesis is primarily concerned with a class of codes, called complementary codes, which minimizes range ambiguities. Most codes, which have been described and analyzed in the literature on radar waveform design, have the drawback that range and doppler ambiguities exist. Examples of these codes are:

1) Linear FM (chirp)

2) Truncated pseudo-noise codes

3) Barker codes.

Of the codes mentioned above, the Barker codes' autocorrelation functions exhibit the smallest range sidelobes, and have been named "perfect" words.

Complementary codes have the feature that their autocorrelation functions have no range sidelobes. Although much work has been done in the area of obtaining properties of these codes, the analysis of the ambiguity functions for these codes has not been done. It is the purpose of this thesis to analyze complementary codes, in both range and doppler, for two cases:

1) Narrow-band analysis

2) Wideband analysis.

By narrow-band we mean that the doppler effect does not significantly alter the envelope of the transmitted signal. The narrow-band analysis will be formulated by utilizing Siebert's ambiguity function.* However,

---

*Siebert's ambiguity function is a modification of Woodward's ambiguity function. The essential difference is that Siebert's ambiguity function is real valued, whereas Woodward's ambiguity function is complex valued.

one of the postulates in the formulation of Siebert's ambiguity function is that doppler does not significantly affect the envelope of the transmitted signal. Hence Siebert's ambiguity function cannot be used in the wideband analysis. We will extend Siebert's ambiguity function to include the wideband case. In Appendix B we will define the region of validity of the narrow-band analysis. The essence of the derivation of the region of validity of the narrow-band analysis is that the time-bandwidth-velocity product must be much less than the velocity of propagation divided by two, in order that we may assume that the envelope of the transmitted signal is not altered by the doppler effect. Then by wideband, we mean that doppler has a significant effect on the envelope of the transmitted signal. Throughout this thesis, we will assume that target acceleration is negligible over the interval of measurement.

Let us now consider complementary codes. Complementary codes or series were originally conceived by M. J. Golay,[3,4] in his work on infrared multi-slit spectrometry. An extensive list of properties for complementary codes was formulated by M. J. Golay and additions, based upon applications of group and vector theory, were formulated by S. Jauregui in his doctoral dissertation.[5]

A set of complementary series may be defined as "a pair of equally long, finite sequences of two kinds of elements which has the property that the number of pairs of like elements with any one given separation in one series is equal to the number of pairs of unlike elements with the same given separation in the other series."[6] These sequences are binary and are aperiodic.

It has been shown that the autocorrelation function of these codes gives rise to a central peak. The height of the peak is dependent on the length of the code, for zero delay, and decreases linearly to zero

for delay equal to the duration of one code symbol, then remains at zero. It is this property of the complementary codes that makes this coding method attractive for use in the detection problem. Because the definition of the complementary codes appears rather formidable, we will utilize the property given above whenever we refer to complementary codes. Appendix F is a partial list of the properties of complementary codes. This list is provided so that complementary codes of almost any length may be generated from basic length codes called kernels. A kernel is defined as a basic length code which cannot be decomposed into shorter length codes by an inversion of the standard generating methods. To the author's best knowledge there are only four kernels that are known to exist.[5] These kernels are listed in Appendix F.

At this point we might indicate what the ideal ambiguity function would be. Since we would like to resolve two targets in range and doppler to an infinite degree, the ideal ambiguity function would be a delta function at the origin of the range, doppler axis. Thusly, the system would have infinite resolution. This can never be achieved; what would be required is a code of infinite length with the duration of each code symbol infinitesimally small. However, we should not discard the idea of an ideal ambiguity function, since it gives us a reference by which to compare other ambiguity functions.

A brief synopsis of each chapter will be now given.

In Chapter II a system model for single codes is postulated and a correlation between a physical waveform in the system and the ambiguity function is given. By single codes we are referring to binary codes such as Barker codes, pseudo-noise codes, etc., i.e., codes which consist of a single sequence; as opposed to complementary codes which consist of a pair of equally long binary sequences. In this chapter

the analysis is entirely narrow-band. The single code ambiguity function is derived to ease computational matters in the derivation of the ambiguity function for complementary codes.

Chapter III contains the derivation and the justification of the form of the narrow-band complementary code ambiguity function.

In Chapter IV a system model is postulated for the complementary codes and the derivation of the complementary code ambiguity function is accomplished. Computer programs were run for the two kernels of length 10 and the kernel of length 26, and ambiguity diagrams were constructed. One property of the entire class of binary codes in which phase-reversal modulation is utilized, is uncovered in this chapter. It is proved that in the doppler domain, the zero crossings of the ambiguity function move closer to the origin of the range-doppler axis as the length of the code is increased; assuming that the duration, T, of a code symbol remains constant. The implication of this phenomenon is that better doppler discrimination is possible for longer code lengths, all other things being equal.

Chapter V contains the investigation of the doppler effect on the transmitted signal and the proof that the envelope of the transmitted signal is altered due to doppler. This chapter in conjunction with Appendices A and D shows that the doppler effect is threefold:

1) The carrier frequency is shifted by the doppler frequency.
2) The envelope of the transmitted signal is compressed or expanded according to whether the target is closing or opening with respect to the receiver.
3) The received and transmitted energies are different; in fact, the received and transmitted energies differ by the same factor as the received and transmitted carrier frequencies. The above statement

assumes a lossless medium and ignores spherical spreading of the transmitted and received waves.

Chapter VI contains the derivation of the wide-band ambiguity function for single codes as well as complementary codes, valid for positive differential doppler and positive range deviation. Unfortunately due to time limitations, computer programs to generate numerical values for the wideband complementary code ambiguity function were not accomplished.

To clarify the discussion of the model of the system, which is postulated in Chapter II, a brief formulation of the autocorrelation function of complementary codes will be given. As mentioned previously, complementary codes consist of two binary sequences, which will be referred to as Code A and Code B or simply A and B. To obtain the autocorrelation function[7] for the complementary code, $R_c(\tau)$, we compute the autocorrelation function for code A, $R_A(\tau)$, and for code B, $R_B(\tau)$. Then $R_c(\tau)$ is obtained by summing $R_A(\tau)$ and $R_B(\tau)$, i.e.,

$$R_c(\tau) = R_A(\tau) + R_B(\tau).$$

The property of interest in the autocorrelation function of the complementary codes is that no range sidelobes exist. All binary codes have autocorrelation functions with range sidelobes. However, $R_A(\tau)$ has range sidelobes which are the negative of the sidelobes of $R_B(\tau)$. Hence when $R_A(\tau)$ and $R_B(\tau)$ are summed, the range sidelobes cancel. Figure 1-1 shows this unique property of the complementary codes.

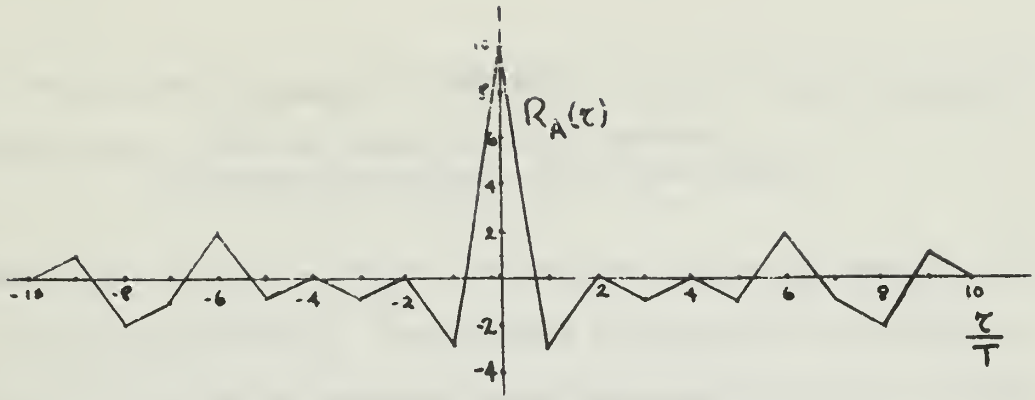

Figure 1-1a

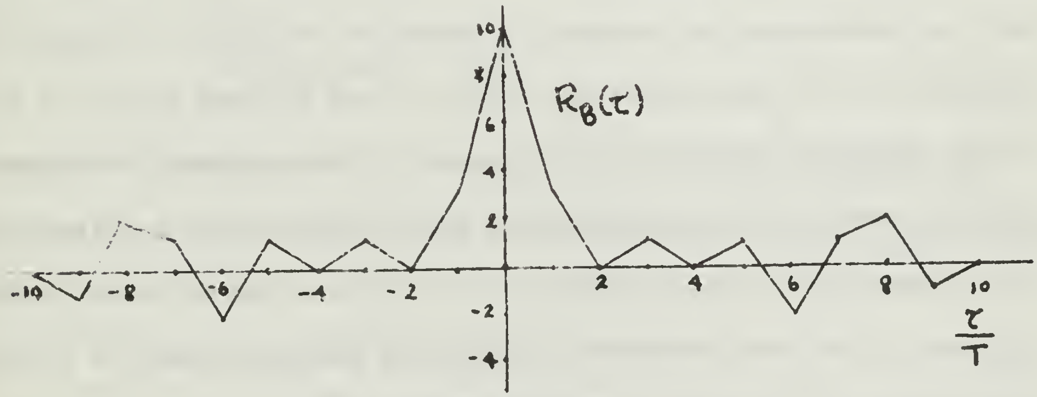

Figure 1-1b

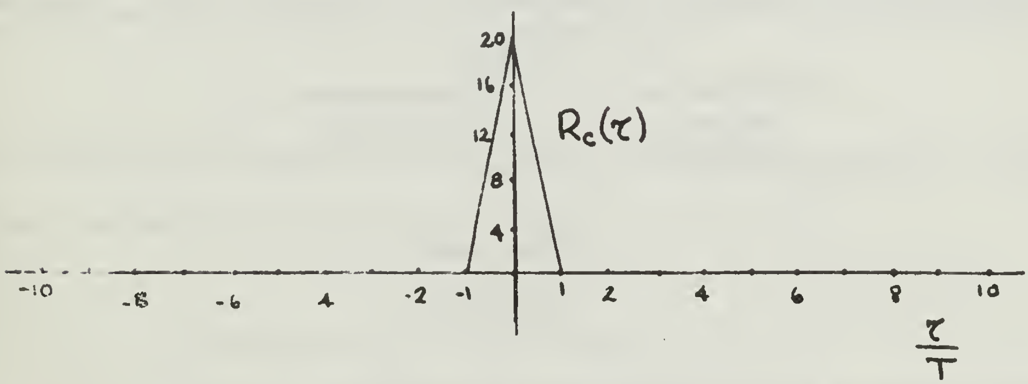

Figure 1-1c

Fig. 1-1a - Autocorrelation function for code A, length 10; A = set $\{-1,+1,+1,-1,+1,-1,+1,+1,+1,-1\}$

Fig. 1-1b - Autocorrelation function for code B, length 10; B = set $\{-1,+1,+1,+1,+1,+1,+1,-1,-1,+1\}$

Fig. 1-1c - Autocorrelation function for the complementary code, length 10.

CHAPTER II

MATCHED FILTER APPROACH FOR THE SINGLE CODE SYSTEM (NARROW-BAND ANALYSIS)

It might be well to look at the single code system before attempting to analyze the complementary coded system. In the matched filter approach the underlying theme is to correlate the ambiguity function with a physical waveform in the system. The ambiguity function is an excellent measure of range and velocity resolvability, i.e., how closely one can distinguish two targets in range and velocity. A common misconception is to state that the output of the matched filter is identical to the ambiguity function for all cases. This statement holds some truth; however, it is not generally correct in carrier modulated systems. Let us depart from this discussion to model our system before attempting to clarify the above statement. The model that is chosen is a slight modification of the model used by Davenport.[8]

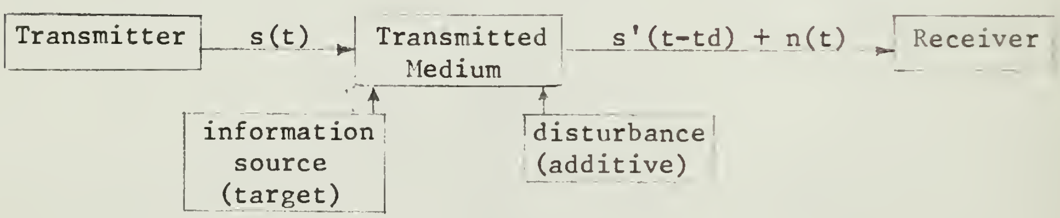

System model

Figure 2-1

The difference between Davenport's model and the model that is chosen is that in the radar, as well as the sonar case, the information source interacts in the medium, whereas in Davenport's system model, the information source interacts in the transmitter.

The transmitted signal is chosen as a phase-reversal modulated signal, where

$$s(t) = \alpha \cos(\omega_0 t - n_i \pi) \qquad 2\text{-}1$$

where $n_i = \begin{cases} 0 \\ 1 \end{cases}$ depending on the value of the ith code symbol

α = normalization constant.

For convenience the signal energy is normalized to unity by specifying that

$$\int s^2(t)\, dt = 1 .$$

It is a well known fact that a phase-reversal modulated signal is identical to a DSB/SC signal; hence the transmitted signal can be written as

$$s(t) = I(t) \cos \omega_0 t, \qquad 2\text{-}2$$

where $I(t) = \alpha \sum_{i=0}^{N} X_i \left\{ u(t-iT) - u[t - (i + 1)T] \right\}$,

and $X_i = \pm 1$, depending on the value of the ith code symbol.

The normalization constant can be easily evaluated by squaring equation 2-2 and performing the integration. Thus

$$\int_{-\infty}^{\infty} s^2(t)\, dt = \frac{\alpha^2}{2} \int_0^{NT} \left[1 + \cos 2\omega_0 t\right] dt \qquad 2\text{-}3a$$

$$= \frac{\alpha^2 NT}{2} + \frac{\alpha^2 \sin 2\omega_0 NT}{4\omega_0} . \qquad 2\text{-}3b$$

The second term in equation 2-3b is very small compared to the first term, for ω_0 large. This term can be interpreted as the difference

between the initial and final value of the carrier phase and will be small. Hence the normalization constant is approximately given by

$$\alpha = \sqrt{\frac{2}{NT}} \, . \qquad \text{2-3c}$$

The received signal contains a noise term, n(t), which will be ignored since the receiver will utilize a matched filter[9] to maximize the signal-to-noise ratio. Thus the received signal, $s'(t-t_d)$, is the transmitted signal modified by the information source, and contains range and velocity information. Let us assume that the target speeds are sufficiently less than the speed of propagation of the wave in the medium (say of the order of $10^{-4} \times c$, where c is the velocity of propagation.) The principal doppler effect, in this case, is to shift the carrier frequency by the amount f_d, where f_d is the doppler frequency; doppler will have little effect on the duration of a code symbol, T. (See Chapter IV for the discussion of the doppler effect on the duration of a code symbol.) With the above conditions postulated, the received signal may be given by

$$s'(t-t_d) = I(t-t_d) \cos[(\omega_0 + \omega_d')(t-t_d)] \, ,$$

$$= \alpha \sum_{i=0}^{N} X_i \{ \Pi(t-t_d-iT) - \Pi[t-t_d-(i+1)T] \cos[(\omega_0 + \omega_d')(t-t_d)] \, , \qquad \text{2-4}$$

where the convention is chosen so that the doppler frequency is positive for closing targets, and negative for opening targets.

At this point the question might be raised as to what are the various waveforms in the receiver. As mentioned earlier in this chapter, a matched filter will be utilized in the system model. To obtain the signals to correlate with the received signal, we translate the transmitted signal by various expected doppler frequencies as indicated in

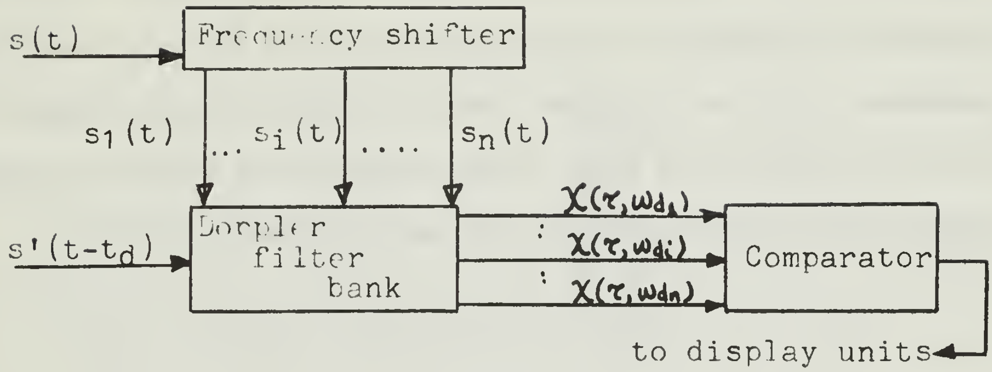

Figure 2-2a

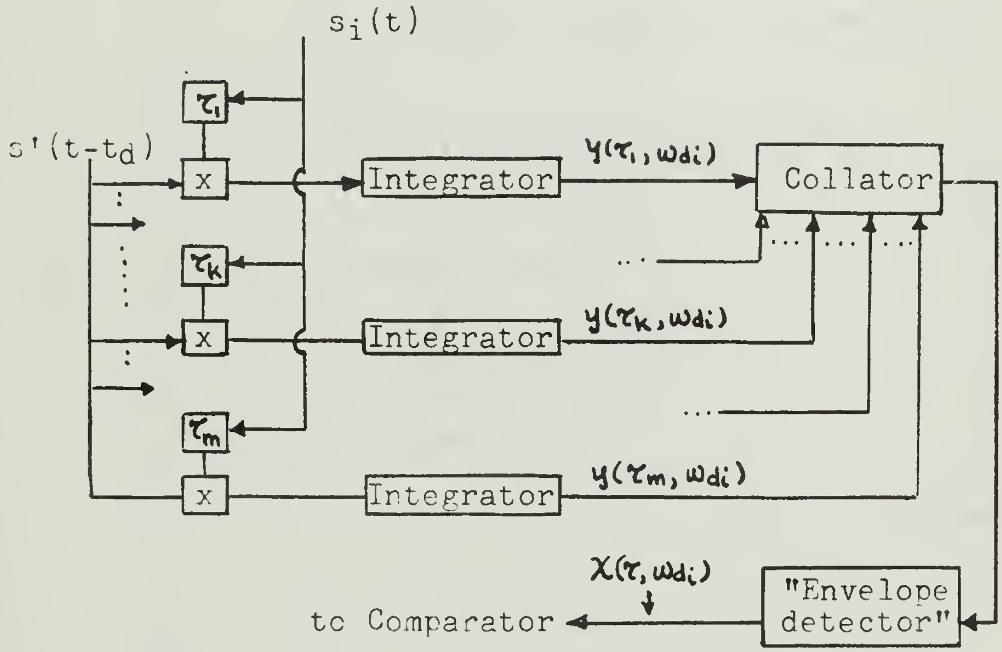

Figure 2-2b

Figure 2-2a Receiver block diagram

2-2b ith doppler filter of the filter bank in Figure 2-2a

Figure 2-2a. The doppler shifted signal is then delayed. The delay is required to account for the propagation time to and from the target. To instrument this system in real time, the delay mechanism might be of the form of a tapped delay line. We shall denote the delayed, doppler shifted signal as the replica signal. The replica signal is given by

$$s_i(t - \tau_k) = I(t - \tau_k)\cos\left[(\omega_o + \omega_{di})(t - \tau_k)\right] \qquad \text{2-5}$$

Let us now analyze the various signals in the receiver. To simplify the analysis, the matched filter block diagram is duplicated from Figure 2-2b.

The output of the matched filter is

$$y_k(\tau_k, \omega_d', \omega_{di}) = \int_{-\infty}^{\infty} s'(t-t_d)\, s_i(t-\tau_k)\, dt \qquad \text{2-6a}$$

$$= \int_{-\infty}^{\infty} I(t-t_d)\cos\left[(\omega_o+\omega_d')(t-t_d)\right] \cdot$$

$$I(t-\tau_k)\cos\left[(\omega_o+\omega_{di})(t-\tau_k)\right] dt \qquad \text{2-6b}$$

Then let

$$t_1 = t - t_d \qquad \text{2-7a}$$

$$\omega_{o1} = \omega_o + \omega_{di} \qquad \text{2-7b}$$

Equation 2-6b becomes

$$y_k(\tau_k, \omega_d', \omega_{di}) = \int_{-\infty}^{\infty} I(t_1)\, I(t_1 + t_d - \tau_k)\cos(\omega_{o1} - \omega_{di} + \omega_d')t_1 \cdot$$

$$\cos\left[\omega_{o1}(t_1 + t_d - \tau_k)\right] dt_1 \quad . \qquad \text{2-8}$$

Figure 2-3

Matched filter for the ith doppler filter
and kth range delay

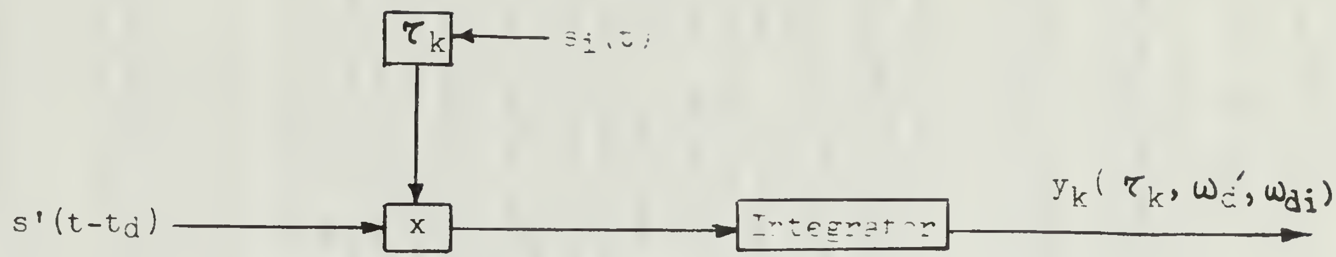

Then let

$$\tau = \tau_k - t_d \tag{2.9a}$$

$$\omega_d = \omega_d' - \omega_{di} \; . \tag{2.9b}$$

If the above changes in variables are effected, then

$$y_k(\tau, \omega_d) = \int_{-\infty}^{\infty} I(t_1) I(t_1 - \tau) \cos(\omega_{01} + \omega_d) t_1 \cos \omega_{01}(t_1 - \tau) dt. \tag{2-10}$$

The variables τ and ω_d deserve some comment. From equation 2-9a, we see that if τ is zero, then the propagation delay to the target has been matched in range bin τ_k. Hence $\frac{\tau_k}{2}$ is the range to the target. From equation 2-9b we see that if ω_d is zero, then ω_{di} is the doppler frequency. Thus both τ and ω_d represent the departure of the target's range and velocity from the estimated range and velocity. The variable t_1 is just the variable of integration, and since it is inconsequential as to what nomenclature is ascribed to it, we shall denote t_1 by t. ω_{01} represents the estimated carrier frequency of the replica signal. Hence the output of the matched filter in the system is given by

$$y_k(\tau, \omega_d) = \int_{-\infty}^{\infty} I(t) I(t - \tau) \cos(\omega_{01} + \omega_d) t \cos \omega_{01}(t - \tau) dt \; , \tag{2-11a}$$

$$= \frac{1}{2} \int_{-\infty}^{\infty} I(t) I(t - \tau) \cos(\omega_d t - \omega_{01}\tau) dt$$

$$+ \frac{1}{2} \int_{-\infty}^{\infty} I(t) I(t - \tau) \cos[(2\omega_{01} + \omega_d) t - \omega_{01}\tau] dt \; . \tag{2-11b}$$

The second term in equation 2-11b has frequencies centered about twice the carrier frequency plus the doppler frequency, and will be rejected. Note that the output of each matched filter is an ordinate in the τ domain.

Next we require a device to collect the output of each of the matched filters in an orderly fashion. Hence the use of the term, collator, to describe that device is appropriate. We shall define the collator in Figure 2-2b as that device which collects the various outputs of the matched filter sequentially as a function of range deviation, τ. To clarify the above definition, we might think of the collator as a graph plotter, where ordinates (outputs of the matched filters) are plotted as a function of range deviation, τ. The "envelope detector" in Figure 2-2b is not an envelope detector in the normal sense, and requires some explanation. As mentioned above, the collator collects the outputs of each matched filter and produces a continuous curve in the τ domain. This curve oscillates at ω_{o1} in the τ domain, but only its envelope has information content. The "envelope detector" refers to that device that takes the envelope of the output of the collator, but in the range deviation or τ domain. In the usual sense of the term, envelope detection is accomplished in the time domain and hence a distinction must be made in our usage of the term envelope detector.

Now let us look at the output of the collator;

$$y(\tau,\omega_d) = \frac{1}{2}\int_{-\infty}^{\infty} I(t)I(t-\tau)\cos(\omega_d t-\omega_{o1}\tau)dt \qquad 2\text{-}12$$

If the Euler identity for the cosine function is utilized, the output from the collator is

$$y(\tau,\omega_d) = \frac{1}{4} e^{j\omega_{c1}\tau} \int_{-\infty}^{\infty} I(t)I(t-\tau)e^{j\omega_d t}dt$$

$$+ \frac{1}{4} e^{-j\omega_{c1}\tau} \int_{-\infty}^{\infty} I(t)I(t-\tau)e^{-j\omega_d t}dt \quad . \qquad 2\text{-}13$$

If we note that the second term of equation 2-13 is the complex conjugate of the first term and that the sum of a quantity, say z, and its complex conjugate is

$$Z + Z^* = 2\,\mathrm{Re}(Z) \;,$$

then

$$y(\tau,\omega_d) = 2\,\mathrm{Re}\left\{\frac{1}{4} e^{j\omega_{c1}\tau} \int_{-\infty}^{\infty} I(t)I(t-\tau)e^{j\omega_d t}dt\right\}. \qquad 2\text{-}14$$

The terms $I(t)$ and $I(t - \tau)$ are the modulation functions and involve the limits of integration and the values of the codes. The modulation functions, according to equation 2-2 are

$$I(t) = \alpha \sum_{i=1}^{N} X_i \left\{ \mathbb{1}(t-iT) - \mathbb{1}[t-(i+1)T] \right\} \;, \qquad 2\text{-}15a$$

$$I(t-\tau) = \alpha \sum_{i=1}^{N} X_i \left\{ \mathbb{1}(t-\tau-iT) - \mathbb{1}[t-\tau-(i+1)T] \right\} . \qquad 2\text{-}15b$$

The unit step functions in equations 2-15a and 2-15b will determine the limits of integration and the X_i's are ± 1, depending on the value of the codes. Figure 2-4 is the plot of the time waveforms of $I(t)$ and $I(t - \tau)$. To obtain the limits of integration, we merely observe the zero crossings of the functions. Hence the output of the collator is given by

Figure 2-4

Time waveforms for the functions $I(t)$ and $I(t-\tau)$ for the code of length 10, where $X = \text{set } \{-1,+1,+1,-1,+1,-1,+1,+1,+1,-1\}$ (Note that the amplitude of $I(t)$ is suppressed intentionally so that the waveforms may be seen in detail)

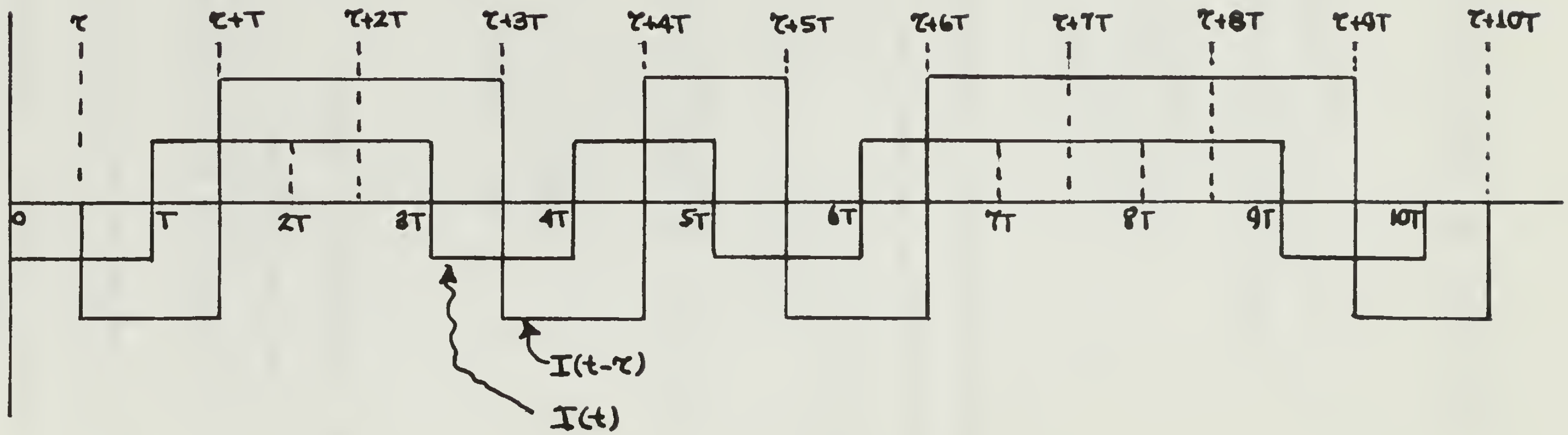

$$y(\tau,\omega_d) = \frac{\alpha^2}{2} \mathcal{R}e \left\langle e^{j\omega_{o1}\tau} \left\{ X_1X_1 \int_{\tau}^{T} e^{j\omega_d t} dt \right.\right.$$

$$+ X_1X_2 \int_{T}^{\tau+T} e^{j\omega_d t} dt + X_2X_2 \int_{\tau+T}^{2T} e^{j\omega_d t} dt$$

$$\left.\left. + X_2X_3 \int_{2T}^{\tau+2T} e^{j\omega_d t} + \cdots\cdots + X_{10}X_{10} \int_{\tau+9T}^{10T} e^{j\omega_d t} dt \right\} \right\rangle .$$

The above equation can be generalized to a code of any length N, and will be written as the sum of two series. Therefore the output of the collator is

$$y(\tau,\omega_d) = \frac{\alpha^2}{2} \mathcal{R}e \left\langle e^{j\omega_{o1}\tau} \left\{ \sum_{i=1}^{N-k} X_iX_{k+i} \int_{\tau+(i-1)T}^{(k+i)T} e^{j\omega_d t} dt \right.\right.$$

$$\left.\left. + \sum_{i=1}^{N-(k+1)} X_iX_{k+i+1} \int_{(k+i)T}^{\tau+iT} e^{j\omega_d t} dt \right\} \right\rangle . \qquad 2\text{-}16$$

where N = length of the code

k = smallest integer $\geq |\tau/T|$

T = the duration of a code symbol = clock period

The first integral in equation 2-16 can be evaluated as

$$C_1 = \int_{\tau+(i-1)T}^{(k+i)T} e^{j\omega_d t} dt = \frac{e^{j\omega_d(k+i)T} - e^{j\omega_d[\tau+(i-1)T]}}{j\omega_d} , \qquad 2\text{-}17a$$

$$= \frac{1}{j\omega_d}\left\{\cos\omega_d(k+i)T + j\sin\omega_d(k+i)T - \cos\omega_d[\tau+(i-1)T]\right.$$

$$\left. -j\sin\omega_d[\tau+(i-1)T]\right\} . \qquad 2\text{-}17b$$

If the following trigonometric substitutions are utilized,

$$\cos x - \cos y = -2\sin\left(\frac{x+y}{2}\right)\sin\left(\frac{x-y}{2}\right)$$

$$\sin x \pm \sin y = 2\sin\left(\frac{x\pm y}{2}\right)\sin\left(\frac{x\mp y}{2}\right) ,$$

equation 2-17b becomes

$$C_1 = \frac{j}{\omega_d}\left\{-2\sin\frac{\omega_d[(2i+k-1)T+\tau]}{2}\sin\frac{\omega_d[(k+1)T-\tau]}{2}\right.$$

$$\left.+j\,2\sin\frac{\omega_d[(k+1)T-\tau]}{2}\cos\frac{\omega_d[(2i+k-1)T+\tau]}{2}\right\}, \qquad 2\text{-}18a$$

$$= \frac{2}{\omega_d}\left\{\sin\frac{\omega_d[(k+1)T-\tau]}{2}\, e^{j\frac{\omega_d[(2i+k-1)T+\tau]}{2}}\right\} . \qquad 2\text{-}18b$$

The second integral in equation 2-16 can be evaluated as

$$C_2 = \int_{(k+i)T}^{\tau+iT} e^{j\omega_d t}dt = \frac{e^{j\omega_d(\tau+iT)} - e^{j\omega_d(k+i)T}}{j\omega_d} . \qquad 2\text{-}19a$$

By similar arguments used to derive equation 2-18d, C_2 becomes

$$C_2 = \frac{2}{j\omega_d}\sin\frac{\omega_d(\tau-kT)}{2}\, e^{j\frac{\omega_d[\tau+(2i+k)T]}{2}} . \qquad 2\text{-}19b$$

We then substitute equations 2-18b and 2-19b into equation 2-16.

$$y(\tau,\omega_d) = \alpha^2 \mathcal{R}e \left\langle \frac{e^{j\omega_{o1}\tau}}{\omega_d} \left\{ \sum_{i=1}^{N-k} X_i X_{k+i} \sin \frac{\omega_d[(k+1)T-\tau]}{2} \cdot e^{j\frac{\omega_d[(2i+k-1)T-\tau]}{2}} + \sum_{i=1}^{N-(k+1)} X_i X_{k+i} \sin \frac{\omega_d(\tau-kT)}{2} \cdot e^{j\frac{\omega_d[\tau+(2i+k)T]}{2}} \right\} \right\rangle . \qquad 2\text{-}20$$

If the exponential terms are combined, and the real part of equation 2-20 taken, then

$$y(\tau,\omega_d) = \frac{\alpha^2}{\omega_d} \sum_{i=1}^{N-k} X_i X_{k+i} \sin \frac{\omega_d[(k+1)T-\tau]}{2} \cdot \cos\left[\frac{\omega_d(2i+k-1)T+(2\omega_{o1}+\omega_d)\tau}{2}\right] + \frac{\alpha^2}{\omega_d} \sum_{i=1}^{N-(k+1)} X_i X_{k+i+1} \cdot \sin \frac{\omega_d(\tau-kT)}{2} \cos\left[\frac{\omega_d(2i+k)T+(2\omega_{o1}+\omega_d)\tau}{2}\right] . \qquad 2\text{-}21$$

In order to plot equation 2-21, it is necessary to obtain the equation in the form of an envelope term multiplied by an RF term. Let

$$z_1 = \frac{\omega_d(2i+k-1)T}{2} , \qquad 2\text{-}22a$$

$$z_2 = \frac{\omega_d(2i+k)T}{2} , \qquad 2\text{-}22b$$

$$\omega_1 = \frac{2\omega_{o1}+\omega_d}{2} , \qquad 2\text{-}22c$$

$$E_1 = X_i X_{k+i} \sin \frac{\omega_d[(k+1)T-\tau]}{2} \quad , \qquad \text{2-22d}$$

$$E_2 = X_i X_{k+i+1} \sin \frac{\omega_d(\tau-kT)}{2} \quad . \qquad \text{2-22e}$$

Then

$$y(\tau,\omega_d) = \frac{\alpha^2}{\omega_d}\left\{\sum_{i=1}^{N-k} E_1 \cos(z_1+\omega_1\tau) + \sum_{i=1}^{N-(k+1)} E_2 \cos(z_2+\omega_1\tau)\right\} . \qquad \text{2-23a}$$

We now utilized the trigonometric identity

$$\cos(a + b) = \cos a \cos b - \sin a \sin b \text{ .}$$

Equation 2-23a becomes

$$y(\tau,\omega_d) = \frac{\alpha^2}{\omega_d}\left\{\sum_{i=1}^{N-k} E_1 \cos z_1 \cos \omega_1\tau - \sum_{i=1}^{N-k} E_1 \sin z_1 \sin \omega_1\tau + \sum_{i=1}^{N-(k+1)} E_2 \cos z_2 \cos \omega_1\tau - \sum_{i=1}^{N-(k+1)} E_2 \sin z_2 \sin \omega_1\tau\right\} ,$$

$$= \frac{\alpha^2}{\omega_d}\left\{\left[\sum_{i=1}^{N-k} E_1 \cos z_1 + \sum_{i=1}^{N-(k+1)} E_2 \cos z_2\right] \cos \omega_1\tau - \left[\sum_{i=1}^{N-k} E_1 \sin z_1 + \sum_{i=1}^{N-(k+1)} E_2 \sin z_2\right] \sin \omega_1\tau\right\} . \qquad \text{2-23b}$$

Then

$$A \cos a - B \sin a = \sqrt{A^2+B^2} \cos\left(a - \tan^{-1}\frac{B}{A}\right) .$$

Thus the output of the collator becomes

$$y(\tau,\omega_d) = \frac{\alpha^2}{\omega_d}\left\{\left[\sum_{i=1}^{N-k} E_1 \cos z_1 + \sum_{i=1}^{N-(k+1)} E_2 \cos z_2\right]^2\right.$$

$$\left. + \left[\sum_{i=1}^{N-k} E_1 \sin z_1 + \sum_{i=1}^{N-(k+1)} E_2 \sin z_2\right]^2\right\}^{1/2} \cos(\omega_1\tau - \phi)\,, \qquad \text{2-23c}$$

where ϕ is the phase due to the amplitude of the sine and cosine terms.

If equations 2-22 a, b, c, d, e, are substituted into equation 2-23c, and if the sine terms are placed in the familiar $\frac{\sin x}{x}$ form, then

$$y(\tau,\omega_d) = \alpha^2 \left\langle \left\{ \frac{[(k+1)T-\tau]}{2} \frac{\sin \frac{\omega_d[(k+1)T-\tau]}{2}}{\frac{\omega_d[(k+1)T-\tau]}{2}} \sum_{i=1}^{N-k} X_i X_{k+i} \cdot \right.\right.$$

$$\cos \frac{\omega_d(2i+k+1)T}{2} + \frac{(\tau+kT)}{2} \frac{\sin \frac{\omega_d(\tau+kT)}{2}}{\frac{\omega_d(\tau+kT)}{2}} \cdot$$

$$\left. \sum_{i=1}^{N-(k+1)} X_i X_{k+i+1} \cos \frac{\omega_d(2i+k)T}{2} \right\}^2 + \left\{ \frac{[(k+1)T-\tau]}{2} \cdot \right.$$

$$\frac{\sin \frac{\omega_d[(k+1)T-\tau]}{2}}{\frac{\omega_d[(k+1)T-\tau]}{2}} \sum_{i=1}^{N-k} X_i X_i \sin \frac{\omega_d(2i+k-1)T}{2}$$

$$+ \frac{(\tau-kT)}{2} \frac{\sin \frac{\omega_d(\tau-kT)}{2}}{\frac{\omega_d(\tau-kT)}{2}} \sum_{i=1}^{N-(k+1)} X_i X_{k+i+1} \cdot$$

$$\left.\left. \sin \frac{\omega_d(2i+k)T}{2} \right\}^2 \right\rangle^{1/2} \cos\left[\left(\omega_{o1} + \frac{\omega_d}{2}\right)\tau - \phi\right]. \qquad \text{2-24}$$

Equation 2-24 is plotted in Figure 2-5; note the RF fine structure under the envelope.

Now let us analyze the ambiguity function. Essentially, definitions and results will be stated from Siebert's paper[1] with the exception of a few terms which will be modified to conform to the nomenclature of this thesis. The ambiguity function as defined by Siebert is

$$\Psi(\tau, \omega_d) = \frac{1}{2} \left| \int_{-\infty}^{\infty} S_o(t) S_o^*(t-\tau) e^{j\omega_d t} dt \right| , \qquad 2\text{-}25$$

where $S_o(t)$ is the complex envelope of the transmitted signal.

In terms of this thesis

$$S(t) = I(t).$$

I(t) is real. Therefore

$$\Psi(\tau, \omega_d) = \frac{1}{2} \left| \int_{-\infty}^{\infty} I(t) I(t-\tau) e^{j\omega_d t} dt \right| . \qquad 2\text{-}26$$

Equation 2-26 departs from equation 2-14 in that the carrier phase term is absent and the magnitude of the integral is taken. Utilizing the same analysis used in obtaining the limits of integration for the output of the collator, we see that equation 2-26 can be written as

$$\Psi(\tau, \omega_d) = \frac{\alpha^2}{2} \left| \sum_{i=1}^{N-k} X_i X_{k+i} \int_{\tau+(i-1)T}^{(k+i)T} e^{j\omega_d t} dt \right.$$

$$\left. + \sum_{i=1}^{N-(k+1)} X_i X_{k+i+1} \int_{(k+i)T}^{\tau+iT} e^{j\omega_d t} dt \right| . \qquad 2\text{-}27$$

Figure 2-5

Waveform of the output of the collator for the code
X = set $\{-1,+1,+1,-1,+1,-1,+1,+1,+1,-1\}$
for the conditions; $\omega_d=0$, and $\tau \geq 0$
(Note that the period of the RF fine structure is greatly exaggerated)

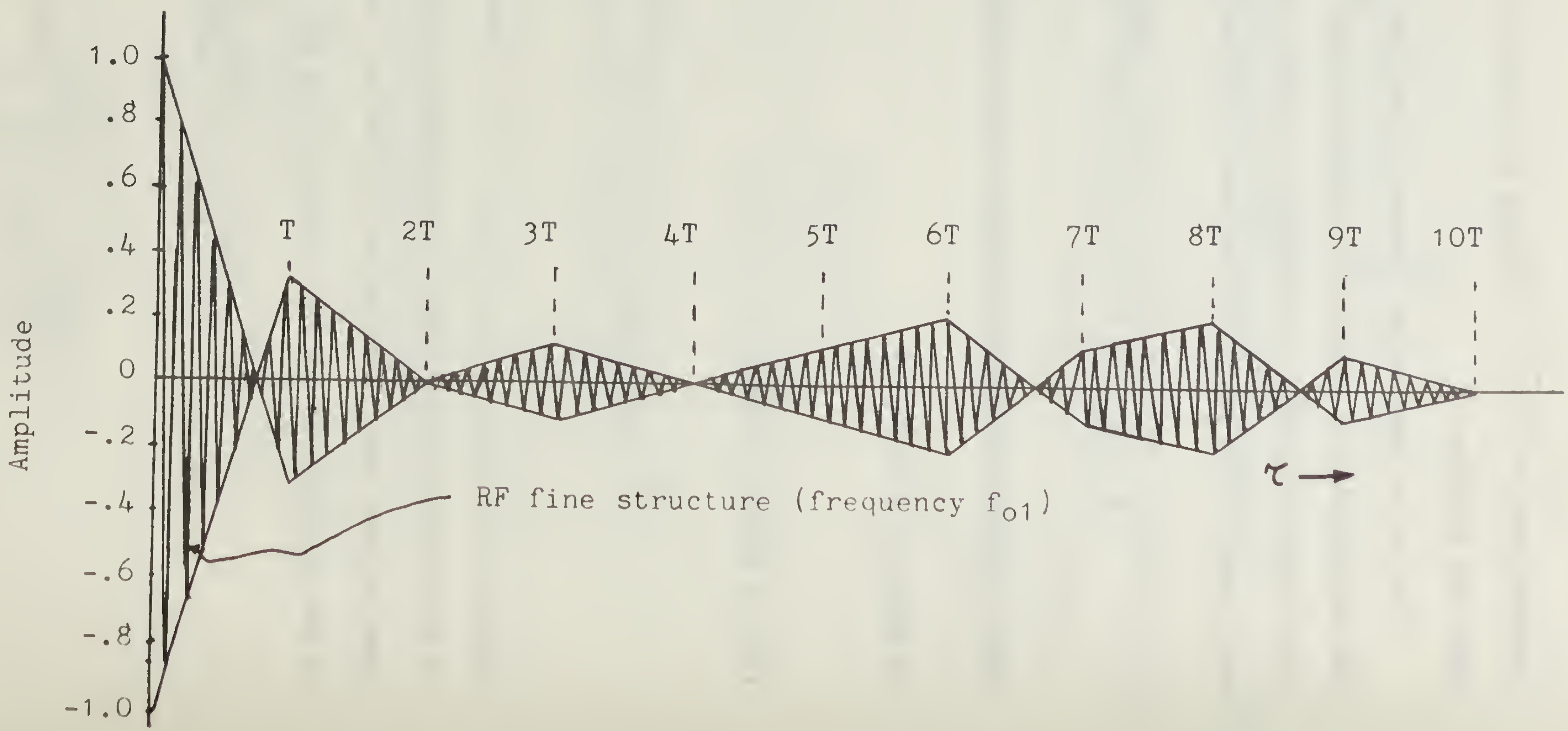

If the results of equations 2-17 through 2-20 are utilized, equation 2-27 becomes

$$\Psi(\tau,\omega_d) = \frac{\alpha^2}{\omega_d}\left|\sum_{i=1}^{N-k} X_i X_{k+i} \sin\frac{\omega_d[(k+1)T-\tau]}{2} \cdot e^{j\frac{\omega_d(2i+k-1)T}{2}} e^{j\frac{\omega_d\tau}{2}} + \sum_{i=1}^{N-(k+1)} X_i X_{k+i+1} \cdot \sin\frac{\omega_d(\tau-kT)}{2} e^{j\frac{\omega_d(2i+k)T}{2}} e^{j\frac{\omega_d\tau}{2}}\right| . \qquad \text{2-28}$$

The term $e^{j\frac{\omega_d\tau}{2}}$ can be factored from equation 2-28. Note that

$$\left|e^{j\frac{\omega_d\tau}{2}}\right| = 1 .$$

If the magnitude of equation 2-28 is taken, then the equation in its final form is

$$\Psi(\tau,\omega_d) = \alpha^2\Big\langle\Bigg\{\frac{[(k+1)T-\tau]}{2}\,\frac{\sin\frac{\omega_d[(k+1)T-\tau]}{2}}{\frac{\omega_d[(k+1)T-\tau]}{2}}\sum_{i=1}^{N-k} X_i X_{k+i} \cdot$$

$$\cos\frac{\omega_d(2i+k)T}{2} + \frac{(\tau-kT)}{2}\,\frac{\sin\frac{\omega_d(\tau-kT)}{2}}{\frac{\omega_d(\tau-kT)}{2}} \cdot$$

$$\sum_{i=1}^{N-(k+1)} X_i X_{k+i+1} \cos\frac{\omega_d(2i+k)T}{2}\Bigg\}^2 + \Bigg\{\frac{[(k+1)T-\tau]}{2} \cdot$$

$$\frac{\sin\frac{\omega_d[(k+1)T-\tau]}{2}}{\frac{\omega_d[(k+1)T-\tau]}{2}}\sum_{i=1}^{N-k} X_i X_{k+i} \sin\frac{\omega_d(2i+k-1)T}{2}$$

$$+ \frac{(\tau-kT)}{2} \frac{\sin\frac{\omega_d(\tau-kT)}{2}}{\frac{\omega_d(\tau-kT)}{2}} \sum_{i=1}^{N-(k+1)} X_i X_{k+i+1} \circ$$

$$\left.\left.\sin\frac{\omega_d(2i+k)T}{2}\right\}^2\right\rangle^{1/2}. \qquad 2\text{-}29$$

In the earlier portions of this chapter, the statement was made that the output of the matched filter is identical to the ambiguity function. We are now prepared to discuss this particular point. In comparing equation 2-24 (the output of the collator) with equation 2-29 (the ambiguity function), we note that the ambiguity function is identical to the envelope of the output of the collator. Hence the difference between the ambiguity function and the output of the matched filter is that there exists an RF fine structure of frequency f_{oi}, in the output of the matched filter which is absent in the ambiguity function. Note that if the phase of the RF fine structure is some odd multiple of $\frac{\pi}{2}$, then the output of the matched filter will be zero. Thus, we can say qualitatively that the ambiguity function measures the positive maximums of the output of the matched filter per cycle of the RF fine structure. To circumvent the problem of outputs of the matched filter being zero near the central peak, we sum and take the envelope of the output of the matched filters. However, care must be taken in choosing the differential range deviations. Suppose that the differential range deviation, $\Delta\tau$, is some multiple of the inverse of twice the frequency of the RF fine structure, i.e.,

$$\Delta\tau = \frac{m}{2(f_o + f_d)} \quad ; \quad m = 1, 2, \cdots \quad .$$

Furthermore, suppose that in any matched filter, the phase difference between the transmitted signal and the received signal is an odd multiple of $\frac{\pi}{2}$ radians. Then the output from all the matched filters will be zero. This point is easy to see because the system will be tracking the zero crossings of the RF fine structure.

The RF fine structure is also troublesome in the area of multiplexing. This point will be discussed in Chapter IV, when we will formulate ideas on the type of multiplexing to be used in the complementary coded system.

The output of the "envelope detector" is given by the envelope of equation 2-24. However, as mentioned earlier, the output of the "envelope detector" is identical to the ambiguity function.

CHAPTER III

DEFINITION OF THE AMBIGUITY FUNCTION FOR COMPLEMENTARY CODES

In this short chapter, we shall extend Siebert's Ambiguity function to the ambiguity function for complementary codes. Let us analyze the signal processing techniques required to produce the desired results in the complementary coded system. In Chapter II, it was shown that in the single code system, the output of the "envelope detector" in Figure 2-2b was identical to the ambiguity function. What then, should be the configuration of the complementary coded system? Should the complementary coded system be, in essence, two single coded systems such that the outputs of the two "envelope detectors" be summed together? Or should the two codes be summed elsewhere?

Let us postulate the complementary coded system to be comprised of two identical single code systems with the outputs of the "envelope dectors" of code A and B summed together. In this case the ambiguity function of the complementary coded system will be the sum of the ambiguity functions of code A and B, i.e.,

$$\Psi_c(\tau,\omega_d) = \Psi_A(\tau,\omega_d) + \Psi_B(\tau,\omega_d)\,. \qquad 3\text{-}1$$

One of the properties of the ambiguity function is that

$$\Psi(\tau,\omega_d)\Big|_{\omega_d=0} = \alpha\left|R(\tau)\right|\,.$$

Hence equation 3-1 for $\omega_d = 0$ becomes

$$\Psi_c(\tau,\omega_d)\Big|_{\omega_d=0} = \alpha|R_A(\tau)| + \alpha|R_B(\tau)| . \qquad 3\text{-}2$$

As indicated in the introduction of this thesis, the desired property of the complementary codes was that off the central peak, the autocorrelation function of code A, $R_A(\tau)$, was the negative of the autocorrelation function of code B, $R_B(\tau)$, so that when the autocorrelation functions were summed, the range sidelobes canceled. Since the proposed definition (equation 3-1) of the ambiguity function contains two positive quantities $|R_A(\tau)|$, and $|R_B(\tau)|$, the definition is inadequate.

As a second approach to the problem, let us define the ambiguity function of the complementary coded system as

$$\Psi_c(\tau,\omega_d) = \frac{1}{2}\left|\int_{-\infty}^{\infty} I_A(t)\, I_A(t-\tau)\, e^{j\omega_d t}\, dt + \int_{-\infty}^{\infty} I_B(t)\, I_B(t-\tau)\, e^{j\omega_d t}\, dt\right| , \qquad 3\text{-}3$$

where $I_A(t)$ = envelope of code A

$I_B(t)$ = envelope of code B.

For zero doppler frequency, equation 3-3 becomes .

$$\Psi_c(\tau,0) = \alpha_c|R_A(\tau) + R_B(\tau)| . \qquad 3\text{-}4$$

It is easy to see that the range sidelobes of code A will cancel the range sidelobes of code B so that the range sidelobes for the complementary coded ambiguity function will be nonexistent for zero doppler frequency. Equation 3-3 will be chosen as the definition of the ambiguity function for the complementary codes.

Equation 3-3 gives us the clue as to the configuration of the complementary coded system. We can infer that the two codes should be summed at the output of the matched filters, then envelope detected.

CHAPTER IV

MATCHED FILTER APPROACH FOR THE COMPLEMENTARY CODED SYSTEM (NARROW-BAND ANALYSIS)

A. BACKGROUND

In the complementary coded system, some form of multiplexing is required since two codes will be utilized to obtain the desired cancellation of the range sidelobes. Of the three obvious types of multiplexing (time division, frequency division, and quaternary coding) only time division, TDM, and frequency division multiplexing, FDM, will be discussed.

B. PROPOSED FDM SYSTEM

Assume for the moment that the FDM system is modelled as below.

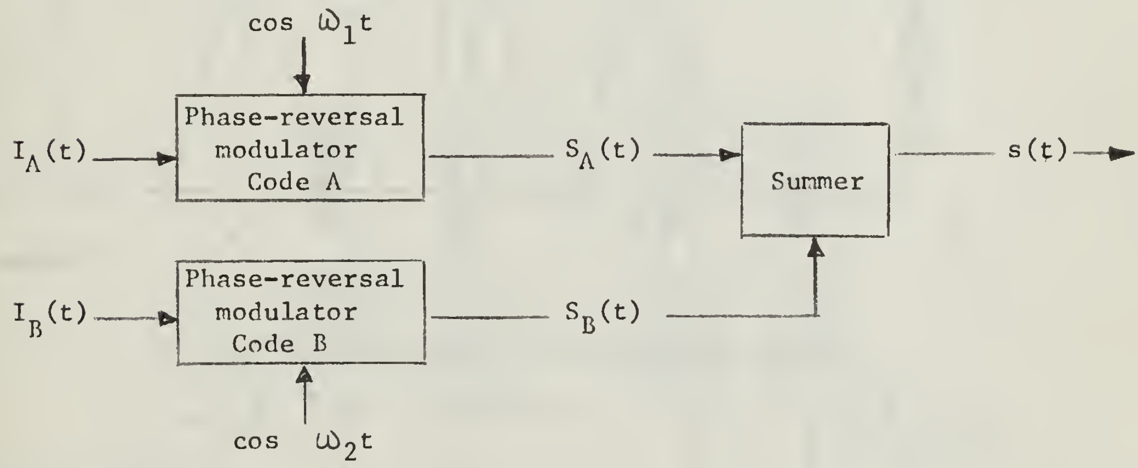

Complementary coded FDM transmitter block diagram

Figure 4-1

It might be well to observe the transmitted spectrum to aid in the understanding of the signal processing schemes that will be required in the receiver. The frequencies, f_1 and f_2, are at RF. The outputs of each of the phase-reversal modulators can be easily obtained from equation 2-2

if appropriate subscripts are used. Hence

$$s_A(t) = \alpha_c \sum_{i=1}^{N} XA_i \{ \Pi(t-iT) - \Pi[t-(i+1)T] \cos \omega_1 t \ , \qquad 4\text{-}1$$

$$s_B(t) = \alpha_c \sum_{i=1}^{N} XB_i \{ \Pi(t-iT) - \Pi[t-(i+1)T] \cos \omega_2 t \ . \qquad 4\text{-}2$$

It is easy to see that the spectrum of the spectrum of the transmitted signal consists of two $\left|\frac{\sin x}{x}\right|$ functions centered at f_1 and f_2.

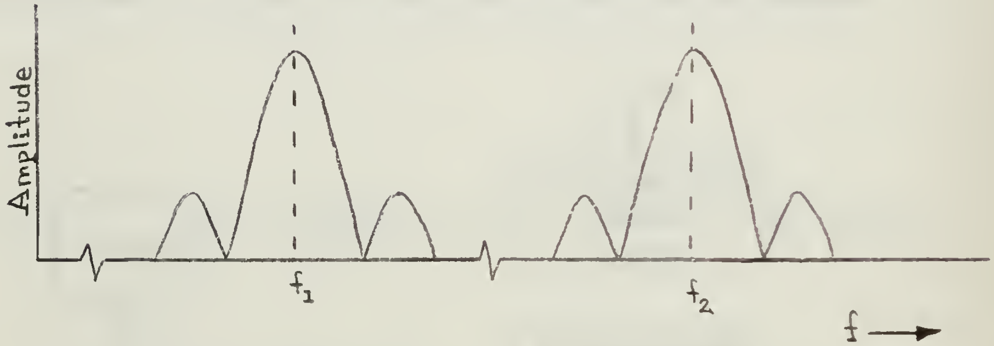

One-sided spectrum of the transmitted signal

Figure 4-2

Thus to detect each code, the system requires bandpass filters centered at the carrier frequency plus the doppler frequency. Hence the system block diagram is given by Figures 4-3a and 4-3b. Since the output of each range bank can be treated the same as in the single code system, equation 2-15 applies with the substitution of appropriate subscripts. Let γ be the envelope quantity in equation 2-15; hence the output from any range bank in Figure 4-3b for code A is given by

Figure 4-3a

FDM receiver block diagram

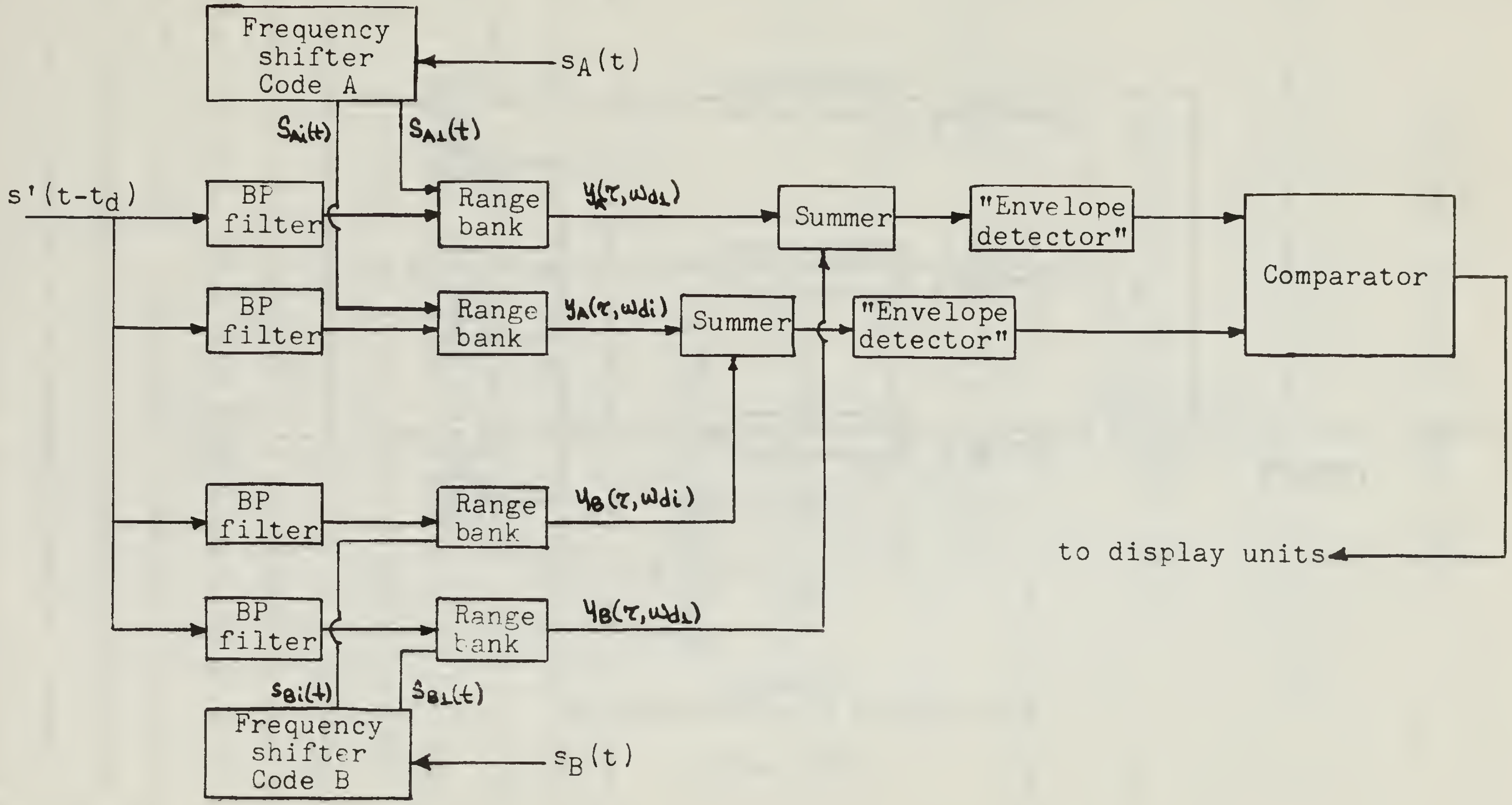

Figure 4-3b

ith range bank in Figure 4-3a
(Code A)

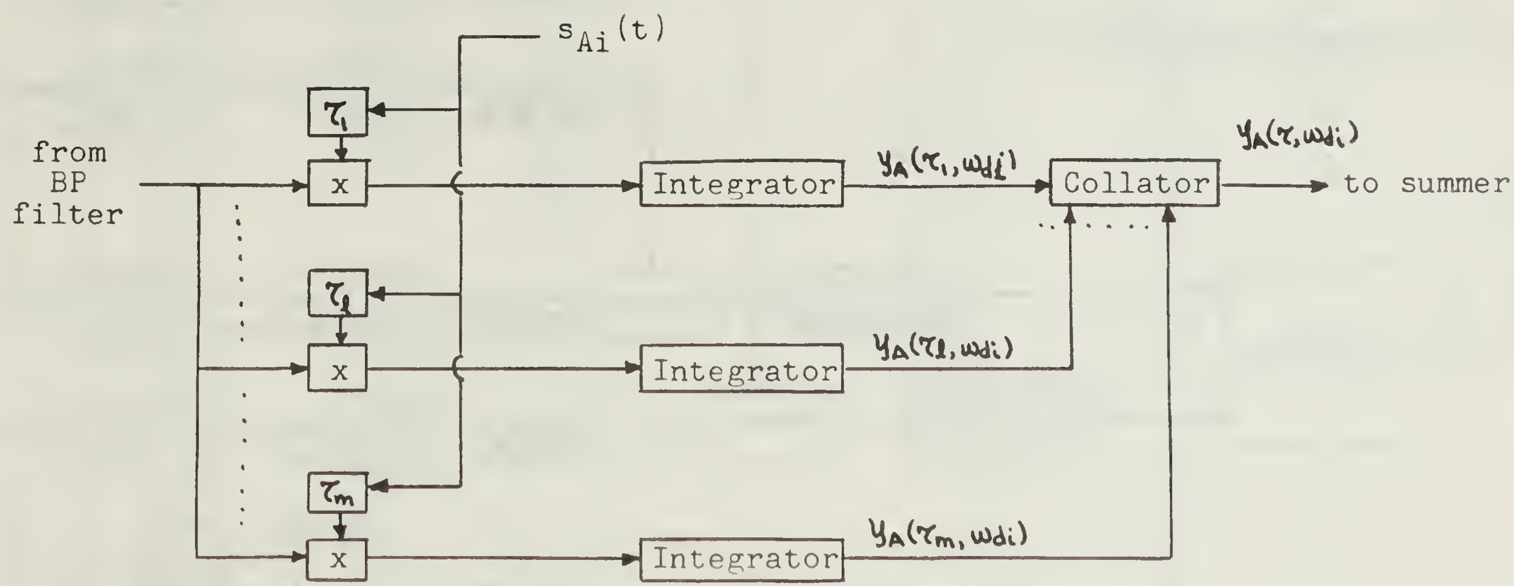

$$y_A(\tau, \omega_d) = \gamma_A \cos\left[\left(\omega_1 + \frac{\omega_d}{2}\right)\tau - \phi_A\right] . \qquad \text{4-3a}$$

The output from the corresponding range bank for code B is

$$y_B(\tau, \omega_d) = \gamma_B \cos\left[\left(\omega_2 + \frac{\omega_d}{2}\right)\tau - \phi_B\right] . \qquad \text{4-3b}$$

The output from the summer in Figure 4-3a is the sum of the outputs from the range banks of code A and B. Therefore

$$\begin{aligned} y(\tau, \omega_d) &= y_A(\tau, \omega_d) + y_B(\tau, \omega_d) \\ &= \gamma_A \cos\left[\left(\omega_1 + \frac{\omega_d}{2}\right)\tau - \phi_A\right] \\ &\quad + \gamma_B \cos\left[\left(\omega_2 + \frac{\omega_d}{2}\right)\tau - \phi_B\right] . \qquad \text{4-4} \end{aligned}$$

The effect of the different frequencies of the RF fine structure for code A and B is to lower the output from the matched filter at the central peak and to increase the range sidelobes. It is true that, if the carrier frequencies of both codes are nearly equal, the range sidelobes will be very small; and in fact, might be quite tolerable. However, bear in mind that the characteristic of interest in a complementary coded system is for range sidelobes to be nonexistent for zero doppler.

In this system the factor which is troublesome is the RF fine structure which is absent in the ambiguity function. Hence the analysis provides a further contradiction to the statement that the output of the matched filter is identical to the ambiguity function. Indeed, it is that factor which is different between the output of the matched filter and the ambiguity function which defeats this method of multiplexing.

C. TDM SYSTEM

Another multiplexing method is TDM. The suceeding portions of this thesis will dwell entirely on phase-reversal TDM systems for complementary codes. The results from Chapter II concerning single code systems can be easily extended to the complementary coded systems. In the transmitter the essential difference is the time multiplexing circuitry; hence the transmitter can be modelled as below.

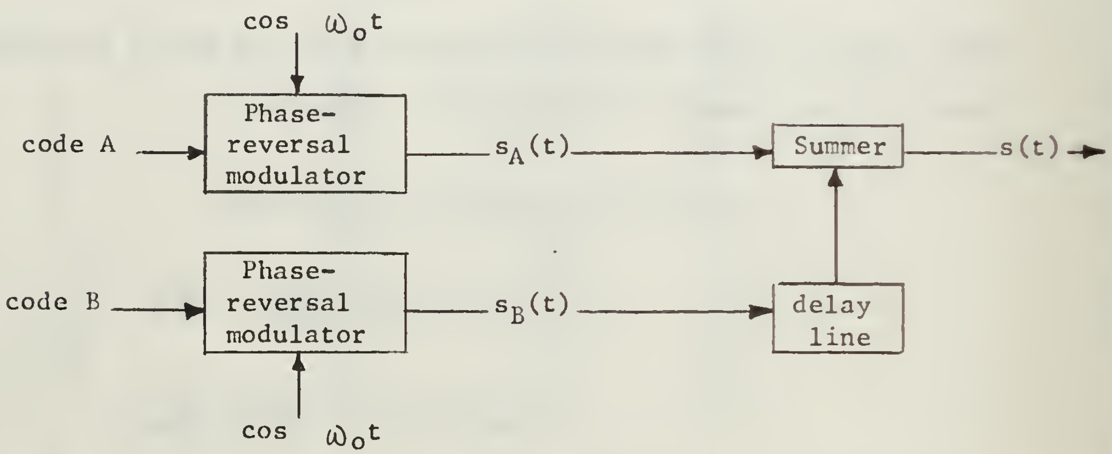

TDM transmitter block diagram

Figure 4-4

As in Chapter II the transmitted energy will be normalized to unity by specifying that

$$\int_{-\infty}^{\infty} s^2(t)\,dt = 1 \quad . \tag{4-5}$$

To obtain the normalization constant, we note that

$$s(t) = \begin{cases} s_A(t) , & \text{for} \quad 0 < t < NT \\ s_B(t) , & \quad NT < t < 2NT \ . \end{cases}$$

$s_A(t)$ and $s_B(t)$ are given by

$$s_A(t) = \alpha_c \sum_{i=0}^{N} XA_i \left\{ 1\!\!1(t-iT) - 1\!\!1[t-(i+1)T] \right\} \cos \omega_0 t \quad , \qquad \text{4-6a}$$

$$s_B(t) = \alpha_c \sum_{i=0}^{N} XB_i \left\{ 1\!\!1(t-iT) - 1\!\!1[t-(i+1)T] \right\} \cos \omega_0 t \quad , \qquad \text{4-6b}$$

where $XA_i = \pm 1$, depending on the value of the ith code symbol of A

$XB_i = \pm 1$, depending on the value of the ith code symbol of B.

Then

$$\int_{-\infty}^{\infty} s^2(t)\,dt = \int_{-\infty}^{\infty} s_A^2(t)\,dt + \int_{-\infty}^{\infty} s_B^2(t)\,dt$$

$$\int_{-\infty}^{\infty} s_A^2(t)\,dt = \alpha_c^2 \frac{NT}{2} + \alpha_c^2 \frac{\sin 2\omega_0 NT}{4\omega_0} \cong \alpha_c^2 \frac{NT}{2}$$

$$\int_{-\infty}^{\infty} s_B^2(t)\,dt = \alpha_c^2 \frac{NT}{2} + \alpha_c^2 \frac{\sin 2\omega_0 NT}{2\omega_0} \cong \alpha_c^2 \frac{NT}{2} \, .$$

Therefore the normalization constant, α_c, is approximately

$$\alpha_c \cong \sqrt{\frac{1}{NT}} \, . \qquad \text{4-7}$$

In the transmitter, code B is delayed and summed with code A. The receiver is modelled in Figure 4-5. To detect the signal the gating circuit in the receiver separates the two codes. The output from each

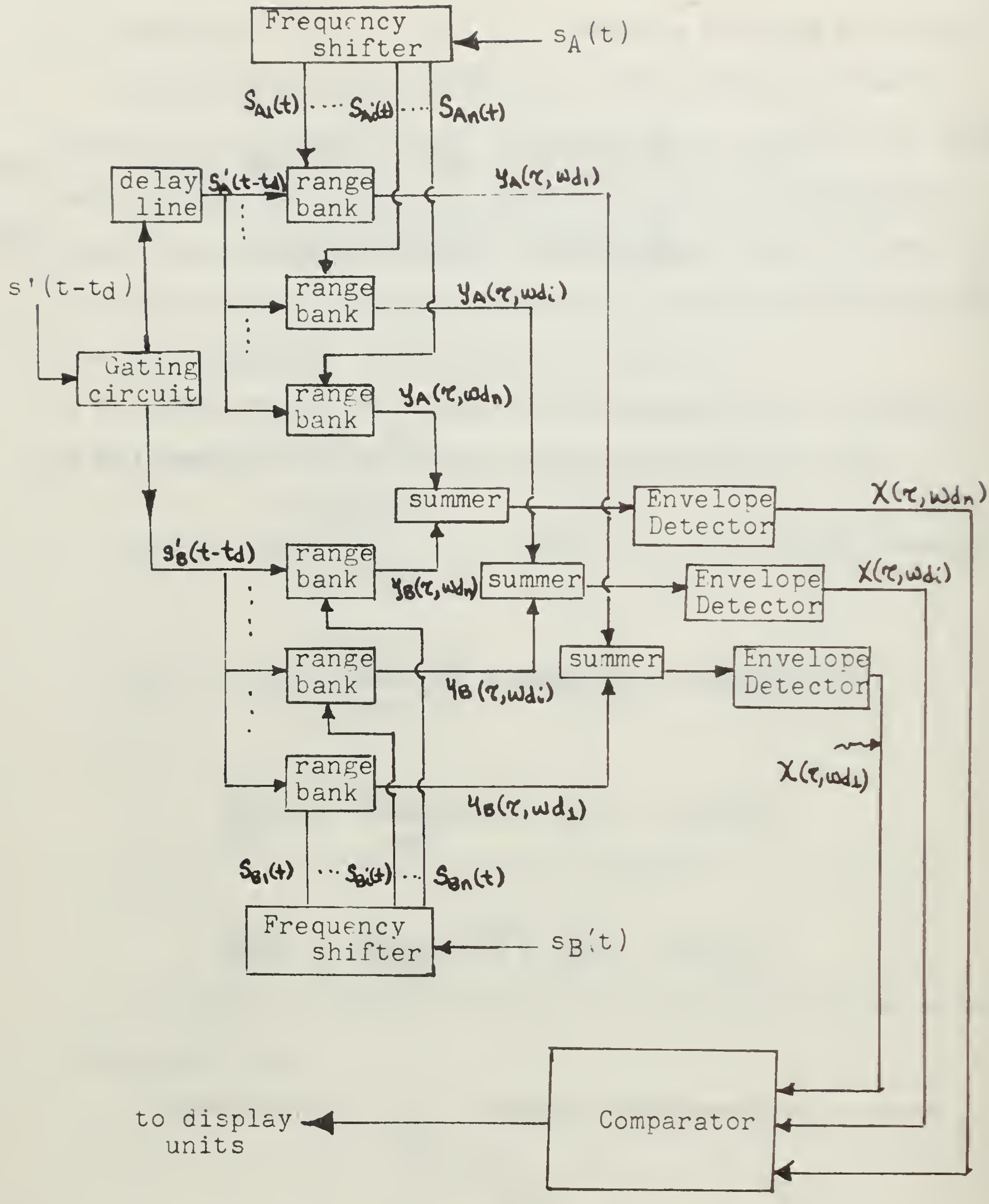

TDM receiver block diagram

Figure 4-5

correlator in Figure 4-5 is identical to the output from a correlator in the single code system. Hence the output from the "envelope detector" is given by

$$\chi(\tau, \omega_d) = \text{Envelope of } \left\{ y_A(\tau, \omega_d) + y_B(\tau, \omega_d) \right\}. \qquad 4\text{-}8$$

Upon examination of equation 2-15, we find that the only terms which depend upon the value of the codes are the X_i's. The rest of the terms are common to both $y_A(\tau, \omega_d)$ and $y_B(\tau, \omega_d)$. Hence if the signed products in equation 2-15 are replaced by signed products for code A and B, i.e.,

$$X_i X_j \text{ is replaced by } (XA_i XA_j + XB_i XB_j)$$

and if the envelope of equation 2-15 is taken, then the output of the "envelope detector" will be given by

$$\chi(\tau, \omega_d) = \alpha_c^2 \Bigg\langle \Bigg\{ \frac{[(k+1)T-\tau]}{2} \frac{\sin \frac{\omega_d[(k+1)T-\tau]}{2}}{\frac{\omega_d[(k+1)T-\tau]}{2}} \sum_{i=1}^{N-k} [XA_i XA_{k+i}$$

$$+ XB_i XB_{k+i}] \cos \frac{\omega_d(2i+k-1)T}{2} + \frac{(\tau - kT)}{2} \frac{\sin \frac{\omega_d(\tau-kT)}{2}}{\frac{\omega_d(\tau-kT)}{2}} \cdot$$

$$\sum_{i=1}^{N-(k+1)} [XA_i XA_{k+i+1} + XB_i XB_{k+i+1}] \cos \frac{\omega_d(2i+k)T}{2} \Bigg\}^2$$

$$+ \Bigg\{ \frac{[(k+1)T-\tau]}{2} \frac{\sin \frac{\omega_d[(k+1)T-\tau]}{2}}{\frac{\omega_d[(k+1)T-\tau]}{2}} \sum_{i=1}^{N-k} [XA_i XA_{k+i}$$

$$+ XB_i XB_{k+i}\Big] \sin \frac{\omega_d(2i+k-1)T}{2} + \frac{(\tau-kT)}{2} \,.$$

$$\frac{\sin \frac{\omega_d(\tau-kT)}{2}}{\frac{\omega_d(\tau-kT)}{2}} \sum_{i=1}^{N-(k+1)} \left[XA_i XA_{k+i+1} + XB_i XB_{k+i+1}\right] \,.$$

$$\left.\left. \sin \frac{\omega_d(2i+k)T}{2}\right\}^2 \right\rangle^{1/2} . \qquad \text{4-9}$$

As stated in Chapter II the output from the "envelope detector" is identical to the ambiguity function. Therefore the ambiguity function for the complementary codes will be given by equation 4-9.

Let us now analyze the narrow-band ambiguity function for complementary codes. For zero doppler equation 4-9 reduces to

$$\Psi_c(\tau,0) = \alpha_c^2 \left| \left\{ \frac{[(k+1)T-\tau]}{2} \sum_{i=1}^{N-k} [XA_i XA_{k+i} + XB_i XB_{k+i}] \right.\right.$$

$$\left.\left. + \frac{(\tau-kT)}{2} \sum_{i=1}^{N-(k+1)} [XA_i XA_{k+i+1} + XB_i XB_{k+i+1}] \right\} \right| , \qquad \text{4-10}$$

$$\equiv \alpha_c^2 \left| R_A(\tau) + R_B(\tau) \right| .$$

Thus we see that from the analysis done in the introduction, the ambiguity function for zero doppler contains no range sidelobes. We note that this property is a direct result of the RF phase synchronization assumed in equations 4-6a, b.

For the case of zero range delay, the ambiguity function reduces to

$$\Psi_c(0,\omega_d) = \alpha_c^2 \left\langle \left\{ \frac{T}{2} \frac{\sin\frac{\omega_d T}{2}}{\frac{\omega_d T}{2}} \sum_{i=1}^{N} [XA_i XA_i + XB_i XB_i] \cdot \cos\frac{\omega_d(2i-1)T}{2} \right\}^2 + \left\{ \frac{T}{2} \frac{\sin\frac{\omega_d T}{2}}{\frac{\omega_d T}{2}} \sum_{i=1}^{N} [XA_i XA_i + XB_i XB_i] \sin\frac{\omega_d(2i-1)T}{2} \right\}^2 \right\rangle^{1/2}. \quad \text{4-11}$$

Note that

$$X_i X_i = 1 .$$

Then if the sine terms are factored, equation 4-11 reduces to

$$\Psi_c(0,\omega_d) = \alpha_c^2 \left| T \frac{\sin\frac{\omega_d T}{2}}{\frac{\omega_d T}{2}} \right| \left\{ \left[\sum_{i=1}^{N} \cos\frac{\omega_d(2i-1)T}{2} \right]^2 + \left[\sum_{i=1}^{N} \sin\frac{\omega_d(2i-1)T}{2} \right]^2 \right\}. \quad \text{4-12}$$

If the Euler identity is utilized

$$e^{j\theta} = \cos\theta + j\sin\theta ,$$

and noting that

$$\left|\sum e^{j\theta}\right| = \left|\sum\cos\theta + j\sum\sin\theta\right| = \left\{(\sum\cos\theta)^2 + (\sum\sin\theta)^2\right\}^{1/2},$$

then, we see that

$$\left|\sum_{i=1}^{N} e^{j\frac{\omega_d(2i-1)T}{2}}\right| = \left|e^{-j\frac{\omega_d T}{2}} \sum_{i=1}^{N} e^{j\omega_d i T}\right| = \left|\sum_{i=1}^{N} e^{j\omega_d i T}\right|$$

$$= \left|\sum_{i=1}^{N} \cos\omega_d i T + j\sum_{i=1}^{N} \sin\omega_d i T\right| .$$

Thus equation 4-12 can be written as

$$\Psi_c(0,\omega_d) = \alpha_c^2 \left| \frac{T}{\frac{\omega_d T}{2}} \sin \frac{\omega_d T}{2} \right| \left| \left\{ \sum_{i=1}^{N} \cos \omega_d i T + j \sum_{i=1}^{N} \sin \omega_d i T \right\} \right| . \qquad 4\text{-}13$$

If the following trigonometric formulas[10] are utilized

$$\sum_{i=1}^{N} \cos i\theta = \cos \frac{(N+1)\theta}{2} \operatorname{cosec} \frac{\theta}{2}$$

$$\sum_{i=1}^{N} \sin i\theta = \sin \frac{(N+1)\theta}{2} \operatorname{cosec} \frac{\theta}{2} ,$$

and

$$\sum_{i=1}^{N} \cos i\theta + j \sum_{i=1}^{N} \sin i\theta = \sin \frac{N\theta}{2} \operatorname{cosec} \frac{\theta}{2} \cdot \left[\cos \frac{(N+1)\theta}{2} + j \sin \frac{(N+1)\theta}{2} \right] ;$$

thus equation 4-13 becomes

$$\Psi_c(0,\omega_d) = \alpha_c^2 \left| T \frac{\sin \frac{\omega_d T}{2}}{\frac{\omega_d T}{2}} \right| \left| \left[\sin \frac{N\omega_d T}{2} \cos \frac{\omega_d T}{2} \, e^{j \frac{(N+1)\omega_d T}{2}} \right| . \qquad 4\text{-}14$$

Then noting that the absolute value of a product is the product of their absolute values, and

$$\left| e^{j\theta} \right| = 1 .$$

Finally we see that equation 4-14 becomes

$$\Psi_c(0,\omega_d) = \alpha_c^2 \left| NT \frac{\sin \frac{N\omega_d T}{2}}{\frac{N\omega_d T}{2}} \right| . \qquad 4\text{-}15$$

If equation 4-15 is plotted, one interesting result is observed.

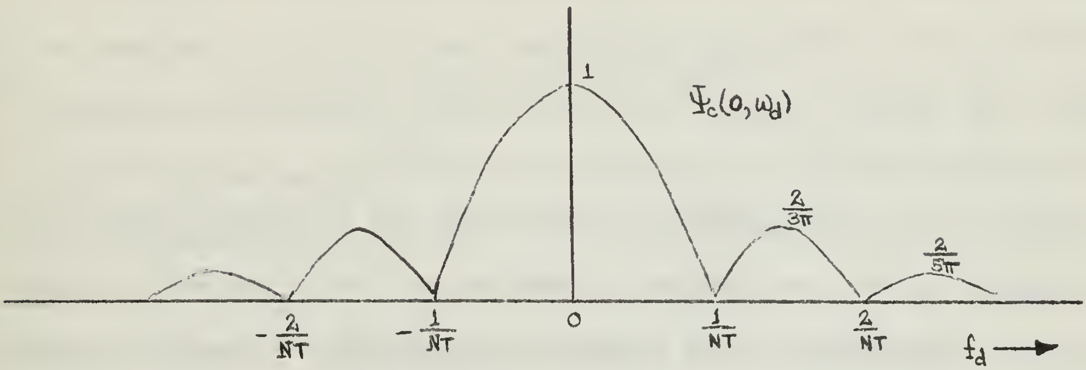

Ambiguity function for complementary codes;

in the doppler domain.

Figure 4-6

The first zero crossing of the ambiguity function occurs at $\frac{1}{NT}$; succeeding zero crossings occur at multiples of $\frac{1}{NT}$. Hence the coded pulse sequence is acting like a single pulse of length NT in the doppler domain. For a better insight into this phenomena, let us review the origin of the $\sin \frac{N\omega_d T}{2}$ term. A glance at equation 4-12a shows us that the term originated as a sum of exponentials, i.e.,

$$\left| \sum_{i=1}^{N} e^{j\frac{\omega_d(2i-1)T}{2}} \right| = \left| \sum_{i=1}^{N} e^{j\omega_d iT} \right| . \qquad 4\text{-}16$$

The criterion for the ambiguity function to be zero in the doppler domain is

$$\sin \frac{N\omega_d T}{2} = 0 \implies \frac{N\omega_d T}{2} = n\pi \; ; \; n = 1, 2, \ldots\ldots . \qquad 4\text{-}17a$$

Or alternatively,

$$N\omega_d T = n 2\pi \; ; \quad n = 1, 2, \cdots \; . \qquad \text{4-17b}$$

Hence we see from equation 4-16 that when the total phase shift is a multiple of 2π, the ambiguity function for zero range delay will be zero. This effect can be viewed as the addition of phasors such that when the function is zero, the phasors have added to form a closed loop. This, of course, occurs when the total phase shift is some multiple of 2π.

One added comment should be made concerning the zero crossings of the ambiguity function in the doppler domain. Since the zero crossings occur at $\frac{1}{NT}$, then, as the length of the code increases, the ambiguity function will be compressed closer to the origin; hence approaching the ideal. However, the length of the code cannot be increased indefinitely without complications. It will be shown in Chapter VI that longer codes will be more sensitive to changes caused by the doppler effect, and unfortunately the length of the code cannot be increased indefinitely without reducing the output from the matched filter. The above compression effect on the ambiguity function is not a property possessed solely by the complementary codes. For example, single phase-reversal codes have ambiguity functions which experience the compression effect for long codes. It is the length of these codes, rather than their internal structure, which produces compression in the doppler domain; assuming that the duration of a code symbol, T, is held constant.

D. SUMMARY OF RESULTS

Equation 4-9 was coded into Fortran and programs were run for the two kernels* of length 10 and the kernel of length 26. Plots of the ambiguity function were made for constant "doppler phase," Φ_d , where this is defined as the recurrent argument in our equations for the ambiguity function, i.e.,

$$\Phi_d = \frac{\omega_d T}{2} = f_d T \pi , \qquad 4\text{-}18$$

where T = duration of a code symbol.

To convert doppler phase into radial velocity, we recall that for the narrow-band case

$$f_d \cong \frac{2v_r}{c} f_o .$$

Therefore,

$$v_r = \frac{c}{2} \frac{f_d}{f_o} = \frac{c}{2} \frac{\Phi_d}{f_o T \pi} . \qquad 4\text{-}19$$

Table 1 gives the conversion from doppler phase to radial velocity for various values of carrier frequency and duration of a code symbol. Doppler phase, Φ_d , was defined in equation 4-18, so that the ambiguity function need not be recomputed for different values of f_o and T.

---

*As stated in the introduction, a kernel is a basic length code which cannot be decomposed into shorter length codes by an inversion of the standard generating methods. Conversely, complementary codes of longer lengths can be generated by appropriately combining the kernels.

Figure 4-7 is the ambiguity diagram for the kernel, A_2 and B_2, code length 10. (The code values for the kernels are listed at the end of Appendix F.) The ambiguity diagram is the term used to describe the three dimensional figure generated from the ambiguity function. The bandwidth* of the ambiguity function in Figure 4-7 is approximately 0.1π. For the system postulated in Figure 2-2, this bandwidth corresponds to a velocity discrimination of 3000 knots, for $T = 1\,\mu$sec, $f_o = 10$ GHz. For $f_o = 1$ GHz and $T = 0.1\,\mu$sec., velocity discrimination is roughly 300,000 knots. Hence complementary codes of this length cannot be used for situations requiring good velocity discrimination.

Figure 4-8 is the ambiguity diagram for the kernel, A_2 and B_2, code length 10, and with Φ_d in increments of 0.125π.

Figure 4-9 is the ambiguity diagram for the kernel, A_1 and B_1, code length 10. Note that the range sidelobes extend out to seven units, whereas the range sidelobes in Figure 4-8 extend to 10 units. However, the amplitudes of the sidelobes for the kernel, A_1 and B_1 are slightly larger than for sequences A_2 and B_2.

Figure 4-10 is the ambiguity diagram for the kernel, A and B, length 26. The range sidelobes extend to 14 units. The maximum amplitude of the range sidelobes is 0.32. The ambiguity diagrams in Figure 4-9 and 4-10 are in the same increments of Φ_d. Note that the bandwidth of the ambiguity function for the kernel, A and B, length 26, is less than the bandwidth of the ambiguity function for the kernel, A_1 and B_1 length 10. This effect is the compression phenomena for longer codes which is discussed in Chapter IV.

---

*The bandwidth of the ambiguity function is here defined as doppler phase (converted to frequency) at the first zero crossing of the ambiguity function for $\tau = 0$.

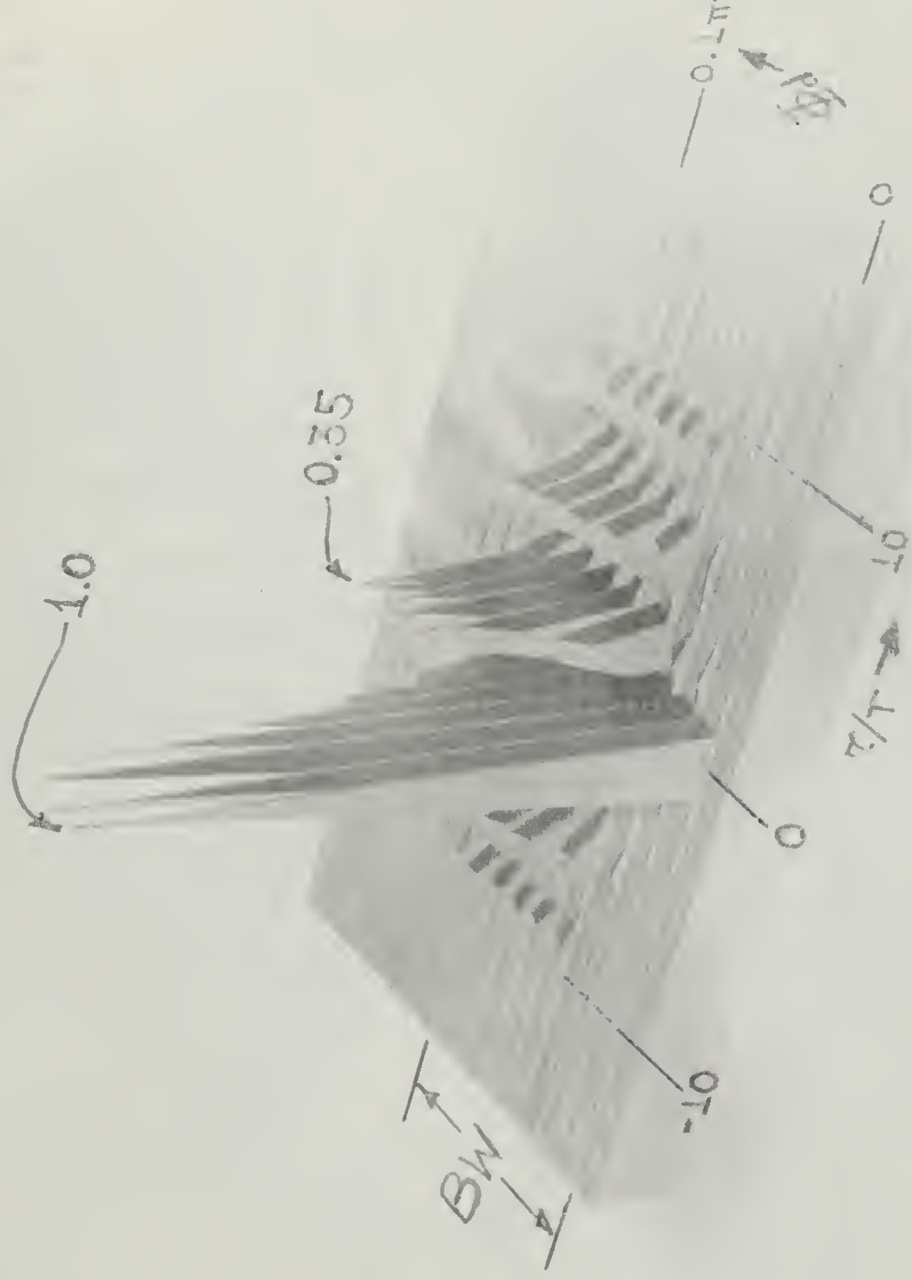
1.0
0.35
0
10
-10
BW

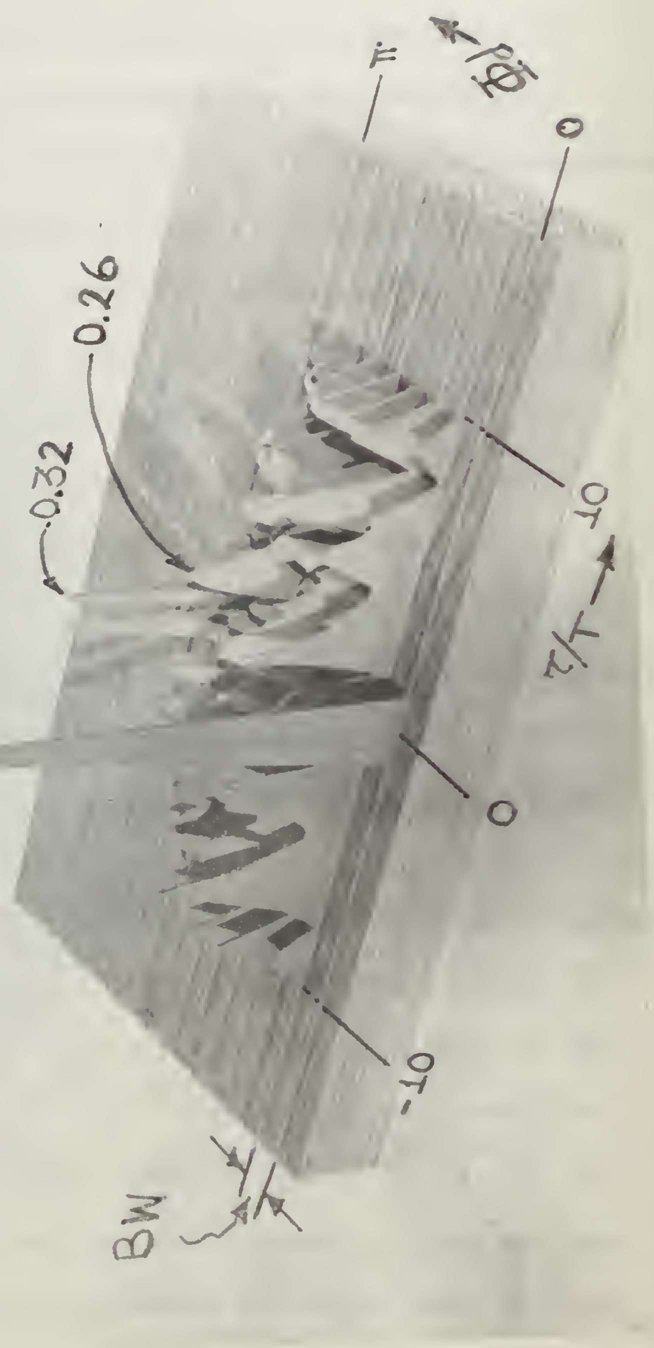
1.0
0.32
0.26
π
Φ
0
10
T/2
0
-10
BW

Figure 4-[illegible]

Ambiguity diagram for the kernel, a_1, b_1;
Length [illegible]; $0 \leq \Phi_d \leq 0.3\pi$; Φ_d in [illegible]π increments

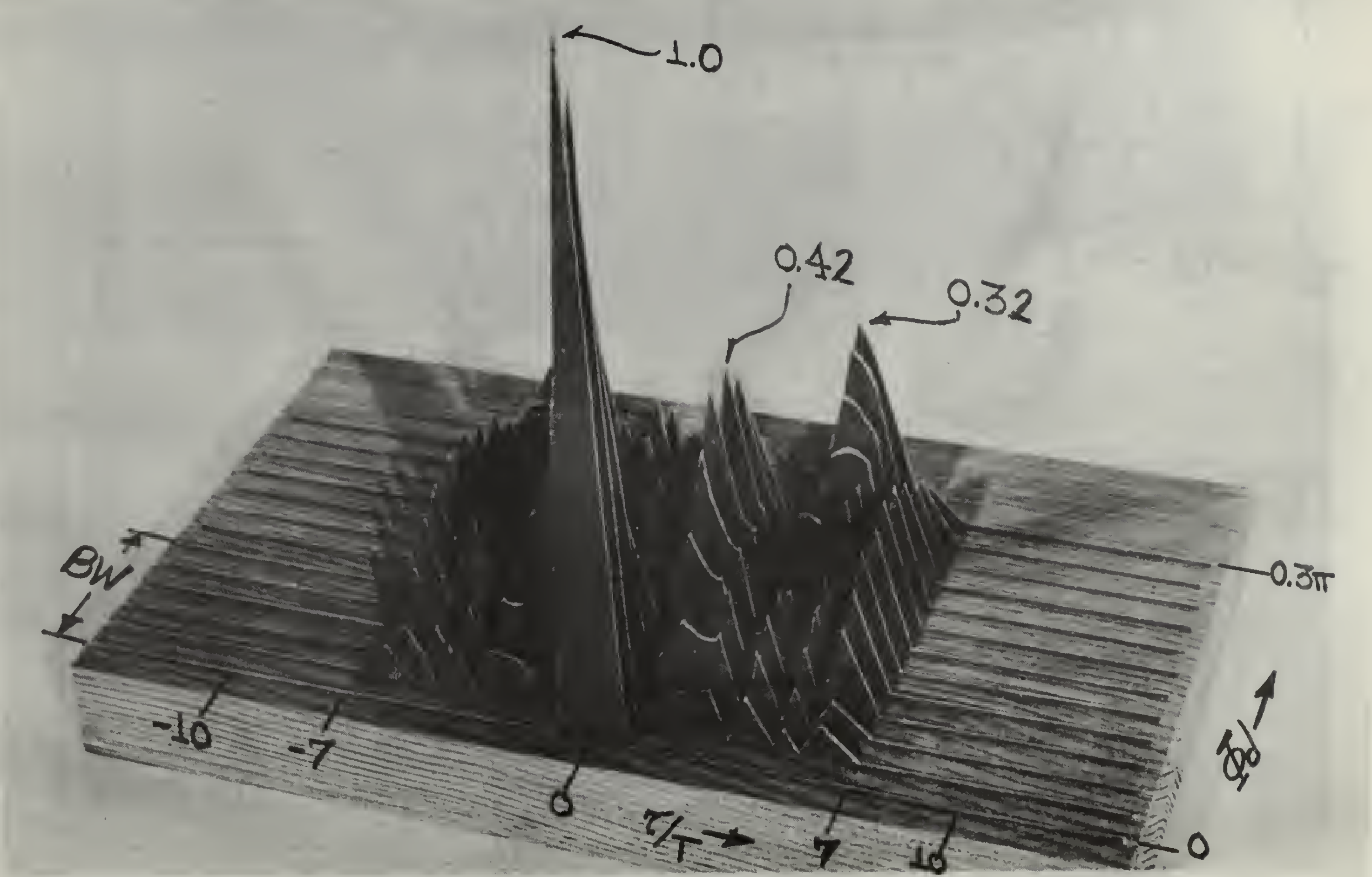

[illegible]

[illegible] for the [illegible]
[illegible] $\le \bar{\Phi}_d \le$ [illegible] ; $\bar{\Phi}_d$ [illegible] π [illegible]

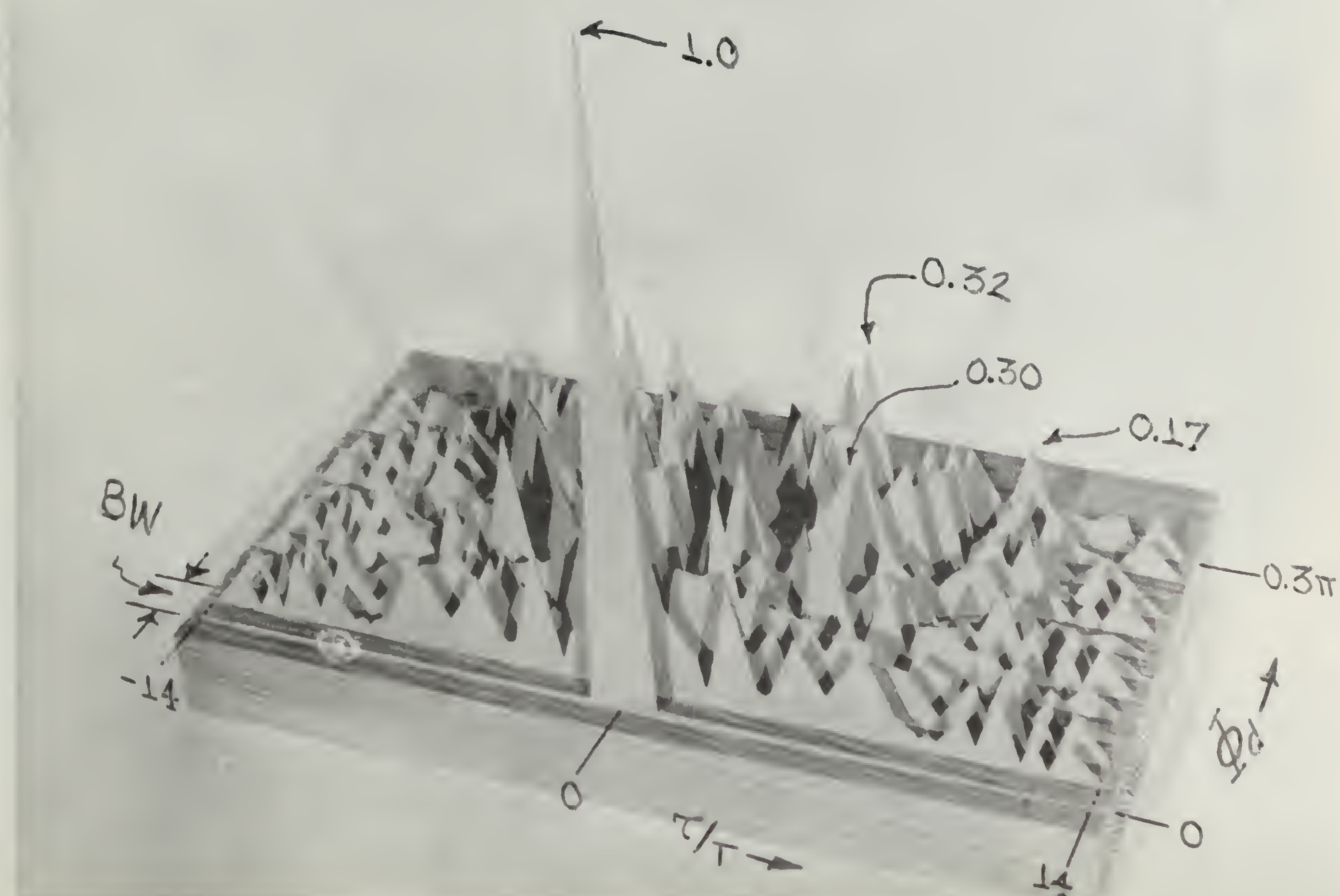

TABLE 1

CONVERSION FROM DOPPLER PHASE, Φ_d , TO TARGET'S RADIAL COMPONENT OF VELOCITY, v_r.

Note: c = velocity of propagation of the wave in the medium (5.91×10^8 knots)

f_o = carrier frequency

T = duration of a code symbol

f_d = doppler frequency

$\Phi_d = \pi f_d T = 2 v_r f_o T \pi / C$

v_r (knots)	f_o (GHz)	T (μ sec.)	Φ_d (π rad)
60	1	1	2.00×10^{-4}
100	↓	↓	3.38×10^{-4}
600			2.00×10^{-3}
1000			3.38×10^{-3}
1600			5.40×10^{-3}
2000			6.75×10^{-3}
3000			1.00×10^{-2}
4000			1.35×10^{-2}
5000			1.69×10^{-2}
6000			2.00×10^{-2}
60000			0.2
60	1	0.1	2.00×10^{-5}
100	↓	↓	3.38×10^{-5}
600			2.00×10^{-4}
1000			3.38×10^{-4}
1600			5.40×10^{-4}
2000			6.75×10^{-4}
3000			1.00×10^{-3}
4000			1.35×10^{-3}
5000			1.69×10^{-3}
6000			2.00×10^{-3}
60000			2.00×10^{-2}

TABLE 1
(cont'd)

v_r (knots)	f_o (GHz)	T (μsec.)	$\bar{\Phi}_d$ (π rad)
60	10	1	2.00×10^{-3}
100	↓	↓	3.38×10^{-3}
600			2.00×10^{-2}
1000			3.38×10^{-2}
1600			5.40×10^{-2}
2000			6.75×10^{-2}
3000			0.1
4000			0.135
5000			0.169
6000			0.2
60000			2.0
60	10	0.1	2.00×10^{-4}
100	↓	↓	3.38×10^{-4}
600			2.00×10^{-3}
1000			3.38×10^{-3}
1600			5.40×10^{-3}
2000			6.75×10^{-3}
3000			1.00×10^{-2}
4000			1.35×10^{-2}
5000			1.69×10^{-2}
6000			2.00×10^{-2}
60000			0.2

CHAPTER V

INVESTIGATION OF THE DOPPLER EFFECT ON THE TRANSMITTED SIGNAL (WIDEBAND ANALYSIS)

A. BACKGROUND

In Chapters II, III, and IV the analysis was done on pulse-coded systems for the narrow-band case. What is meant by narrow-band is that doppler has negligible effect on the envelope of the transmitted signal, but shifts the carrier frequency by the doppler frequency. It is the purpose of this chapter to discuss the doppler effect on the envelope of the waveform and to derive the expression for the time waveform of the received signal (wideband case). As stated in the introduction, target acceleration is assumed to be negligible over the interval of measurement.

B. EFFECT OF DOPPLER ON THE TRANSMITTED SIGNAL'S FREQUENCY COMPONENTS

Assume that s(t) is any arbitrary transmitted signal. Then the Fourier transform (if it exists) is a measure of the frequency content of the signal. It is assumed that s(t) is sufficiently well behaved to have a Fourier transform. If the shorthand notation is utilized, the Fourier transform of s(t) is

$$\mathcal{F}[s(t)] = \mathcal{S}(f) .$$

It is well known that the doppler effect is to shift the frequency components of the signal such that the new frequency f' is given by

$$f' = \left(\frac{1 + v_r/c}{1 + v_r/c} \right) f \,^{*}, \qquad \text{5-1}$$

---

*This equation is a statement of the two-way doppler effect for radar and sonar. For the radar case Torres[11] has indicated that if the

where v_r = radial component of velocity between the target and the transmitter

c = speed of propagation of the wave in the medium

Note: The convention is chosen so that v_r is positive for closing targets and negative for opening targets.

Define a quantity, the doppler factor, D, such that

$$f' = Df \; . \qquad \text{5-2a}$$

Alternatively,

$$D = \frac{1 + v_r/c}{1 - v_r/c} \; . \qquad \text{5-2b}$$

The doppler factor may be given in terms of the doppler frequency f_d. Note that the doppler frequency is defined as the change in the carrier frequency due to the doppler effect. Hence

$$f_d = f_o' - f_o \; . \qquad \text{5-3b}$$

Then

$$f_d = Df_o - f_o = (D - 1)f_o \; . \qquad \text{5-3c}$$

---

velocity vectors of the transmitter and the target are noncollinear, the angle at which the energy arrives at the receiver (assuming that the same antenna is used for transmitting and receiving) differs from the angle at which the energy was transmitted due to the angular aberration phenomenon.[16]

In the sonar case equation 5-1 applies if the medium is at rest with respect to the transmitter.

The above equation may be rearranged so that

$$D = 1 + \frac{f_d}{f_o} \qquad \text{5-4a}$$

If the ratio $\frac{v_r}{c} \ll 1$, then the doppler factor may be approximated by

$$D \cong 1 + \frac{2v_r}{c} \quad . \qquad \text{5-4b}$$

Hence the doppler frequency is approximately

$$f_d = \frac{2v_r}{c} f_o \quad . \qquad \text{5-5}$$

Next let us examine the received signal's Fourier transform, S'(f). (The prime notation is used to indicate that the received signal differs from the transmitted signal.) Since the effect of doppler is to shift all the frequency components of the original signal by a multiplicative factor, D, the received signal's transform is given by

$$S'(f) = S(f/D) \quad .^{*} \qquad \text{5-6}$$

C. TIME WAVEFORM OF THE DOPPLER SHIFTED SIGNAL

It was established in the previous section that the received signal's Fourier transform was related to the transmitted signal's transform by a change in argument. Hence the inverse transform of the received signal's Fourier transform will yield the time waveform of the received signal.

---

*We arrived at the amplitude factor being unity from considerations of the special theory of relativity. In Appendix A we proved that the transmitted and received energy is dependent on the relative velocity between the transmitter and the target. This result was also obtained by A. W. Rihaczek.[12] To obtain the energy of the received signal, we integrate the squared magnitude of equation 5-6 over all frequencies. Thus the energy amplitude factor is introduced via the change in frequency scale.

Since the time waveform and its Fourier transform form a one to one correspondence, the time waveform obtained by the inverse transform of the received signal's Fourier transform will be unique. If the inverse Fourier transform is taken, then

$$s'(t) = \mathcal{F}^{-1}\left[S\left(\tfrac{f}{D}\right)\right] = \int_{-\infty}^{\infty} S\left(\tfrac{f}{D}\right) e^{j\omega t}\, df \quad . \qquad 5\text{-}7$$

By a change in variable

$$f' = \frac{f}{D}$$

$$df' = \frac{df}{D} \quad ,$$

then equation 5-7 becomes

$$s'(t) = D\int_{-\infty}^{\infty} S(f')\, e^{j2\pi f'(Dt)}\, df' \quad . \qquad 5\text{-}8$$

Equation 5-8 has the same form as the transmitted signal with the exception of the amplitude factor D and the change in the time variable to Dt. Therefore

$$s'(t) = Ds(Dt) = \mathcal{F}^{-1}\left[S\left(\tfrac{f}{D}\right)\right] \qquad 5\text{-}9$$

Equation 5-9 is a well known transform pair and is referred to by R. M. Bracewell [13] as the "Similarity Theorem." Since the received signal is of the same functional form as the transmitted signal except for

a change in argument and in amplitude, s'(t) may be written as

$$s'(t) = DI(Dt)\cos\omega_o Dt \qquad \text{5-10a}$$

$$= D\alpha\sum_{i=1}^{N} X_i\left\{\mathbb{1}(Dt-iT)-\mathbb{1}[Dt-(i+1)T]\right\}\cos\omega_o Dt, \qquad \text{5-10b}$$

Note that the unit step function $\mathbb{1}(Dt-iT)$ may be written as $\mathbb{1}[D(t-i\frac{T}{D})]$ and

$$\mathbb{1}[D(t-i\tfrac{T}{D})] \equiv \mathbb{1}(t-i\tfrac{T}{D}) .$$

Define

$$T_D = T/D. \qquad \text{5-11}$$

Then

$$\omega_o D = \omega_o(1+\frac{f_d}{f_o}) = \omega_o + \omega_d . \qquad \text{5-12}$$

Hence equation 5-10b becomes

$$s'(t) = D\alpha\sum_{i=1}^{N} X_i\left\{\mathbb{1}(t-iT_D)-\mathbb{1}[t-(i+1)T_D]\right\}\cos(\omega_o+\omega_d)t . \qquad \text{5-13}$$

Equation 5-13 is the time waveform for the wideband doppler shifted signal. Note that the wideband signal reduces to the narrow-band signal if the doppler factor is nearly unity.

If equation 5-13 is examined carefully, we see that doppler produces three effects.

1) The carrier frequency is shifted by the doppler frequency.
2) The duration of a code symbol is altered by the doppler factor.
3) The received energy differs from the transmitted energy by the doppler factor.

The reason for the carrier frequency being shifted by doppler is obvious, and Appendix A shows the relationship between the received and transmitted energy. However, why is the duration of a code symbol altered by the doppler effect?

Let us determine the physical significance of the alteration of the duration of a code symbol.

Let

η = number of cycles of RF in the duration of one code symbol of the transmitted signal

η' = number of cycles of RF in the duration of one code symbol of the received signal.

Then

$$\eta = \frac{\text{duration of one code symbol for the transmitted signal}}{\text{duration of one cycle of the transmitted signal}} \qquad \text{5-14a}$$

$$= \frac{T}{1/f_o} = f_o T \qquad \text{5-14b}$$

$$\eta' = \frac{\text{duration of one code symbol for the received signal}}{\text{duration of one cycle of the received signal}} \qquad \text{5-15a}$$

$$= \frac{T_D}{1/f_o'} = f_o' T_D \,. \qquad \text{5-15b}$$

From equation 5-11

$$T_D = \frac{T}{D} \,,$$

Figure 5-1

Time waveforms of the transmitted and received signals for the duration of one code symbol

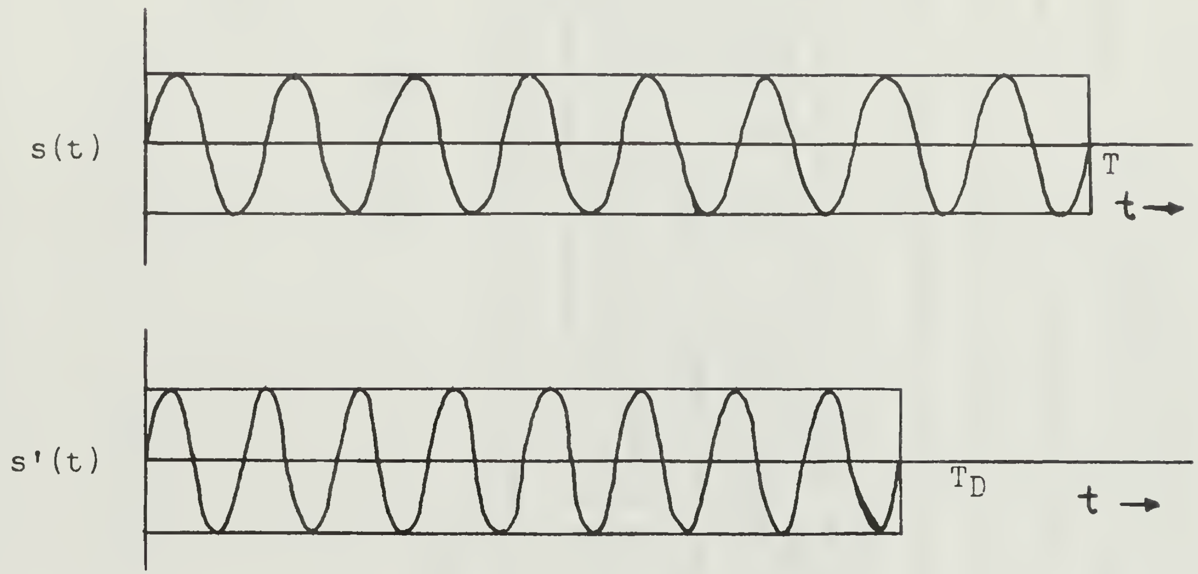

and from equation 5-3b

$$f_o' = Df_o .$$

Therefore

$$\eta' = (Df_o)(\frac{T}{D}) = f_o T . \qquad 5\text{-}16$$

Hence

$$\eta' = \eta . \qquad 5\text{-}17$$

Thus we see that the number of cycles of RF in the transmitted and received signals remains constant. Hence the implication of the doppler effect is that when the transmitted signal's carrier undergoes a shift due to doppler, the duration of a code symbol changes so that the total number of cycles of RF for the transmitted and received signals remains constant. This is compatible with the special theory of relativity as shown in Appendix D.

CHAPTER VI

WIDEBAND AMBIGUITY FUNCTION FOR COMPLEMENTARY CODES

A. BACKGROUND

It might be well to indicate those situations in which the doppler effect on the envelope of the transmitted signal cannot be ignored. Certainly for relative velocities, between the target and the transmitter, near the velocity of propagation of the wave in the medium, this effect cannot be ignored. Another situation involves the duration of the pulse train. As indicated in Chapter V, the doppler shifted waveform undergoes a compression or expansion; hence if the total duration of the shifted waveform is compressed or expanded, approaching the duration of one code symbol, energy will be lost in the correlation process. The criterion for the use of the narrow-band analysis is given in Appendix B and is duplicated here. Hence if

$$\frac{|f_d|}{f_0} \ll \frac{1}{N} . \qquad 6\text{-}1$$

Or alternatively,

$$NTW|v_r| \ll \frac{c}{2} \quad ,^{*} \qquad \text{(See equation B-14)} \qquad 6\text{-}2$$

Then the narrow-band analysis applies.

---

*This result is indicated by A. W. Rihaczek[12], and E. J. Kelly and R. P. Wishner.[14]

Equation 6-2 is a statement of the velocity-time-bandwidth-product uncertainty relationship.

B. SYSTEM BLOCK DIAGRAM

The system block diagram for the wideband case is essentially the same as the narrow-band case with the exception of two critical areas. A guard interval is necessary between code A and code B to allow for time expansion or compression of the two codes due to the doppler effect on the envelope of the received signal. Also the delayed replica of the transmitted signal must be clocked at the rate corresponding to the expected clock rate of the received signal and the carrier frequency must be shifted by the doppler frequency. Suppose that the replica signal were shifted by the doppler frequency, but not clocked at the expected rate; then degradation of the output of the matched filter would be expected. In fact, the above statement implies that we are requiring a narrow-band system to detect a wideband signal. From the point of view of equipment complexity, it is more economical just to shift the carrier frequency of the transmitted signal to obtain the replica signal. Appendix C contains the analysis of the replica signal just being shifted in carrier frequency for the wideband case. It is expected that no serious degradation of the output of the matched filter, and hence the "envelope detector," will be evidenced, so long as the time-bandwidth-product-velocity uncertainty relationship is not violated. (Equation 6-2)

C. WIDEBAND AMBIGUITY FUNCTION FOR SINGLE CODES

In the wideband case the replica signal is obtained by clocking the transmitted signal at the expected rate and translating this signal by the expected doppler frequency. For convenience the wideband matched filter block diagram is given below.

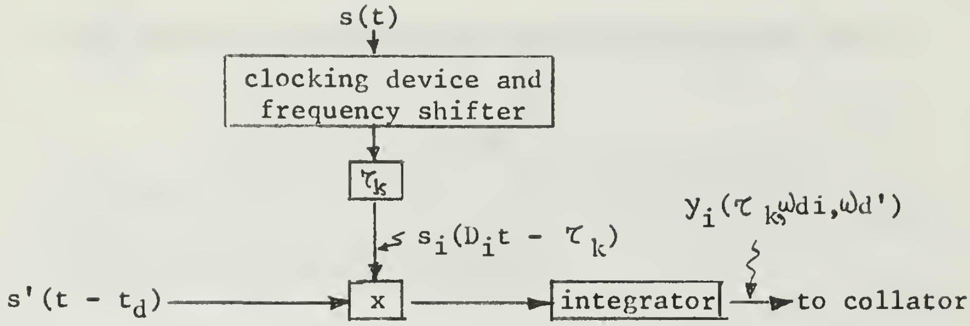

Wideband matched filter

Figure 6-1

The replica signal is given by

$$s_i(D_i t - \tau_k) = I(D_i t - \tau_k) \cos \omega_o (D_i t - \tau_k) , \qquad \text{6-3a}$$

where D_i = expected doppler factor

$$= 1 + \frac{f_{di}}{fo} \qquad \text{6-3b}$$

ω_{di} = expected doppler radian frequency,

The received signal is given by

$$s'(t-t_d) = D' I[D'(t-t_d)] \cos[(\omega_o + \omega_d')(t-t_d)] , \qquad \text{6-4a}$$

where D' = target's doppler factor

$$= 1 + \frac{f_d'}{fo} \qquad \text{6-4b}$$

ω_d' = target's doppler radian frequency,

Then the output from the matched filter is given by

$$y_i(\tau_k, \omega_{di}, \omega_d') = \int_{-\infty}^{\infty} s'(t-t_d)\, s_i(D_i t - \tau_k)\, dt$$

$$= D' \int_{-\infty}^{\infty} I[D'(t-t_d)] \cos[(\omega_o + \omega_d')(t-t_d)] \cdot$$

$$I[D_i(t - \frac{\tau_k}{D_i})] \cos[(\omega_o + \omega_{di})(t - \frac{\tau_k}{D_i})]\, dt \, . \qquad \text{6-5a}$$

Now let us shift the time reference by letting

$$t_1 = t - t_d \, .$$

Thus equation 6-5a becomes

$$y_i = D' \int_{-\infty}^{\infty} I(D't_1)\, I[D_i(t_1 + t_d - \frac{\tau_k}{D_i})] \cos(\omega_o + \omega_d')t_1 \cdot$$

$$\cos[(\omega_o + \omega_{di})(t_1 + t_d - \frac{\tau_k}{D_i})]\, dt_1 \, . \qquad \text{6-5b}$$

Then define

$$\tau_1 = \frac{\tau_k}{D_i} - t_d \, . \qquad \text{6-6}$$

Since t_1 is the variable of integration, it may be replaced by t with no loss in generality. Hence the output of the matched filter may be written as

$$y_i = D' \int_{-\infty}^{\infty} I(D't)\, I[D_i(t-\tau_1)] \cos(\omega_o + \omega_d')t \cdot$$

$$\cos[(\omega_c + \omega_{di})(t-\tau_1)]\, dt \quad , \qquad \text{6-7a}$$

$$= \frac{D'}{2}\int_{-\infty}^{\infty} I(D't)\, I[D_i(t-\tau_1)] \cos[(\omega_d' - \omega_{di})t + (\omega_o + \omega_{di})\tau_1]\, dt$$

$$+ \frac{D'}{2}\int_{-\infty}^{\infty} I(D't)\, I[D_i(t-\tau_1)] \cos[(2\omega_o + \omega_d')t - (\omega_o + \omega_{di})\tau_1]\, dt \, . \qquad \text{6-7b}$$

The second term in equation 6-7b will be rejected, provided that $(\omega_d' - \omega_{di}) \ll (2\omega_o + \omega_d')$. As in the narrow-band case, the output of the matched filter is an ordinate in the τ domain. Then, the collator collects these ordinates in the τ domain. The output of the collator is given by

$$y(\tau_1, \omega_{di}, \omega_d') = \frac{D'}{2}\int_{-\infty}^{\infty} I(D't)\, I[D_i(t-\tau_1)] \cos[(\omega_d' - \omega_{di})t + (\omega_o + \omega_{di})\tau_1]\, dt \, . \qquad \text{6-8}$$

Let

$$\omega_{o1} = \omega_o + \omega_{di} \qquad \text{6-9a}$$

$$\omega_{d1} = \omega_d' - \omega_{di} \, . \qquad \text{6-9b}$$

If the Euler identity for the cosine function is used, equation 6-8 becomes

$$y(\tau_1, \omega_{di}, \omega_d') = \mathrm{Re}\left\{ e^{j\omega_{o1}\tau_1} \frac{D'}{2}\int_{-\infty}^{\infty} I(D't)\, I[D_i(t-\tau_1)]\, e^{j\omega_{d1}t}\, dt \right\} . \qquad \text{6-10}$$

The output of the "envelope detector" will be given by

$$X(\tau_1, \omega_{di}, \omega_d') = \mathcal{E}nv\left\langle \mathrm{Re}\left\{ e^{j\omega_{o1}\tau_1} \frac{D'}{2}\int_{-\infty}^{\infty} I(D't)\, I[D_i(t-\tau_1)]\, e^{j\omega_{d1}t}\, dt \right\} \right\rangle .$$

To the extent that we can ascribe an envelope to the output of the summer, then

$$\mathcal{E}nv\left\langle \mathcal{R}e\left\{ e^{j\omega_{o1}\tau_1} \frac{D'}{2}\int_{-\infty}^{\infty} I(D't)I[D_i(t-\tau_1)]e^{j\omega_{d1}t}\,dt \right\}\right\rangle \cong$$

$$\left| \frac{D'}{2}\int_{-\infty}^{\infty} I(D't)I[D_i(t-\tau_1)]\,e^{j\omega_{d1}t}\,dt \right| .^{*} \qquad 6\text{-}11$$

In Chapter II, it was proved that for the narrow-band system the output of the "envelope detector" is identical to the ambiguity function. For the wideband case the ambiguity function will be defined by

$$\Psi'(\tau_1, \omega_{di}, \omega_d') = \left| \frac{D'}{2}\int_{-\infty}^{\infty} I(D't)\,I\left[D_i(t-\tau_1)\right] e^{j\omega_{d1}t}\,dt \right| . \qquad 6\text{-}12$$

It is only to the extent that the approximation made in equation 6-11 holds, that it is possible to give a physical interpretation to the wideband ambiguity function.

Let us now reference the received signal to the replica signal by letting

$$t_i = D_i t.$$

Thus equation 6-12 becomes

$$\Psi'(\tau_1, \omega_{di}, \omega_d') = \left| \frac{D'}{D_i}\,\frac{1}{2}\int_{-\infty}^{\infty} I\left(\frac{D'}{D_i}t_i\right) I(t_i - D_i\tau_1)\,e^{j\frac{\omega_{d1}}{D_i}t_i}\,dt_i \right| . \qquad 6\text{-}13$$

---

*If the integral in equation 6-11 is a "relatively" slowly varying function of τ_1, as compared with $e^{j\omega_{o1}\tau_1}$, then this approximation is valid.

Then define

$$D_\Delta = \frac{D'}{D_i} = \frac{f_o + f_d'}{f_o + f_{di}} , \qquad 6\text{-}14$$

$$\tau = D_i \tau_1 = \tau_k - D_i t_d , \qquad 6\text{-}15$$

$$\omega_\Delta = \frac{\omega_{di}}{D_i} = \left(\frac{\omega_d' - \omega_{di}}{\omega_o + \omega_{di}}\right) \omega_o , \qquad 6\text{-}16$$

$$= (D_\Delta - 1)\,\omega_o . \qquad 6\text{-}16b$$

Therefore the wideband ambiguity function becomes

$$\Psi'(\tau, \omega_\Delta) = \left| \frac{D_\Delta}{2} \int_{-\infty}^{\infty} I(D_\Delta t_i)\, I(t_i - \tau)\, e^{j\omega_\Delta t_i}\, dt_i \right| . \qquad 6\text{-}17$$

Note that either equation 6-17 or equation 6-13 may be chosen as the definition of the wideband ambiguity function.

One of the properties of the narrow-band ambiguity function is that it is symmetrical in range deviation, τ , and doppler, ω_d. However, the wideband single code ambiguity function seems to exhibit no simple symmetry property. Thus, we will obtain equations for the wideband single code ambiguity function, explicit for a limited case, to indicate the method that is involved.

The wideband single code ambiguity function will be calculated for $\omega_\Delta > 0$, $\tau > 0$. These equations will be limited to the case of the received signal's envelope being compressed or expanded by not more than the duration of one code symbol of the replica signal. Appendix E

contains the analysis of the limits of integration and the code values in the interval of integration for the wideband, single code ambiguity function. We have divided the ambiguity function into two intervals of range deviation.

1. For range deviations, τ , in the interval

$$(m-1)\frac{T'}{\Delta T} \le \frac{\tau}{\Delta T} \le \frac{T'}{\Delta T} - N + 1 - (m+1)\frac{T_{Di}}{\Delta T}\ ; \quad m = 1, 2, \cdots N,$$

we have

$$\Psi'(\tau,\omega_\Delta) = \frac{D_\Delta \alpha^2}{2} \left| \sum_{i=1}^{N-p} X_i X_{i+p} \int_{\tau+(i-1)T_{Di}}^{(i+p)T'} e^{j\omega_\Delta t}\,dt \right.$$

$$\left. + \sum_{i=1}^{N-(p+1)} X_i X_{i+p+1} \int_{(i+p)T'}^{\tau+iT_{Di}} e^{j\omega_\Delta t}\,dt \right| , \qquad \text{6-18}$$

where N = length of the code

$X_i = \pm 1$ depending on the ith value of the code symbol

D_i = replica signal's doppler factor $= 1 + \frac{f_{di}}{f_o}$

D' = received signal's doppler factor $= 1 + \frac{f_d'}{f_o}$

$D_\Delta = \frac{D'}{D_i} = \frac{f_o + f_d'}{f_o + f_{di}}$

$\omega_\Delta = (D_\Delta - 1)\,\omega_o$ 6-19

T = transmitted signal's duration of a code symbol

T_{Di} = replica signal's duration of a code symbol $= \frac{T}{D_i}$

T_D' = received signal's duration of a code symbol $= \frac{T}{D'}$

$T' = \frac{T_D'}{D_\Delta}$

$$\left.\begin{aligned}
\Delta T &= \text{magnitude of the difference in the duration of a code symbol} \\
&= \left| T_{Di} - T' \right| \\
p &= \text{smallest integer} \geq \left| \tau / T_{Di} \right| \\
j &= \sqrt{-1} \ \text{(denotes a complex quantity)} \\
\alpha &= \text{normalization constant} = \sqrt{\frac{2}{NT}} .
\end{aligned}\right\} \quad \text{6-19 (cont.)}$$

Then if the integration is performed, equation 6-18 becomes

$$\Psi'(\tau,\omega_\Delta) = D_\Delta \alpha^2 \left| \sum_{i=1}^{N-p} X_i X_{i+p} \frac{[(i+p)T' - (i-1)T_{Di} - \tau]}{2} \cdot \frac{\sin \frac{\omega_\Delta[(i+p)T' - (i-1)T_{Di} - \tau]}{2}}{\frac{\omega_\Delta[(i+p)T' - (i-1)T_{Di} - \tau]}{2}} \, e^{j\frac{\omega_\Delta[(i+p)T' + (i-1)T_{Di}]}{2}} \right.$$

$$\left. + \sum_{i=1}^{N-(p+1)} X_i X_{i+p+1} \frac{[\tau + iT_{Di} - (i+p)T']}{2} \cdot \frac{\sin \frac{\omega_\Delta[\tau + iT_{Di} - (i+p)T']}{2}}{\frac{\omega_\Delta[\tau + iT_{Di} - (i+p)T']}{2}} \, e^{j\frac{\omega_\Delta[iT_{Di} + (i+p)T']}{2}} \right| . \qquad \text{6-20}$$

2. For range deviations, τ, in the interval

$$\frac{T'}{\Delta T} - N + 1 + (m-1)\frac{T_{Di}}{\Delta T} \leq \frac{\tau}{\Delta T} \leq m\frac{T'}{\Delta T} \quad ; \qquad m = 1,2,\cdot\cdot,N ;$$

we have

$$\Psi'(\tau,\omega_\Delta) = \frac{D_\Delta \alpha^2}{2} \left| \sum_{i=1}^{n-\ell-k} X_i X_{i+k} \int_{\tau+(i-1)T_{Di}}^{(i+k)T'} e^{j\omega_\Delta t} dt \right.$$

$$+ \sum_{i=1}^{n-\ell-(k+1)} X_i X_{i+k+1} \int_{(i+k)T'}^{\tau + iT_{Di}} e^{j\omega_\Delta t} dt$$

$$+ X_{n-\ell-k} X_{n-\ell+1} \int_{(n-\ell)T'}^{(n-\ell+1)T'} e^{j\omega_\Delta t}\, dt$$

$$+ \sum_{i=n-\ell}^{N-2} X_{i+k} X_{i+2} \int_{(i+1)T'}^{\tau+(i-k)T_{Di}} e^{j\omega_\Delta t}\, dt$$

$$+ \sum_{i=n-\ell}^{N-2} X_{i+k+1} X_{i+2} \int_{\tau+(i-k)T_{Di}}^{(i+2)T'} e^{j\omega_\Delta t}\, dt \Bigg| , \qquad 6\text{-}21$$

where the definitions in equation 6-19 apply and

$$n = \frac{T'}{\Delta T}$$

$$n_1 = \frac{T_{Di}}{\Delta T}$$

$$q = \text{smallest integer} \geq \left|\tau/\Delta T\right|$$

$$l = q \text{ modulo } (n_1)$$

$$k = \text{smallest integer} \geq \left|\tau/T_{Di}\right| .$$

If the integrals in equation 6-21 are evaluated, then the ambiguity function becomes

$$\Psi'(\tau,\omega_\Delta) = D_\Delta \alpha^2 \Bigg| \sum_{i=1}^{n-\ell-k} X_i X_{i+k} \frac{[(i+k)T' - (i-1)T_{Di} - \tau]}{2} \cdot$$

$$\frac{\sin \frac{\omega_\Delta[(i+k)T' - (i-1)T_{Di} - \tau]}{2}}{\frac{\omega_\Delta[(i+k)T' - (i-1)T_{Di} - \tau]}{2}} e^{j\frac{\omega_\Delta[(i+k)T' + (i-1)T_{Di}]}{2}}$$

$$+ \sum_{i=1}^{n-\ell-(k+1)} X_i X_{i+k+1} \frac{[\tau + iT_{Di} - (i+k)T']}{2} \cdot$$

$$\frac{\sin \frac{\omega_\Delta[\tau + iT_{Di} - (i+k)T']}{2}}{\frac{\omega_\Delta[\tau + iT_{Di} - (i+k)T']}{2}} \; e^{j\frac{\omega_\Delta[iT_{Di} + (i+k)T']}{2}}$$

$$+ X_{n-l-k} X_{n-l+1} \frac{T'}{2} \frac{\sin \frac{\omega_\Delta T'}{2}}{\frac{\omega_\Delta T'}{2}} e^{j\frac{\omega_\Delta[(2n-2l+1)T' - \tau]}{2}}$$

$$+ \sum_{i=n-l}^{N-2} X_{i-k} X_{i+2} \frac{[\tau + (i-k)T_{Di} - (i+1)T']}{2} \circ$$

$$\frac{\sin \frac{\omega_\Delta[\tau + (i-k)T_{Di} - (i+1)T']}{2}}{\frac{\omega_\Delta[\tau + (i-k)T_{Di} - (i+1)T']}{2}} \; e^{j\frac{\omega_\Delta[(i-k)T_{Di} + (i+1)T']}{2}}$$

$$+ \sum_{i=n-l}^{N-2} X_{i-k+1} X_{i+2} \frac{[(i+2)T' - (i+k)T_{Di} - \tau]}{2} \circ$$

$$\left. \frac{\sin \frac{\omega_\Delta[(i+2)T' - (i+k)T_{Di} - \tau]}{2}}{\frac{\omega_\Delta[(i+2)T' - (i+k)T_{Di} - \tau]}{2}} \; e^{j\frac{\omega_\Delta[(i+2)T' + (i-k)T_{Di}]}{2}} \right| . \qquad 6\text{-}22$$

D. WIDEBAND AMBIGUITY FUNCTION FOR COMPLEMENTARY CODES

As stated in Chapter IV-C, to obtain the ambiguity function for a complementary code, given the ambiguity function for single codes, one merely replaces the signed product for the single codes by the signed products for the complementary codes.

1. Consider range deviation, τ , in the interval

$$(m-1)\frac{T'}{\Delta T} \le \frac{\tau}{\Delta T} \le \frac{T'}{\Delta T} - N + 1 - (m+1)\frac{T_{Di}}{\Delta T} \quad ; \qquad m = 1,2,\cdots,N.$$

Then if the signed products for the single codes in equation 6-20 are replaced by the signed products for the complementary codes, the ambiguity function for the complementary codes will be given by

$$\Psi_c'(\tau,\omega_\Delta) = D_\Delta \alpha_c^2 \Bigg| \sum_{i=1}^{N-\rho} [XA_i XA_{i+\rho} + XB_i XB_{i+\rho}] \circ$$

$$\frac{[(i+\rho)T' - (i-1)T_{Di} - \tau]}{2} \frac{\sin \frac{\omega_\Delta[(i+\rho)T' - (i-1)T_{Di} - \tau]}{2}}{\frac{\omega_\Delta[(i+\rho)T' - (i-1)T_{Di} - \tau]}{2}} \circ$$

$$e^{j\frac{\omega_\Delta[(i+\rho)T' + (i-1)T_{Di}]}{2}} + \sum_{i=1}^{N-(\rho+1)} [XA_i XA_{i+\rho+1}$$

$$+ XB_i XB_{i+\rho+1}] \frac{[\tau + iT_{Di} - (i+\rho)T']}{2} \circ$$

$$\frac{\sin \frac{\omega_\Delta[\tau + iT_{Di} - (i+\rho)T']}{2}}{\frac{\omega_\Delta[\tau + iT_{Di} - (i+\rho)T']}{2}} e^{j\frac{\omega_\Delta[iT_{Di} + (i+\rho)T']}{2}} \Bigg| , \qquad 6\text{-}23$$

where $\alpha_c = \sqrt{\frac{1}{NT}}$.

2. Now consider range deviation, τ, in the interval

$$\frac{T'}{\Delta T} - N + 1 + (m-1)\frac{T_{Di}}{\Delta T} \leq \frac{\tau}{\Delta T} \leq m\frac{T'}{\Delta T}; \quad m = 1, 2, \cdots N .$$

Then if the signed products in equation 6-22 are replaced by the signed products for the complementary codes, the ambiguity function for the complementary codes will be given by

$$\Psi_c'(\tau,\omega_\Delta) = D_\Delta \alpha_c^2 \left| \sum_{i=1}^{n-\ell-k} \left[XA_i XA_{i+k} + XB_i XB_{i+k} \right] \cdot \right.$$

$$\frac{[(i+k)T' - (i-1)T_{Di} - \tau]}{2} \frac{\sin \frac{\omega_\Delta[(i+k)T' - (i-1)T_{Di} - \tau]}{2}}{\frac{\omega_\Delta[(i+k)T' - (i-1)T_{Di} - \tau]}{2}} \cdot$$

$$e^{j\frac{\omega_\Delta[(i+k)T' + (i-1)T_{Di}]}{2}} + \sum_{i=1}^{n-\ell-(k+1)} \left[XA_i XA_{i+k+1} \right.$$

$$\left. + XB_i XB_{i+k+1} \right] \frac{[\tau + iT_{Di} - (i+k)T']}{2} \cdot$$

$$\frac{\sin \frac{\omega_\Delta[\tau + iT_{Di} - (i+k)T']}{2}}{\frac{\omega_\Delta[\tau + iT_{Di} - (i+k)T']}{2}} \; e^{j\frac{\omega_\Delta[iT_{Di} + (i+k)T']}{2}}$$

$$+ \left[XA_{n-\ell-k} XA_{n-\ell+1} + XB_{n-\ell-k} XB_{n-\ell+1} \right] \frac{T'}{2} \cdot$$

$$\frac{\sin \frac{\omega_\Delta T}{2}}{\frac{\omega_\Delta T}{2}} \; e^{j\frac{\omega_\Delta[(2n-2\ell+1)T' - \tau]}{2}}$$

$$+ \sum_{i=n-\ell}^{N-2} \left[XA_{i-k} XA_{i+2} + XB_{i-k} XB_{i+2} \right] \cdot$$

$$\frac{[\tau+(i-k)T_{Di}-(i+1)T']}{2}\;\frac{\sin\frac{\omega_\Delta[\tau+(i-k)T_{Di}-(i+1)T']}{2}}{\frac{\omega_\Delta[\tau+(i-k)T_{Di}-(i+1)T']}{2}}$$

$$e^{j\frac{\omega_\Delta[(i-k)T_{Di}+(i+1)T']}{2}} + \sum_{i=n-\ell}^{N-2}[XA_{i-k+1}XA_{i+2}$$

$$+XB_{i-k+1}XB_{i+2}]\,\frac{[(i+2)T'-(i+k)T_{Di}-\tau]}{2}\,\circ$$

$$\left.\frac{\sin\frac{\omega_\Delta[(i+2)T'-(i+k)T_{Di}-\tau]}{2}}{\frac{\omega_\Delta[(i+2)T'-(i+k)T_{Di}-\tau]}{2}}\;e^{j\frac{\omega_\Delta[(i+2)T'-(i+k)T_{Di}]}{2}}\right|\,. \qquad 6\text{-}24$$

CHAPTER VII

CONCLUSIONS

A. SUMMARY

The research presented in this thesis had two primary objectives. The first objective was to formulate the ambiguity function of the complementary codes for the narrow-band case. The second objective was to formulate the ambiguity function of the complementary codes for the wideband case. We shall summarize the results of these investigations, but not necessarily in the order presented in the thesis.

1. NARROW-BAND ANALYSIS

In the narrow-band case, Siebert's ambiguity function was extended to include complementary codes. The ambiguity function of complementary codes was defined so that its autocorrelation function contained no range sidelobes. From the definition we determined that the two codes should be combined at the outputs of the matched filters to effect the necessary cancellation of range sidelobes. During the course of research into the ambiguity function of complementary codes, we discovered that, once the ambiguity function for a single codes has been derived, then to derive the ambiguity function for a complementary code is a simple task -- replace the signed products of the single code with the sum of the signed products of sequences A and B, i.e.,

$$\text{replace } (X_i X_j) \text{ by } (XA_i XA_j + XB_i XB_j) \text{ .}$$

In the derivation of the ambiguity function for single codes, it was proved that the ambiguity function was identical to the output of the "envelope detector." (The "envelope detector" refers to the device in the system that takes the envelope of the signal, but in the range

or τ domain. This use of the term differs from conventional terminology in that, usually, envelope detection is done in the time domain.) Although this result is not unique, it helps to clarify some of the misinterpretations of the ambiguity function. It is a common misconception to state that the output of the matched filter is identical to the ambiguity function.

One result obtained in the analysis of the ambiguity function of complementary codes is that in the doppler domain, the zero crossings of the ambiguity function move closer to the origin as the length of the code increases, if the duration of a code symbol is held constant. The implication of this result is that longer codes permit better velocity discrimination. However, this process of increasing the code length to obtain better velocity discrimination cannot be continued indefinitely without incurring a penalty. The penalty is that if the velocity-time-bandwidth-product uncertainty relationship is violated, then distortions of the envelope of the received signal must be taken into account. This amounts to having to clock the replica signal at the expected rate and hence increasing the complexity of the system.

2. WIDEBAND ANALYSIS

In the wideband analysis, it can be shown that the doppler effect is three-fold.

a. The carrier frequency is shifted by the doppler frequency.

b. The envelope of the transmitted signal is compressed or expanded according to whether the target is closing or opening with respect to the receiver.

c. The received energy differs from the transmitted energy by the same factor as the received and transmitted carrier frequencies.

Although all three effects can be proved from the special theory of relativity, only the last two were proved in this manner. The distortion of the envelope of the received signal was also proved as a logical consequence of the application of Fourier analysis, and the doppler effect on the carrier frequency. A. W. Rihaczek[12] proved, by considering a photon, that the received and transmitted energies differ. Our approach to the problem was to make a Lorentz transformation of the field tensor.

It was proved that for binary phase-reversal modulated signals, if

$$NTW|v_r| \ll \frac{c}{2},$$

then the narrow-band analysis applies.

The wideband ambiguity function was derived here; however this result had been previously accomplished by A. W. Rihazek[12], and Kelly and Wishner[14]. We merely clarified certain aspects of the analysis. Then the equations for the single code and complementary code wideband ambiguity functions were derived. These equations are limited to the case of signal's envelope being altered by not more than the duration of one code symbol. They are, indeed, formidable, and a computer is required to obtain the ambiguity diagrams. Due to time limitations, the wideband ambiguity diagrams were not completed.

B. AREAS OF POTENTIAL STUDY

Many areas of future research follow directly from this thesis. A logical extension of this thesis would be to construct the wideband ambiguity diagrams for complementary codes and single codes (Barker codes, truncated pseudo-noise codes, etc.) Also the region of validity for the narrow-band analysis should be more precisely defined. We found that, in the preliminary analysis of the computer runs for the wideband ambiguity function of complementary codes, the wideband ambiguity function

for complementary codes began to deviate substantially from the narrow-band ambiguity function at approximately

$$NTW\left|v_r\right| = 0.1\ c/2$$

APPENDIX A

ENERGY OF THE RECEIVED SIGNAL DERIVED FROM CONSIDERATIONS OF THE SPECIAL THEORY OF RELATIVITY

Consider the reference frame, S, with the transmitter located at the origin of the coordinate system. Assume that the target is a perfect reflector, which is moving at a velocity, v_r, relative to the transmitter. The target is situated at the origin of the reference system, S'. A suitable set of axes is chosen so that the x direction of both of the systems, S and S', is collinear with the relative velocity vector, v_r. Figure A-1 reflects a suitable choice of axes. Note that in Figure A-1, the convention for positive velocity is away from the transmitter and is a standard convention for most physics textbooks. Although this convention is contrary to the one chosen in the main text of this thesis, no confusion should arise here.

The transmitter emits a plane wave of finite duration, NT. Let field quantities as seen in the transmitter reference frame be E_y and H_z.

Next, we require the field quantities as seen by the target in reference system, S'. These quantities can be obtained by application of the Lorentz transformations of the field-strength tensor[15]. They are given by

$$\begin{aligned} E_x' &= E_x = 0 & H_x' &= H_x = 0 \\ E_y' &= \gamma(E_y - \beta H_z) & H_y' &= \gamma(H_y + \beta E_z) = 0 \qquad \text{A-1} \\ E_z' &= \gamma(E_z + \beta H_y) = 0 & H_z' &= \gamma(H_z - \beta E_y) \ , \end{aligned}$$

where

$$\beta = v_r/c$$

$$\gamma = [1 - (v_r/c)^2]^{-1/2} = (1-\beta^2)^{-1/2} \ .$$

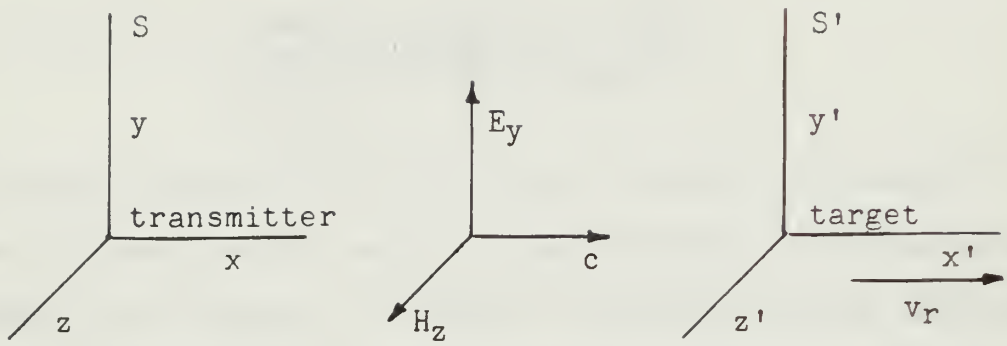

Reference frames for the target and the transmitter

Figure A-1

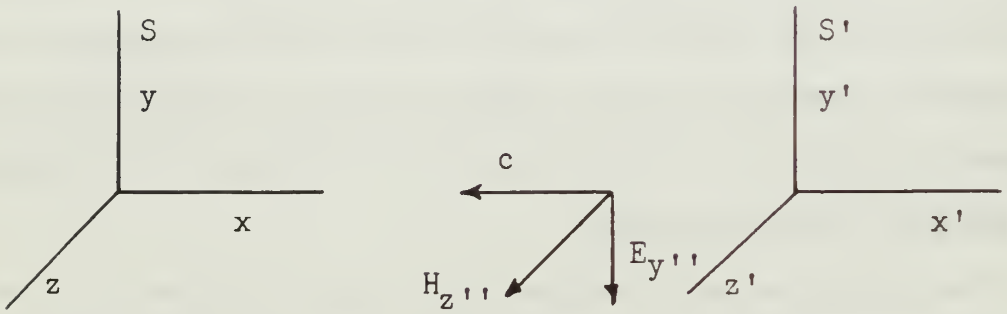

The plane wave after reflection

Figure A-2

The plane wave after reflection
as viewed by the transmitter

Figure A-3

Then we want the reflected wave's field components as viewed by the target. These field components can be easily obtained by applying the boundary conditions for a perfect reflector. Therefore, the field quantities as seen by the target are given by

$$E_x'' = 0 \qquad H_x'' = 0$$
$$E_y'' = -E_y' \qquad H_y'' = 0 \qquad \text{A-4}$$
$$E_z'' = 0 \qquad H_z'' = +H_z' \ .$$

Finally, we require the field quantities as viewed by the transmitter. The reflected wave's components can be easily obtained by applying the transformation rules in equation 1, and noting that the velocity component is now in the negative x direction; hence we must replace v_r by $-v_r$. Let us denote the reflected field quantities by a triple prime notation. Thus

$$E_x''' = 0 \qquad H_x''' = 0$$
$$E_y''' = \gamma(E_y'' + \beta H_z'') \qquad H_y''' = 0 \qquad \text{A-5}$$
$$E_z''' = 0 \qquad H_z''' = \gamma(H_z'' + \beta E_y'').$$

If equation A-4 is substituted into equation A-5,

$$E_y''' = \gamma(-E_y' + \beta H_z')$$
$$H_z''' = \gamma(H_z' - \beta E_y'). \qquad \text{A-6}$$

Then substituting equation A-1 into equation A-6

$$E_y''' = \gamma\{[-\gamma(E_y - \beta H_z)] + \beta\gamma(H_z - \beta E_y)\}$$
$$= -\gamma^2(1 + \beta^2)E_y + 2\gamma^2\beta H_z \qquad \text{A-7}$$
$$H_z''' = \gamma\{\gamma(H_z - \beta E_y) - \beta\gamma(E_y - \beta H_z)\}$$
$$= \gamma^2(1 + \beta^2)H_z - 2\gamma^2\beta E_y \ . \qquad \text{A-8}$$

The solutions for Maxwell's equations are such that

$$E_y = \frac{H_z}{Z_o} = H_z \; ;$$

since $Z_o = \sqrt{\frac{\mu_o}{\epsilon_o}} = 1$, if the field quantities are in Gaussian units.

Therefore, equation A-7 becomes

$$E_y''' = \left[-\gamma^2(1 + \beta^2) + 2\gamma^2\beta \right] E_y$$
$$= -\gamma^2(1 - \beta)^2 E_y \, , \qquad \text{A-9}$$

and

$$H_z''' = \gamma^2(1 + \beta^2) H_z - 2\gamma^2\beta H_z$$
$$= \gamma^2(1 - \beta)^2 H_z \; . \qquad \text{A-10}$$

The power density can be obtained by Poynting's Theorem, and is given by

$$\vec{P} = \frac{1}{2} \mathrm{Re} \left\{ \frac{c}{4\pi} \vec{E} \times \vec{H}^* \right\} \, , \qquad \text{A-11}$$

Thus the power density of the reflected wave as seen by the transmitter is

$$\vec{P}''' = \frac{1}{2} \mathrm{Re} \left\{ \frac{c}{4\pi} \vec{E}''' \times \vec{H}''' \right\} \, ,$$

$$\left| \vec{P}''' \right| = \frac{1}{2} \mathrm{Re} \left\{ \frac{c}{4\pi} E_y''' H_z''' \right\}$$

$$= \frac{c}{8\pi} \gamma^4 (1-\beta)^4 \left| E_o \right|^2 = \frac{c}{8\pi} \left(\frac{1-\beta}{1+\beta} \right)^2 \left| E_o \right|^2 , \qquad \text{A-12}$$

where E_o is the amplitude of E_y.

The power density of the transmitted wave is

$$|\vec{P}| = \frac{c}{8\pi}|E_o|^2. \qquad \text{A-13}$$

The energy density of the wave can be determined by integrating the power density over the duration of the signal. Note that the power density is uniform over the planar surface. Thus the energy density of the transmitted wave is

$$\mathcal{E} = \int_{-\infty}^{\infty} |\vec{P}|\,dt = \frac{c}{8\pi}|E_o|^2 NT. \qquad \text{A-14}$$

And the energy density of the reflected wave is given by

$$\mathcal{E}''' = \int_{-\infty}^{\infty} |\vec{P}'''|\,dt = \frac{c}{8\pi}|E_o|^2\left(\frac{1-\beta}{1+\beta}\right)^2 NT''', \qquad \text{A-15}$$

where N = length of the code

T''' = duration of a code symbol for the received signal

T = duration of a code symbol for the transmitted signal.

During the analysis presented in Chapter V and Appendix D, it is shown that the received signal's duration of a code symbol is altered by the doppler effect so that

$$T''' = \frac{T}{D},$$

where

$$D = \frac{1 - V_r/c}{1 + V_r/c}.$$

Thus equation A-15 becomes

$$\mathcal{E}''' = \frac{c}{8\pi}|E_o|^2\left(\frac{1-\beta}{1+\beta}\right)^2 N\left(\frac{T}{D}\right)$$

$$= \frac{c}{8\pi}|E_o|^2 DNT \quad . \qquad \text{A-16}$$

Then the ratio of the received signal's energy density to the transmitted signal's energy density is given by

$$\frac{\mathcal{E}'''}{\mathcal{E}} = \frac{\frac{c}{8\pi}|E_o|^2 DNT}{\frac{c}{8\pi}|E_o|^2 NT}$$

$$= D \ . \qquad \text{A-17}$$

APPENDIX B

CRITERION FOR THE USE OF THE NARROW-BAND APPROXIMATION (VELOCITY-TIME-BANDWIDTH-PRODUCT UNCERTAINTY RELATIONSHIP)

In this appendix we shall derive, from rather elementary considerations, the region of validity for the narrow-band approximation. This approximation is made in Chapters II and III and assumes that doppler has negligible effect on the envelope of the signal. Chapter V contains the derivation of the time waveform of the doppler shifted signal for the wideband case. (For purposes of clarification, the terms, doppler shifted signal and the received signal, are used synonymously.) We concluded that the effect of doppler was threefold:

1. The duration, T_D, of a code symbol for the doppler shifted waveform was altered so that

$$T_D = T/D. \qquad \text{B-1}$$

2. The carrier frequency was shifted by the doppler frequency.
3. The received signal's energy density differed from the transmitted signal's energy density by the doppler factor.

If the doppler shifted signal's duration of a code symbol is altered by doppler so that the total duration of the signal is expanded or compressed by the duration of a code symbol of the transmitted signal, we expect degradation of the output of the matched filter. In particular, if the code is completely random, then for zero range deviation the output of the matched filter will be zero. Hence we shall use as our criterion of the narrow-band approximation, that the total duration of the received signal must be compressed or expanded by much less than the duration of a code symbol of the transmitted signal, T. Let us examine two cases.

1. Case I: The total duration of the received is compressed by much less than the duration of a code symbol of the transmitted signal. (This statement implies that positive doppler is present.)

Figure B-1 indicates the envelopes of the transmitted signal, $I(t)$, and the received signal, $I(Dt)$, for some arbitrary code. Hence for the condition that the total duration of the received signal is compressed by much less than the duration of a code symbol of the transmitted signal, the following inequality applies:

$$NT_D \gg (N - 1)T \; . \qquad \text{B-2}$$

If the above inequality is rearranged,

$$T/T_D \ll (N/(N - 1) \; . \qquad \text{B-3}$$

From equation B-1

$$T/T_D = D \ll N/(N - 1) \; ,$$

Therefore

$$1 + f_d/f_o \ll N/(N - 1) \; .$$

And

$$f_d/f_o \ll 1/(N - 1) \; . \qquad \text{B-4}$$

Alternatively,

$$\frac{1 + v_r/c}{1 - v_r/c} \ll N/(N - 1) \; .$$

If $N \gg 1$, then

$$v_r/c \ll 1/2N \; . \qquad \text{B-5}$$

Figure B-1

Time waveforms of the received and transmitted signals for the case of the received signal's envelope being compressed by less than the duration of a code symbol of the transmitted signal. (Note that the received signal's amplitude is supressed so that the waveforms may be seen in detail.)

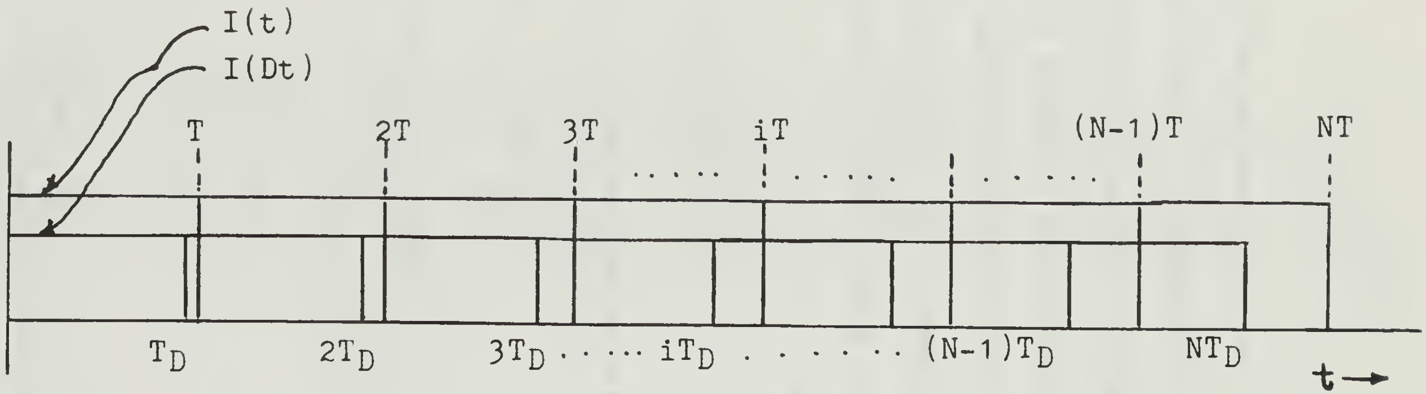

Note that the time-bandwidth product is equal to N.*

Hence

$$NTW\, v_r \ll c/2 \; . \qquad \text{B-6}$$

2. Case II: The total duration of the received signal is expanded by much less than the duration of a code symbol of the transmitted signal. (This statement implies that negative doppler is present.)

Figure B-2 indicates the envelopes of the transmitted signal and the received signal for some arbitrary code. Hence for the condition that the total duration of the received signal is expanded by much less than the duration of a code symbol of the transmitted signal, the following inequality applies:

$$NT \gg (N - 1)T_D \; . \qquad \text{B-7}$$

The above inequality may be rearranged so that

$$T/T_D \gg (N - 1)/N \; . \qquad \text{B-8}$$

Note that the doppler frequency is negative in this case. Hence the doppler factor may be written as

$$D = 1 - \frac{|f_d|}{f_o} \; . \qquad \text{B-9}$$

---

*We have defined bandwidth as the video bandwidth to the first null of the rectangular pulse spectrum, i.e., W = 1/T. This is approximately equal to the "effective" RF bandwidth. Thus NTW = N. The time-bandwidth product, as used by Torres, was defined in such a fashion (using standard deviation in both time and frequency domains) as to be a complete and precise description for a Gaussian pulse. If rectangular or other shaped pulses are used, a numerical factor of the order of magnitude of unity may be introduced into his precise inequality. Hence there exists an apparently discrepancy of a factor of 2 between Torres' inequality and our inequality B-6.

Figure B-2

Time waveforms of the received and transmitted signals for the case of the received signal's envelope being expanded by less than the duration of a code symbol of the transmitted signal. (Note that the received signal's amplitude is supressed so that the waveforms may be seen in detail.)

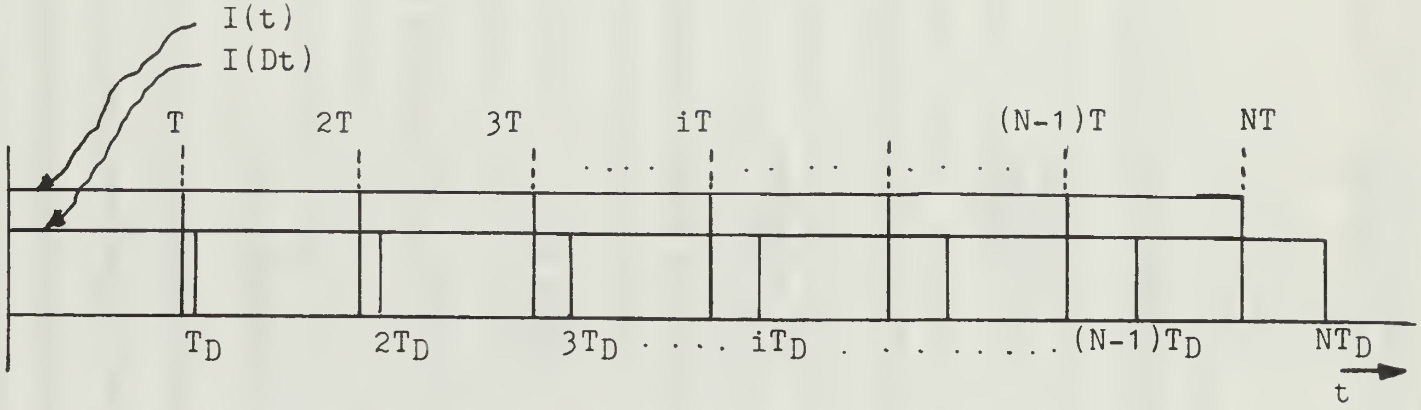

If equation B-9 is substituted into the inequality B-8, then

$$1 - \frac{|f_d|}{f_o} \gg \frac{N - 1}{N}$$

$$\frac{f_d}{f_o} \ll \frac{1}{N} \, . \qquad \text{B-10}$$

Alternatively, the doppler factor may be given by

$$D = \frac{1 - \frac{|v_r|}{c}}{1 + \frac{|v_r|}{c}} \, . \qquad \text{B-11}$$

Hence, substituting equation B-11 into the inequality B-8, then

$$\frac{|v_r|}{c} \ll \frac{1}{2N - 1} \, . \qquad \text{B-12}$$

If the length of the code is much greater than unity

$$\frac{|v_r|}{c} \ll \frac{1}{2N} \, . \qquad \text{B-13}$$

Then, we note that the time-bandwidth product is equal to the length of the code, N. Hence

$$NTW \, |v_r| \ll \frac{c}{2} \, . \qquad \text{B-14}$$

Thus if the time-bandwidth product multiplied by the radial component of relative velocity is much less than one-half the velocity of the wave in the medium, then the narrow-band assumption applies. Inequality B-14 is a statement of the velocity-time-bandwidth-product uncertainty relationship.

APPENDIX C

EFFECT OF DOPPLER MISMATCH, DUE TO THE REPLICA SIGNAL ONLY BEING TRANSLATED IN FREQUENCY, ON THE OUTPUT OF THE "ENVELOPE DETECTOR"

1. BACKGROUND

For the wideband case, the system block diagram contained range banks, such that in one range bank, the received signal is correlated with an exact replica of itself. Note that the replica signal has the same carrier frequency and clock period as the received signal. Hence, in generating this signal from the transmitted signal, the system must contain a clocking device, such as a shift register, as well as a frequency translator. Naturally the clocking device adds to the complexity and hence the cost of the system. Suppose that in trying to reduce the complexity of this system, we merely translate the frequency of the transmitted signal by the doppler frequency. How is the output of the "envelope detector" affected? If the replica signal is obtained by a mere frequency translation, we are, in effect, requiring a narrow-band system to detect a wideband signal. Thus we expect no serious degradation of the output of the envelope detector, so long as the time-bandwidth-product uncertainty relationship (equation 6-2) is not violated.

2. OUTPUT OF THE ENVELOPE DETECTOR (SINGLE CODE SYSTEM)

We will investigate the single code system prior to the complementary coded system, since once the equations for the single code system are obtained, it is a simple task to obtain the equations for the complementary coded system. Figures 2-2a and 2-2b will be used as the system block diagram, since our receiver is a narrow-band system. The received signal, $s'(t)$, will be given by equations 5-10a and 5-10b. The replica signal, $s_M(t)$, is simply the transmitted signal translated by the doppler frequency;

hence it is identical to the narrow-band received signal. Then $s_M(t)$ is given by equation 2-4. Thus

$$s'(t) = D' I(D't) \cos(\omega_o + \omega_d')t \ , \tag{C-1a}$$

$$s_M(t) = I(t) \cos(\omega_o + \omega_{di}) t \ . \tag{C-1b}$$

Then the output of the mismatched filter in Figure 2-2b is given by

$$y_M(\tau, \omega_{di}, \omega_d')\Big|_{\omega_{di}=\omega_d'} = \frac{D'}{2} \cos \omega_o\tau \int_{-\infty}^{\infty} I(D't) I(t-\tau)\, dt$$

$$+ \frac{D'}{2} \int_{-\infty}^{\infty} I(D't) I(t-\tau) \cos[2(\omega_o + \omega_d')t - (\omega_o + \omega_d')\tau]\, dt \ . \tag{C-2}$$

The second term in equation C-2 will be rejected by the integrator. Then the mismatched output of the "envelope detector" will be given by

$$X_M(\tau, \omega_{di}, \omega_d')\Big|_{\omega_{di}=\omega_d'} = \frac{D'}{2} \left| \int_{-\infty}^{\infty} I(D't) I(t-\tau)\, dt \right| \ . \tag{C-3}$$

From equation 6-17 we see that the mismatched output from the "envelope detector" is related to the wide-band ambiguity function by

$$X_M(\tau, \omega_\Delta) = \Psi'(\tau, \omega_\Delta)\Big|_{D_i=1} \ . \tag{C-4}$$

Recall from equation 6-14 that

$$D_\Delta = D'/D_i.$$

Then the differential doppler factor, in this case, is

$$D_\Delta = D'. \tag{C-5}$$

Next, let us obtain the mismatched output of the "envelope detector" for the case of the replica signal's doppler frequency matched to the received signal's doppler frequency. This can be obtained by setting $D_i = 1$, and $\omega_\Delta = 0$, in equations 6-20 and 6-22.

1. For range deviations, τ, in the interval

$$(m-1)\frac{T_D'}{\Delta T} \le \frac{\tau}{\Delta T} \le \frac{T_D'}{\Delta T} - N + 1 - (m+1)\frac{T}{\Delta T} \quad ; \qquad m = 1, 2, \cdots, N,$$

we have

$$\chi_M(\tau,0) = D'\alpha^2 \Bigg| \sum_{i=1}^{N-p} X_i X_{i+p} \frac{[(i+p)T_D' - (i-1)T - \tau]}{2} + \sum_{i=1}^{N-(p+1)} X_i X_{i+p+1} \frac{[\tau + iT - (i+p)T']}{2} \Bigg|, \tag{C-6}$$

where N = length of the code

$X_i = \pm 1$ depending on the ith value of the code symbol

D' = received signal's doppler factor

$= 1 + \dfrac{f_{di}}{f_o}$

$D_\Delta = D'$

(C-7)

$$
\left.
\begin{aligned}
T &= \text{transmitted signal's duration of a code symbol} \\
T_D' &= \text{received signal's duration of a code symbol} \\
&= T/D' \\
\Delta T &= \text{magnitude of the difference in the duration of a code} \\
&\quad \text{symbol} = |T - T_D'| \\
p &= \text{smallest integer} \geq |\tau/T| \;.
\end{aligned}
\right\}
\quad \text{C-7 (cont.)}
$$

2. For range deviations, τ, in the interval

$$\frac{T_D'}{\Delta T} - N + 1 + (m-1)\frac{T}{\Delta T} \leq \frac{\tau}{\Delta T} \leq m\frac{T_D'}{\Delta T} \quad ; \qquad m = 1,2,\cdots,N.$$

We have

$$\mathcal{X}_M(\tau,0) = D'\alpha^2 \Bigg| \sum_{i=1}^{n-\ell-k} X_i X_{i+k} \frac{[(i+k)T_D' - (i-1)T - \tau]}{2}$$

$$+ \sum_{i=1}^{n-\ell-(k+1)} X_i X_{i+k+1} \frac{[\tau + iT - (i+k)T_D']}{2}$$

$$+ X_{n-\ell-k} X_{n-\ell+1} \frac{T_D'}{2}$$

$$+ \sum_{i=n-\ell}^{N-2} X_{i-k} X_{i-2} \frac{[\tau + (i-k)T - (i+1)T_D']}{2}$$

$$+ \sum_{i=n-\ell}^{N-2} X_{i-k+1} X_{i-2} \frac{[(i+2)T_D' - (i+k)T - \tau]}{2} \Bigg|, \qquad \text{C-8}$$

where the definitions in equation C-7 apply and

$$\left.\begin{aligned} n &= T_D'/\Delta T \\ n_1 &= T/\Delta T \\ q &= \text{smallest integer} \geq |\tau/\Delta T| \\ k &= \text{smallest integer} \geq |\tau/T| \,. \end{aligned}\right\} \qquad \text{C-9}$$

3. OUTPUT OF THE ENVELOPE DETECTOR (COMPLEMENTARY CODED SYSTEM)

As indicated in Chapter 4-C, it is easy to obtain the equations for the complementary coded system once the equations for the single code system are obtained by simply replacing the signed products of the single codes by the signed product for the complementary codes. Hence if

$$X_i X_j \text{ is replaced by } XA_i XA_j + XB_i XB_j$$

in equations C-6 and C-8; then the resulting equations will be the mismatched output of the envelope detector for the complementary coded system.

APPENDIX D

DURATION OF A CODE SYMBOL DERIVED FROM CONSIDERATIONS OF THE SPECIAL THEORY OF RELATIVITY

In Chapter V it was proved that the transmitted signal's duration of a code symbol, T, differed from the received signal's duration of a code symbol, T', by the inverse of the doppler factor, D. This result was obtained from considerations of the doppler effect on the carrier frequency and also by the use of the Fourier transform.

In this Appendix we will prove the same result, but from considerations of the special theory of relativity.

Consider the reference frame, S, with the transmitter located at the origin of the coordinate system. Next, consider a moving frame, S', with the target located at the origin. A suitable set of axes is chosen so that the x direction of both S and S' is collinear with the velocity vector, v_r. At some initial time, i.e., $t = 0$, we shall assume that the two frames are coincident. At $t = 0$, the transmitter emits a plane wave pulse of duration, T. The pulse travels at the speed of light. Then we can view the pulse as extending in space so that its trailing edge has an x coordinate of $-cT$. For $t \geq 0$, the moving frame travels in the +x direction with a velocity v_r. Note that the convention for positive velocity is away from the transmitter and is a standard convention for most physics textbooks. Although this convention is contrary to the one chosen in the main text of this thesis, no confusion should arise here.

At time $t = T$, the trailing edge of the pulse reaches the origin of S, and the leading edge of the pulse is now at $x = cT$. Now let us consider the spacial distribution of the pulse in the moving frame. In the moving frame the x coordinate, x', and the time in this frame, t',

can be derived from their counterparts in the reference frame from the Lorentz transformations.[16] Thus

$$x' = \gamma(x - v_r t) \qquad \text{D-1}$$

$$t' = \gamma(t - \frac{v_r}{c^2} x), \qquad \text{D-2}$$

where

$$\gamma = \left[1 - \left(\frac{v_r}{c}\right)^2\right]^{-1/2} .$$

Let us denote, as in Figure D-1, the trailing edge of the pulse as event 1. For event 1, the x coordinate of the trailing edge of the pulse in the moving frame is given by

$$x_1' = \gamma(x - v_r t)\Big|_{\substack{x = o \\ t = T}}$$

$$= -\gamma v_r T . \qquad \text{D-3}$$

For event 1, the time elapsed in the moving frame is given by

$$t_1' = \gamma(t - \frac{v_r}{c^2} x)\Big|_{\substack{x = o \\ t = T}}$$

$$= \gamma T . \qquad \text{D-4}$$

Since the pulse is traveling at the speed of light, the total time for the trailing edge of the pulse to pass the observer at the origin of the moving frame is given by

$$T' = t_1' - \frac{x_1'}{c} = \gamma T + \frac{\gamma v_r T}{c} ,$$

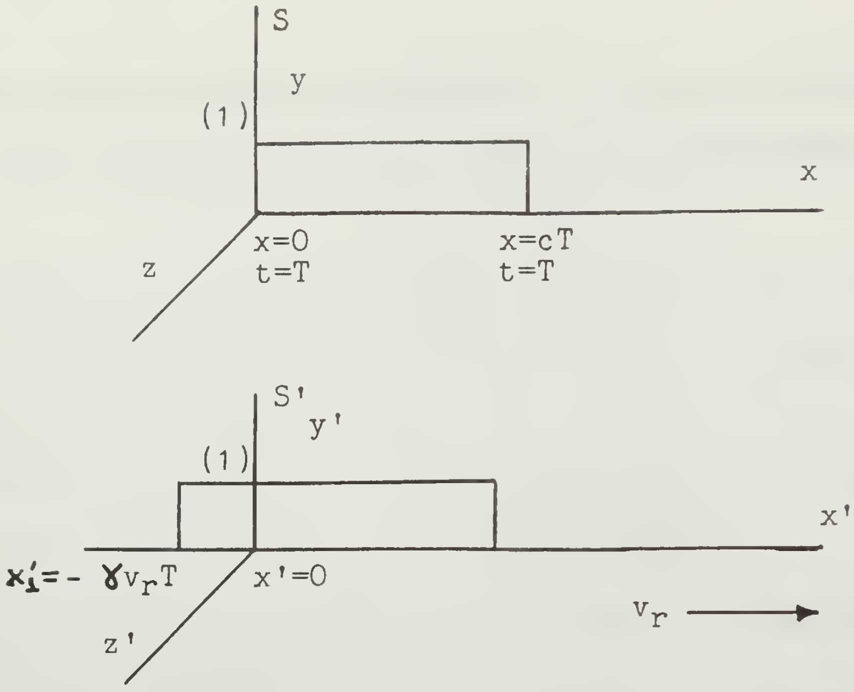

Reference frames for the
transmitter and the target

Figure D-1

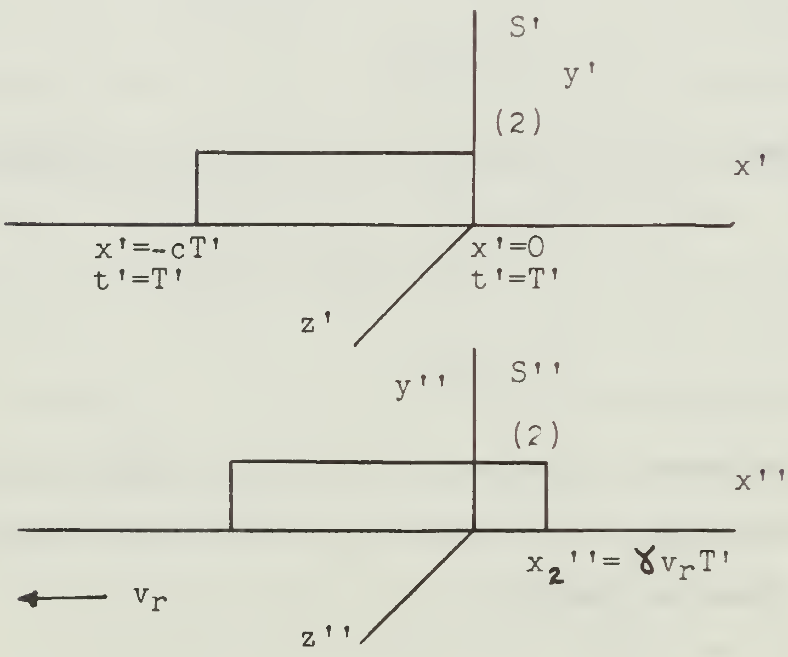

Reference frames for the
target and the receiver

Figure D-2

$$= \gamma\left(1 + \frac{v_r}{c}\right)T ,$$

$$= \sqrt{\frac{1 + v_r/c}{1 - v_r/c}}\; T. \qquad \text{D-5}$$

Equation D-5 is a statement of the expansion or compression of the duration of a pulse for the case of one-way doppler.

Now we would like to consider the duration of the pulse which is reflected from the target, as seen by an observer (the receiver) at the origin of the reference frame, S. To avoid confusion let us denote this reference frame as S''; however, bear in mind that we are assuming that the transmitter and receiver are at the same physical location. We can view the reflected wave as being retransmitted from the target.

Consider S', the target's frame, and S'', the receiver's frame, to be coincident at t' = 0. From S', the receiver seems to be moving at a velocity v_r in the negative x direction. Then at t' = 0, the leading edge of the pulse is at the origin of both frames. At t' = T', the trailing edge of the pulse is at the origin of the frame, S'. Let us denote this as event 2. To obtain the x coordinate of the trailing edge of the pulse as seen by the observer on S'', we utilize the Lorentz transformations as given by equations D-1 and D-2, but remembering to replace v_r by $-v_r$. Thus for event 2

$$x_2'' = \gamma(x' + v_r t')\Big|_{\substack{x'=0 \\ t'=T}}$$

$$= \gamma v_r T', \qquad \text{D-6}$$

For event 2 the time elapsed in S'' is

$$t_2'' = \gamma\left(t' - \frac{v_r}{c}x'\right)\Big|_{\substack{x'=0\\ t'=T}}$$

$$= \gamma T' \qquad \text{D-7}$$

Then the total time required for the trailing edge of the pulse to reach the observer on S'' is given by

$$T'' = t_2'' + \frac{x_2''}{c} = \gamma T' + \frac{\gamma v_r T'}{c}$$

$$= \gamma\left(1 + \frac{v_r}{c}\right)T'$$

$$= \sqrt{\frac{1 + v_r/c}{1 - v_r/c}}\; T'. \qquad \text{D-8}$$

Then if equation D-5 is substituted into equation D-8

$$T''' = \left(\frac{1 + v_r/c}{1 - v_r/c}\right)T$$

$$= T/D , \qquad \text{D-9}$$

where

$$D = \frac{1 - v_r/c}{1 + v_r/c} .$$

The factor which compresses or expands the duration of the pulse is identical to the one obtained by the Fourier transform analysis done in Chapter V, with the exception of the difference in sign of the velocity due to the change in sign convention adapted in this Appendix. In our initial assumptions, we assumed that the duration of the transmitted pulse was T. It is easy to see that if a series of N pulses, each of duration T, were transmitted, then the compression or expansion factor would be identical to the one in equation D-9. Hence we have proved that the doppler effect alters the duration of a code symbol by the factor D.

APPENDIX E

DETERMINATION OF THE LIMITS OF INTEGRATION FOR THE WIDEBAND SINGLE CODE AMBIGUITY FUNCTION

In this Appendix we would like to determine the limits of integration and their corresponding code values in the interval of integration for the wideband single code ambiguity function. In the formulation of the equations for the wideband single code ambiguity function, there are four quadrants to consider. We will consider only the first quadrant, i.e., $\omega_\Delta > 0$, $\tau > 0$, and will limit the validity of the equations to the case of the received signal's total pulse duration being expanded or compressed by not more than the duration of one code symbol of the replica signal.

By equation 6-17, the wideband single code ambiguity function is defined as

$$\Psi'(\tau, \omega_\Delta) = \left| \frac{D_\Delta}{2} \int_{-\infty}^{\infty} I(D_\Delta t) I(t-\tau) e^{j\omega_\Delta t} dt \right| . \qquad \text{E-1}$$

Hence to determine the limits of integration and the code values in the interval of integration, we must analyze $I(D_\Delta t)$ and $I(t - \tau)$. $I(D_\Delta t)$ is the envelope of the received signal (time referenced to the replica signal), and is given by

$$I(D_\Delta t) = \alpha \sum_{i=1}^{N} \left\{ 1\!\!1(D_\Delta t - iT_D') - 1\!\!1[D_\Delta t - (i+1)T_D'] \right\} . \qquad \text{E-2}$$

Then define

$$T' = T_D'/D . \qquad \text{E-3}$$

Therefore, equation E-2 becomes

$$I(D_\Delta t) = \alpha \sum_{i=1}^{N} X_i \left\{ 1\!\!1(t - iT') - 1\!\!1[t-(i+1)T'] \right\} . \qquad \text{E-3}$$

The envelope of the replica signal is given by

$$I(t-\tau) = \alpha \sum_{i=1}^{N} X_i \left\{ 1\!\!1(t-\tau-iT_{D_i}) - 1\!\!1[t-\tau-(i+1)T_{D_i}] \right\} . \qquad \text{E-4}$$

Figure E-1 is a set of waveforms of the received and replica signals' envelopes. We have chosen, in Figure E-1, a code of length 6, with the code values of $\{+1, -1, +1, +1, -1, +1\}$ as an example. From this example we will obtain an equation that will apply, in general, to codes of any length. Note that the amplitude of the received signal's envelope in Figure E-1 is less than the amplitude of the replica signal's envelope. This is done deliberately so that both waveforms may be seen in detail; however, bear in mind that both envelopes are, in actuality, of the same amplitude.

For positive doppler we recall that the received signal's waveform will be compressed. Figure E-1 is a series of waveforms of $I(D_\Delta t)$ and $I(t)$, in which we hold $I(D_\Delta t)$ fixed and shift $I(t - \tau)$ to the right, corresponding to positive range deviation, τ. In doing so, we see that the limits of integration (as a general rule) change for τ in increments of ΔT, where

$$\Delta T = |T_{Di} - T'| \quad . \qquad \text{E-5}$$

Next, we would like to express the interval of integration (and hence the limits of integration) in the form of a series. Let us now look for

Figure E-1

Time waveforms of the received and replica signals' envelope, where the code values are (+1, -1, +1, +1, -1, +1), for positive doppler frequency and positive range deviation, τ.

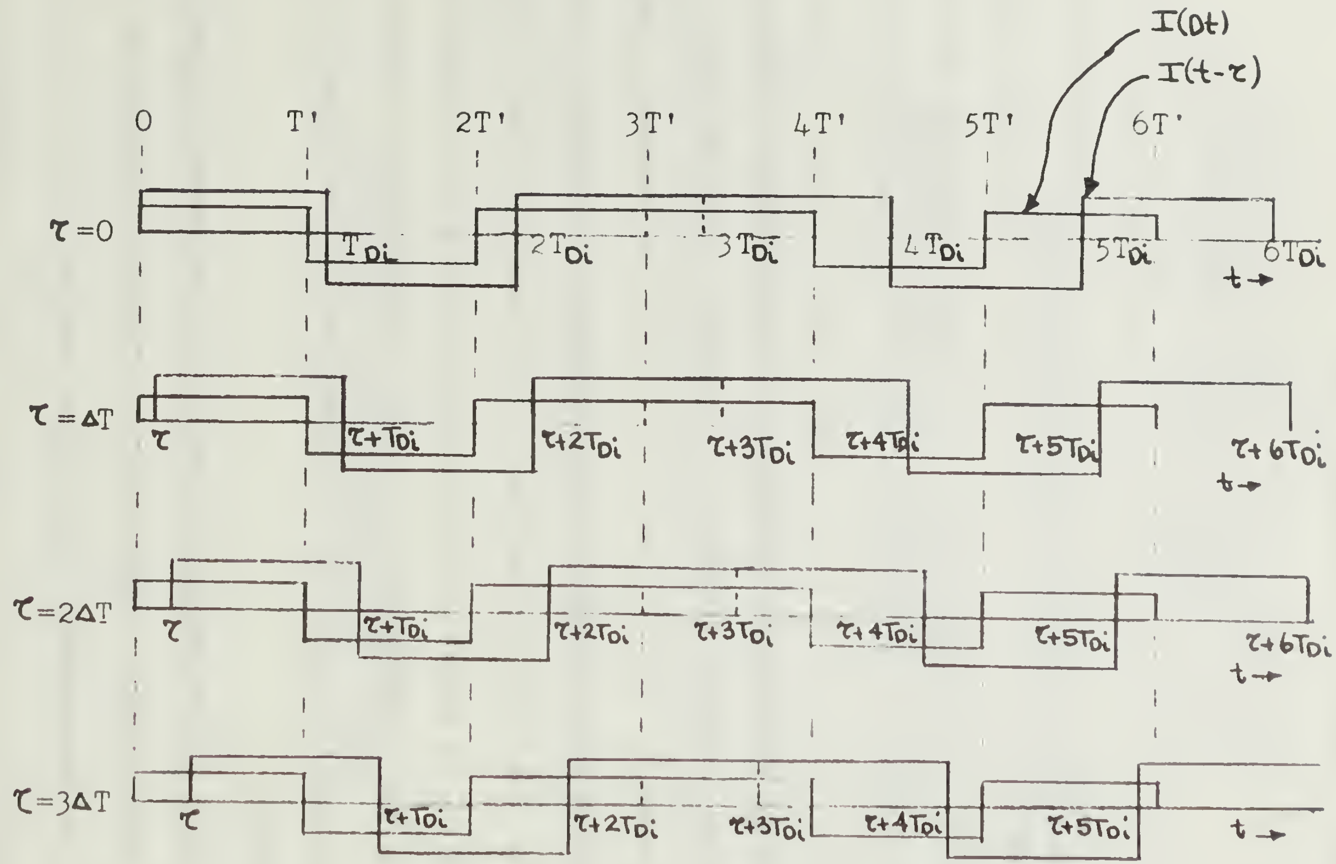

Figure E-1
(cont.)

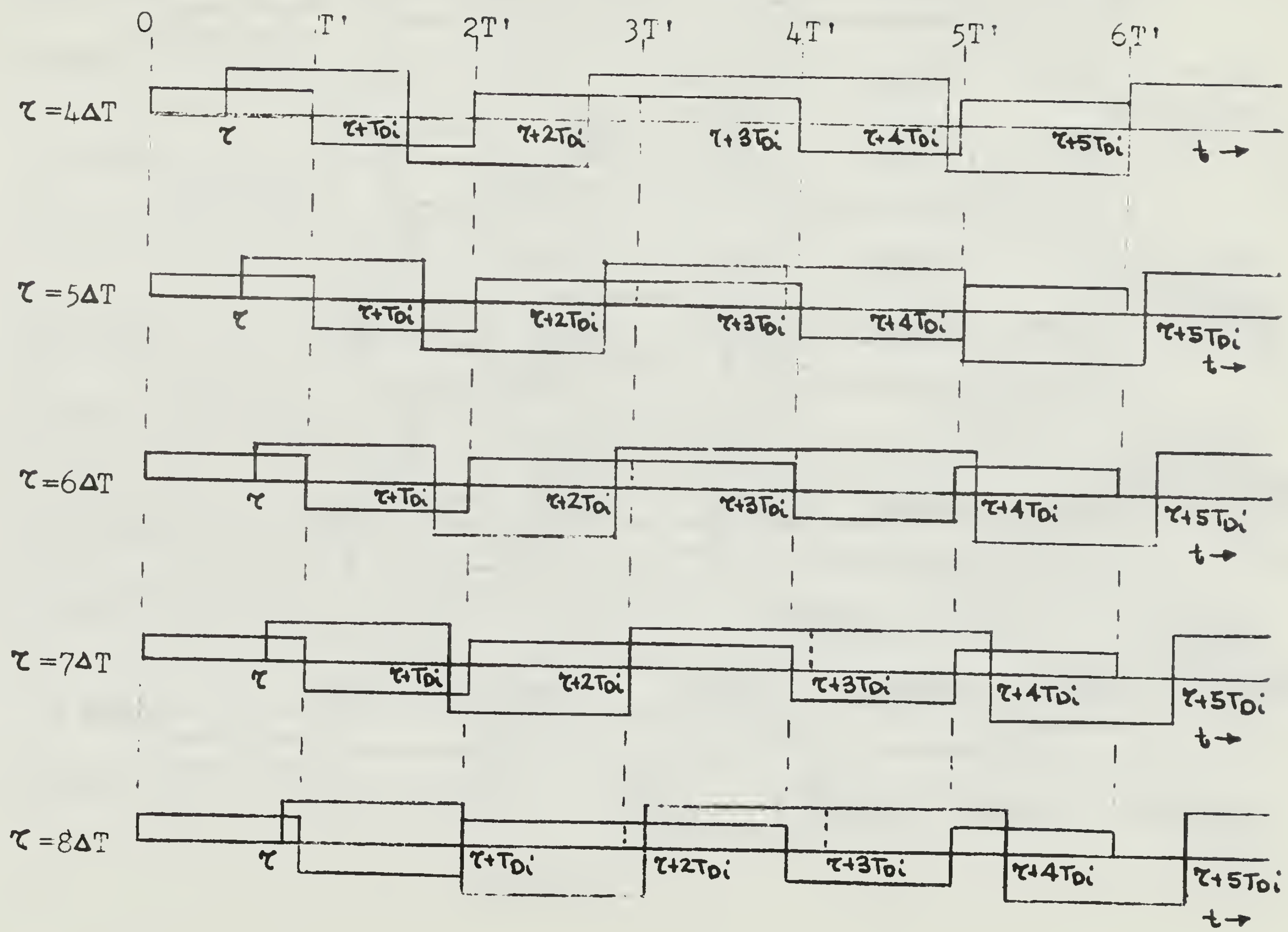

Figure E-1
(cont.)

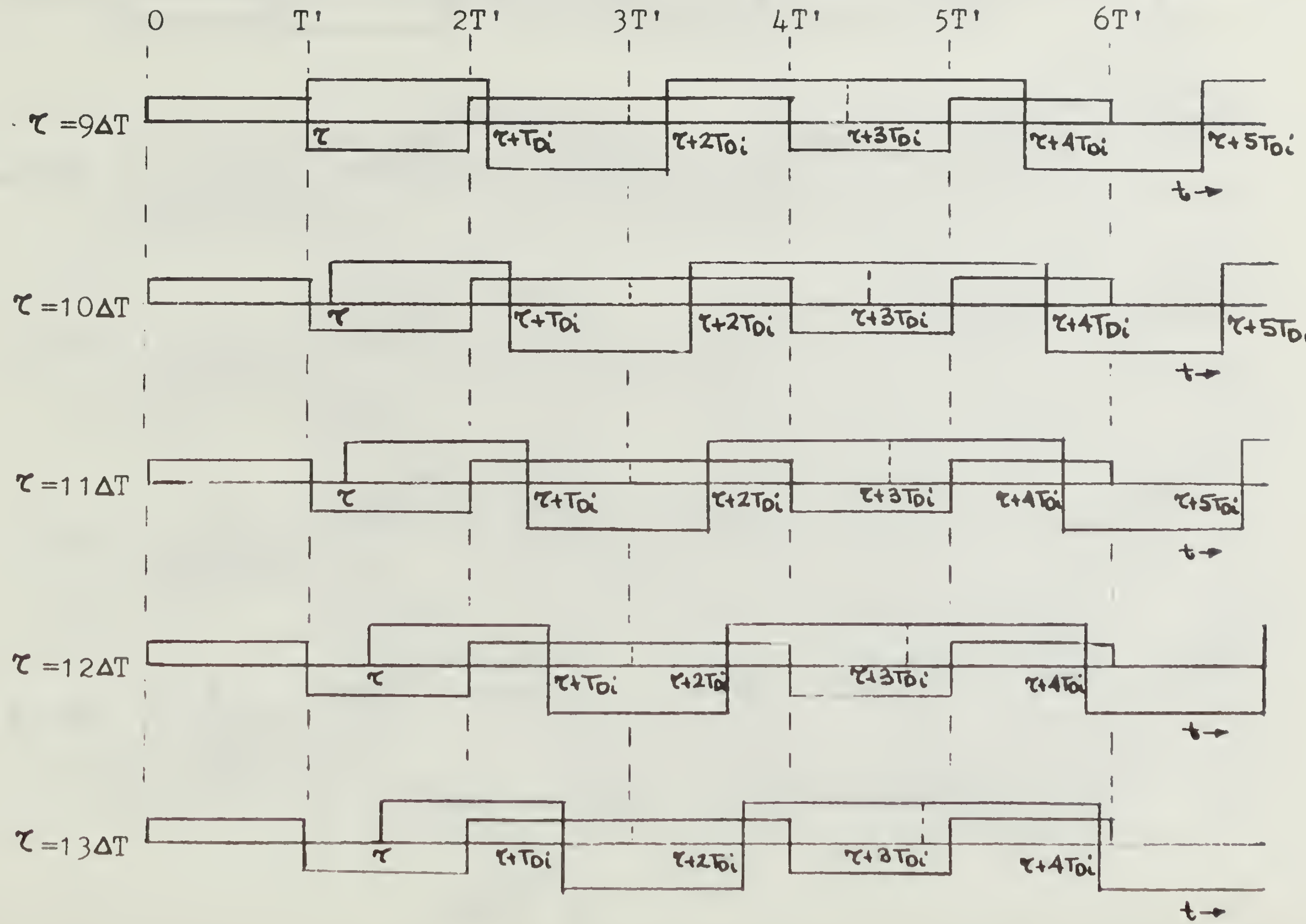

Figure E-1
(cont.)

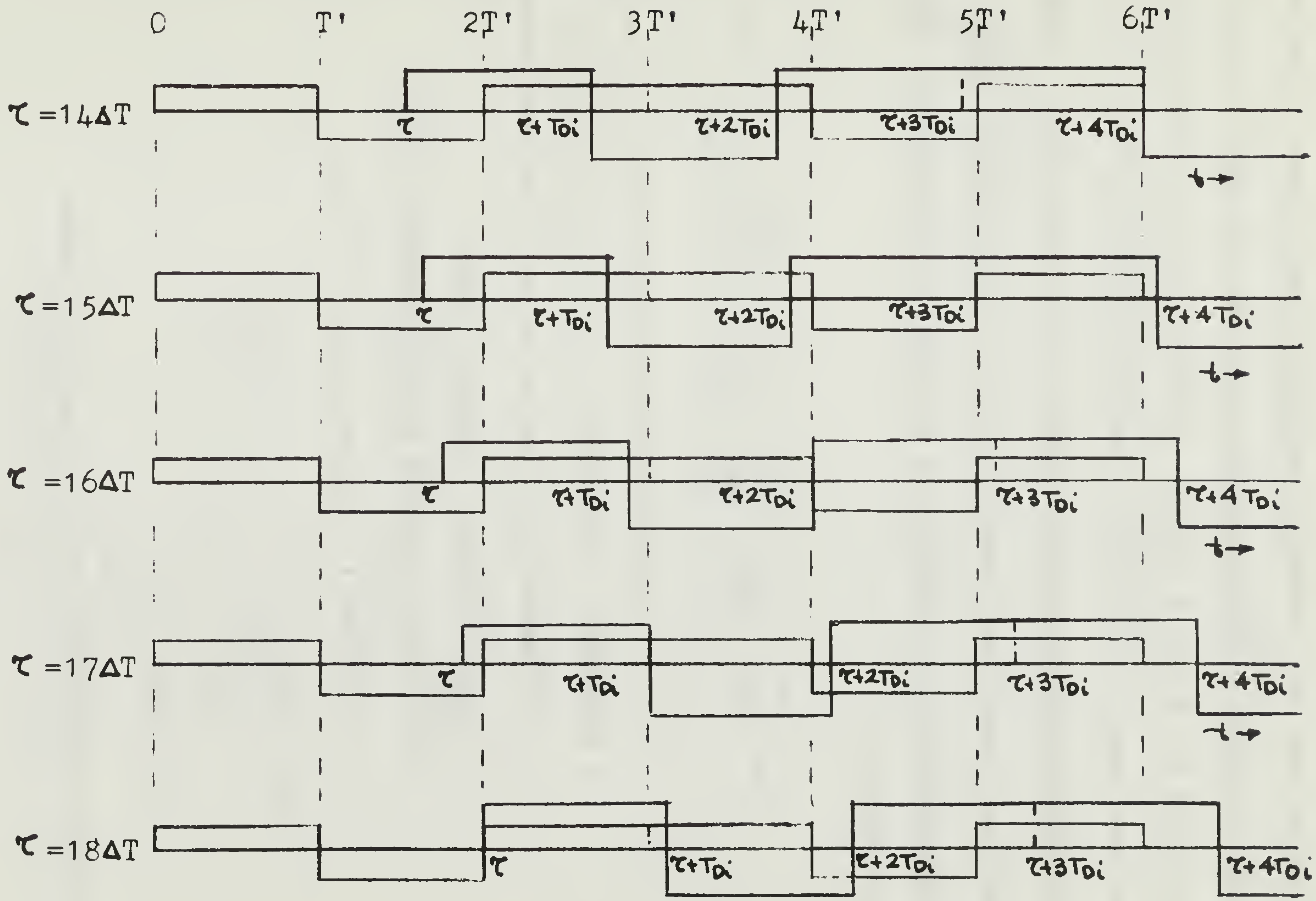

symmetries in Figure E-1. Note that for $0 < \tau < 4\,\Delta T$, the limits of integration over each interval, in addition to the code values of the received and replica signals, remain constant. We also see that this occurs again for $9\,\Delta T < \tau < 13\,\Delta T$. However, we have lost the duration of one code symbol of the replica signal. Similarly, for $19\,\Delta T < \tau < 23\,\Delta T$, we see that we have lost the duration of two code symbols. From this analysis, we can obtain a general formula to express the limits of integration and the code values in the interval of integration. Hence for τ in the interval

$$(m-1)\frac{T'}{\Delta T} \le \frac{\tau}{\Delta T} \le \frac{T'}{\Delta T} - N + 1 - (m+1)\frac{T_{Di}}{\Delta T} \; ; \quad m = 1,2,\cdots N,$$

where

$$\left.\begin{aligned}
N &= \text{length of the code} \\
X_i &= \pm 1 \text{ depending on the ith value of the code symbol} \\
D_i &= \text{replica signal's doppler factor} \\
D' &= \text{received signal's doppler factor} \\
D_\Delta &= \text{differential doppler factor} = D'/D_i \\
T_{Di} &= T/D_i \\
T' &= T_{Di}/D \\
\Delta T &= |T_{Di} - T'| \;.
\end{aligned}\right\} \qquad \text{E-6}$$

The wideband single code ambiguity function becomes

$$\Psi'(\tau,\omega_\Delta) = \frac{D_\Delta \alpha^2}{2} \left| \sum_{i=1}^{N-\rho} X_i X_{i+\rho} \int_{\tau+(i-1)T_{Di}}^{(i+\rho)T'} e^{j\omega_\Delta t}\,dt \right.$$

$$\left. + \sum_{i=1}^{N-(\rho+1)} X_i X_{i+\rho+1} \int_{(i+\rho)T'}^{\tau+iT_{Di}} e^{j\omega_\Delta t}\,dt \right| , \qquad \text{E-7}$$

in which the definitions in equation E-6 apply and

$$\left.\begin{aligned} p &= \text{smallest integer} \geq |\tau/T'| \\ \alpha &= \text{normalization constant} = \sqrt{2/NT} \\ \omega_\Delta &= \left(\frac{\omega_d' - \omega_{di}}{\omega_o + \omega_{di}}\right)\omega_o = (D_\Delta - 1)\,\omega_o\,. \end{aligned}\right\} \quad \text{E-8}$$

To complete the analysis, we would like to obtain the code values and limits of integration for the intervals, $4\,\Delta T < \tau < 8\,\Delta T$, $14\,\Delta T < \tau < 18\,\Delta T$, and so on. As a general rule, the interval of range deviation becomes

$$\frac{T'}{\Delta T} - N + 1 + (m-1)\frac{T_{Di}}{\Delta T} \leq \frac{\tau}{\Delta T} \leq m\frac{T'}{\Delta T}\,; \qquad m = 1, 2, \cdots, N.$$

We see that we may express the ambiguity function for this interval as the sum of five terms, i.e.,

$$\Psi'(\tau,\omega_\Delta) = \frac{D_\Delta \alpha^2}{2}\left|\sum_{i=1}^{n-\ell-k} X_i X_{i+k}\int_{\tau+(i-1)T_{Di}}^{(i+k)T'} e^{j\omega_\Delta t}\,dt\right.$$

$$+\sum_{i=1}^{n-\ell-(k+1)} X_i X_{i+k+1}\int_{(i+k)T'}^{\tau+iT_{Di}} e^{j\omega_\Delta t}\,dt$$

$$+X_{n-\ell-k}X_{n-\ell+1}\int_{(n-\ell)T'}^{(n-\ell+1)T'} e^{j\omega_\Delta t}\,dt$$

$$+\sum_{i=n-\ell}^{N-2} X_{i-k} X_{i+2}\int_{(i+1)T'}^{\tau+(i-k)T_{Di}} e^{j\omega_\Delta t}\,dt$$

$$+\sum_{i=n-\ell}^{N-2} X_{i+k+1} X_{i+2} \int_{\tau+(i-k)T_{Di}}^{(i+2)T'} e^{j\omega_\Delta t}\,dt \Bigg| , \qquad \text{E-9}$$

where the definitions in equations E-6 and E-8 apply and

$$\left.\begin{aligned}
n &= \frac{T'}{\Delta T} \\
n &= \frac{T_{Di}}{\Delta T} \\
q &= \text{smallest integer} \\
l &= q \text{ modulo } (n_1\quad) \\
k &= \text{smallest integer} \geq |\tau / T_{Di}| .
\end{aligned}\right\} \qquad \text{E-10}$$

APPENDIX F

PROPERTIES OF COMPLEMENTARY SEQUENCES 3, 15

This Appendix is a compilation of some of the properties of complementary sequences. At the end of this appendix is a list of the known kernels, of which there are four.

1. Definition: A pair of binary sequences of equal length, with the number of like pairs of one sequence, A, equal to the number of unlike pairs of the other sequence, B, for each possible spacing except at zero spacing, where the pairs of both sequences are like, is said to be a complementary sequence.

2. Given sequences A and B each of length n. Then complementing the code, i.e., complementing each element in the code, of A or B or both, results in a complementary code.

3. Definition: Time inversing of a code is to interchange the 1st and last bit, the second and next to the last bit, and so on.

4. Time inversing the A code, B code or both results in a complementary sequence.

5. Definition: The altering of a code is a transformation where every other bit of both codes is complemented.

6. The result of altering a complementary sequence is again a complementary sequence.

7. Definition: A kernel is a basic length code which cannot be decomposed into shorter length codes by an inversion of the standard generating methods.

8. Definition: Complementary sequences which are not kernels are called composite complementary sequences.

9. If $A = a_1,\ldots\ldots\ldots,a_n$

$B = b_1,\ldots\ldots\ldots,b_n$

is a complementary sequence pair, then

$C = a_1,\ldots\ldots\ldots,a_n,b_1,\ldots\ldots\ldots,b_n$

$D = a_1,\ldots\ldots\ldots,a_n\bar{b}_1,\ldots\ldots\ldots,\bar{b}_n$*

form a complementary sequence pair.

10. If $A = a_1,\ldots\ldots\ldots,a_n$

$B = b_1,\ldots\ldots\ldots,b_n$

is a complementary sequence pair, then

$C = a_1,b_1,a_2,b_2,\ldots\ldots\ldots\ldots a_n,b_n$

$D = a_1,\bar{b}_1,a_2,\bar{b}_2,\ldots\ldots\ldots\ldots a_n,\bar{b}_n$

form a complementary sequence pair.

11. The following is a list of the known kernels:

a. length 2

$A = \{-1,-1\}$
$B = \{-1,+1\}$

b. length 10

$A_1 = \{-1,+1,+1,-1,+1,-1,+1,+1,+1,-1\}$
$B_1 = \{-1,+1,+1,+1,+1,+1,+1,-1,-1,+1\}$

$A_2 = \{+1,-1,+1,-1,+1,+1,+1,+1,-1,-1\}$
$B_2 = \{+1,+1,+1,+1,-1,+1,+1,-1,-1,+1\}$

c. length 26

$A = \{+1,-1,+1,+1,-1,-1,+1,-1,-1,-1,-1,+1,-1,$
$+1,-1,-1,-1,-1,+1,+1,-1,-1,-1,+1,-1,+1\}$

$B = \{-1,+1,-1,-1,+1,+1,-1,+1,+1,+1,+1,-1,-1,$
$-1,-1,-1,-1,-1,+1,+1,-1,-1,-1,+1,-1,+1\}$

---

*$\bar{b}_i$ indicates the complement of b_i

REFERENCES

1. W. M. Siebert, "A Radar Detection Philosophy," IRE Trans. on Info. Theory, Vol. IT-2, pp. 204-221, Sept. 1956.

2. P. M. Woodward, Probability and Information Theory With Applications to Radar, New York: McGraw-Hill, 1953.

3. M. J. Golay, "Multi-Slit Spectrometry," Journal, Optical Society of America, Vol. 39, pp.437-444, June 1949.

4. M. J. Golay, "Static Multi-Slit Spectrometry and Its Application to the Panoramic Display of Infrared Spectra," Journal, Optical Society of America, Vol. 41, pp. 468-472, July 1951.

5. S. Jauregui, "A Theoretical Study of Complementary Binary Code Sequences and a Computer Search for New Kernels," PhD Dissertation, Naval Postgraduate School, Monterey, Calif., May 1962.

6. M. J. Golay, "Complementary Series," IRE Trans. on Info. Theory, Vol. IT-7, pp.82-87, April 1961.

7. R. H. Pettit, "Pulse Sequences With Good Autocorrelation Properties," Microwave Journal, Vol. 10-3, pp.63-67, Feb. 1967.

8. E. J. Baghdady, Lectures on Communication System Theory, pp. 2-3, New York: McGraw-Hill, 1961.

9. G. L. Turin, "An Introduction to Matched Filters," IRE Trans. on Info. Theory, Vol. IT-6, pp. 311-329, June 1960.

10. L. B. Jolley, Summation of Series, pp. 78-79, New York: Dover Publications, Inc., 1961.

11. J. L. Torres, "Relativistic Theory of Wide-Bandwidth Radar," Rept. SEL-1602-1, Stanford Electronics Lab., March 1966.

12. A. W. Rihaczek, "Delay-Doppler Ambiguity Function for Wideband Signals," IEEE Trans. on Aerospace and Electronic Systems, Vol. AES-3, pp. 705-711, July 1967.

13. R. M. Bracewell, The Fourier Transform and Its Applications, pp. 101-104, New York: McGraw-Hill, 1965.

14. E. J. Kelly and R. P. Wishner, "Matched Filter Theory for High-Velocity, Accelerating Targets," IEEE Trans. on Military Electronics, Vol. MIL-9, pp. 56-69, Jan. 1965.

15. J. D. Jackson, Classical Electrodynamics, pp. 347-387, John Wiley and Sons, Inc., 1962.

16. A. Einstein et al, The Principle of Relativity, pp. 37-65, Dover Publications, Inc., 1923.

INITIAL DISTRIBUTION LIST

		No. Copies
1.	Defense Documentation Center Cameron Station Alexandria, Virginia 22314	20
2.	Library Naval Postgraduate School Monterey, California 93940	2
3.	Commander, Air Systems Command (Code AIR-09B) Department of the Navy Washington, D. C. 20360	1
4.	Professor C. F. Klamm (Thesis Advisor) Department of Electrical Engineering Naval Postgraduate School Monterey, California 93940	5
5.	Professor K. E. Woehler Department of Physics Naval Postgraduate School Monterey, California 93940	1
6.	Professor D. B. Hoisington Department of Electrical Engineering Naval Postgraduate School Monterey, California 93940	1
7.	LT Richard M. Akita, USN c/o Mr. Glenn Tateno 45-880 Keneke St. Kaneohe, Hawaii 96744	5
8.	CAPT Justin H. Wickens, USMC c/o Dr. C. R. White 1461 Lone Pine Drive Macon, Georgia 31201	1
9.	Dean C. E. Menneken Dean of Research Naval Postgraduate School Monterey, California 93940	1
10.	Professor W. P. Cunningham Department of Physics Naval Postgraduate School Monterey, California 93940	1

11. LCDR Stephen Jauregui, USN 1
National Security Agency
Fort Meade, Maryland

12. LCDR Theodore J. Kuligowski, USN 1
306 Alta Ave.
Roseville, California 95678

UNCLASSIFIED

UNCLASSIFIED

Security Classification

DOCUMENT CONTROL DATA - R & D

(Security classification of title, body of abstract and indexing annotation must be entered when the overall report is classified)

1. ORIGINATING ACTIVITY (Corporate author)

Naval Postgraduate School
Monterey, California 93940

2a. REPORT SECURITY CLASSIFICATION

Unclassified

2b. GROUP

3. REPORT TITLE

AN INVESTIGATION OF THE NARROW-BAND AND WIDEBAND AMBIGUITY FUNCTIONS FOR COMPLEMENTARY CODES

4. DESCRIPTIVE NOTES (Type of report and inclusive dates)

Masters thesis, June 1968

5. AUTHOR(S) (First name, middle initial, last name)

Richard M. Akita
Lieutenant, United States Navy

6. REPORT DATE

June 1968

7a. TOTAL NO. OF PAGES

126

7b. NO. OF REFS

16

8a. CONTRACT OR GRANT NO.

b. PROJECT NO.

c.

d.

9a. ORIGINATOR'S REPORT NUMBER(S)

9b. OTHER REPORT NO(S) (Any other numbers that may be assigned this report)

10. DISTRIBUTION STATEMENT

[redacted] Delimited per AD846238. 27 Feb 1978

11. SUPPLEMENTARY NOTES

12. SPONSORING MILITARY ACTIVITY

13. ABSTRACT

A complementary code pair has the property that its autocorrelation function contains no range sidelobes. This property makes complementary codes attractive for use in signal waveform design for detection and tracking systems. An extensive list of the properties of these codes has been formulated by M. J. Golay and additions were made by S. Jauregui. However, the ambiguity functions of complementary codes have not been previously formulated.

This thesis considers the ambiguity functions of complementary codes for two cases:

1. Narrow-band analysis
2. Wideband analysis.

In the narrow-band analysis it is assumed that the doppler effect does not significantly alter the envelope of the transmitted signal. Siebert's definition of the ambiguity function is utilized in the formulation of the narrow-band complementary code ambiguity function.

In the wideband analysis it is shown that the doppler effect significantly alters the envelope of the transmitted signal. This alteration of the envelope of the transmitted signal becomes significant when the product of two factors, the relative velocity between the transmitter and the target and the time-bandwidth product, approaches one-half the velocity of propagation in the medium. Siebert's ambiguity function is extended to include the wideband case.

UNCLASSIFIED

DD FORM 1 NOV 65 1473 (PAGE 1)

S/N 0101-807-6811

UNCLASSIFIED

Security Classification

A-31408

14 KEY WORDS	LINK A		LINK B		LINK C	
	ROLE	WT	ROLE	WT	ROLE	WT
COMPLEMENTARY CODES/AMBIGUITY FUNCTION/ SIGNAL WAVEFORM DESIGN/RADAR/SONAR						

DD FORM 1 NOV 65 1473 (BACK)

S/N 0101-807-6821

A-31409

UNCLASSIFIED

UNCLASSIFIED